INFORMATION TO USERS

This manuscript has been reproduced from the microfilm master. UMI films the text directly from the original or copy submitted. Thus, some thesis and dissertation copies are in typewriter face, while others may be from any type of computer printer.

The quality of this reproduction is dependent upon the quality of the copy submitted. Broken or indistinct print, colored or poor quality illustrations and photographs, print bleedthrough, substandard margins, and improper alignment can adversely affect reproduction.

In the unlikely event that the author did not send UMI a complete manuscript and there are missing pages, these will be noted. Also, if unauthorized copyright material had to be removed, a note will indicate the deletion.

Oversize materials (e.g., maps, drawings, charts) are reproduced by sectioning the original, beginning at the upper left-hand corner and continuing from left to right in equal sections with small overlaps. Each original is also photographed in one exposure and is included in reduced form at the back of the book.

Photographs included in the original manuscript have been reproduced xerographically in this copy. Higher quality 6" x 9" black and white photographic prints are available for any photographs or illustrations appearing in this copy for an additional charge. Contact UMI directly to order.

UMI

A Bell & Howell Information Company
300 North Zeeb Road, Ann Arbor MI 48106-1346 USA
313/761-4700 800/521-0600

Analysis and Cancellation of Interference in Wireless Communications

by

MAO ZENG
M. Sc., Tsinghua University, Beijing, 1993
B. Eng. & B. Sc., Tsinghua University, Beijing, 1990

A Dissertation Submitted in Partial Fulfillment of the
Requirements for the Degree of

DOCTOR OF PHILOSOPHY

in the Department of Electrical and Computer Engineering

We accept this dissertation as conforming to the required standard

---

Dr. Qiang Wang, Supervisor, Dept. of Electrical and Computer Engineering

---

Dr. Vijay. K. Bhargava, Member, Dept. of Electrical and Computer Engineering

---

Dr. Panajotis Agathoklis, Member, Dept. of Electrical and Computer Engineering

---

Dr. Jane J. Ye, Outside Member, Dept. of Mathematics and Statistics

---

Dr. James A. Ritcey, External Examiner (University of Washington)

Supervisor: Prof. Qiang Wang

ABSTRACT

Wireless communications have recently gained much popularity in various commercial applications. Because of the peculiar characteristic of radio channels, the ability for communicators to stand various kinds of interference in the open air is one of the most important issues in wireless communications. The focus of this dissertation is on the analysis and cancellation of narrowband interference(NBI) which is one very detrimental form of interference.

To facilitate the analysis of SFH/DPSK under tone interfere, an analytical framework is developed for determination of the probability distribution of a corrupted differential phase. The concept of the phase characteristic function is introduced and its characterizations such as factorization are investigated. Based on it, expressions are derived for the general probability distribution of a received differential phase corrupted by signal tone interference and Gaussian noise under non-fading as well as different fading environments. Furthermore, we also derive the probability distribution of a received differential phase perturbed by multiple tone interference. Subsequently, an extensive analysis of SFH/DPSK is carried out in terms of bit error rate performance given different signalling schemes, fading environments and jamming strategies using band multitone and frequency jitter.

Finally, we propose a new technique for rejection of narrowband interference based on multiple symbol detection of coherent or differential phase shift keying. We first show that the direct use of multiple symbol detection offers poor performance when narrowband interference is dominant. Our proposed technique employs a special signalling or coding scheme which is shown to be robust against narrowband interference. Our evaluation of bit error rate shows significant performance improvement in narrowband interference vis-a-vis direct multiple symbol detection. When viewed as a coding scheme, the proposed signalling scheme is significantly simpler for achieving the same coding gain than conventional error correction codes.

Examiners:

Dr. Qiang Wang, Supervisor, Dept. of Electrical and Computer Engineering

Dr. Vijay. K. Bhargava, Member, Dept. of Electrical and Computer Engineering

Dr. Panajotis Agathoklis, Member, Dept. of Electrical and Computer Engineering

Dr. Jane J. Ye, Outside Member, Dept. of Mathematics and Statistics

Dr. James A. Ritcey, External Examiner (University of Washington)

Table of Contents

List of Figures

List of Tables

Acknowledgments

I wish to express my profound gratitude to my supervisor, Professor Qiang Wang, whose invaluable ideas, stimulating discussions, constant encouragement and unflagging support have guided this thesis research to its present state. The influence of his expertise can be seen throughout this work.

I am greatly indebted to Professor Vijay K. Bhargava, for his continued help, inspiration and understanding. His relentless efforts in nurturing an intellectual environment and facilitating research have been great benefit to me.

I am grateful to Professors Panajotis Agathoklis and Jane J. Ye for serving on my supervisory committee, and Professor James A. Ritcey for agreeing to be the external examiner in my Ph. D oral examination. Their time and effort are highly appreciated.

My sincere thanks are also extended to all my colleagues at Telecommunication Lab, for their warm friendship and cooperation in numerous ways. It has been an enjoyable and academically valuable experience working in this wonderful lab.

I have been truly grateful to Professor Xuelong Zhu for inspiring me to pursue my graduate study and for his guidance and encouragement during my years at Tsinghua University, P. R. China.

Special thanks go to the University of Victoria for its financial support in the form of a University of Victoria Fellowship, and Natural Science and Engineering Research Council of Canada and British Columbia Advanced Systems Institute for their financial assistance.

To
My Beloved Parents

Chapter 1

Introduction

1.1 Motivation of Research

Historically, communication has been restricted primarily to voice traffic between two fixed locations rather than people. The ability to communicate with people on the move has evolved remarkably since Guglielmo Marconi first demonstrated radio's ability to provide continuous contact with ships sailing the English channel[1][2]. That was in 1897, and since then new wireless communications methods and services have been enthusiastically adopted by people throughout the world. In recent years, wireless communications have gained much popularity in various commercial applications such as ISM (industrial, scientific and medical) band license-free radio, forthcoming PCS (personal communication services), mobile data and wireless LAN (local area network), etc., fueled by digital and RF circuit fabrication improvement, new large-scale circuit integration, and other miniaturization technologies which make portable radio equipment smaller, cheaper, and more reliable[3]-[7]. This increased popularity is in addition to the wide use of wireless communications for many years in military applications such as anti-jam radio[8] and satellite communications[9].

Interference is the major limiting factor in the performance of wireless communication systems, this is because the wireless channel is non-stationary and typically full of contamination such as natural and man-made interference. Such a poor channel quality has been recognized as the biggest obstacle for design of wireless communication sys-

tems. Therefore, one special requirement of a wireless communication system is that it must be able to stand various kinds of interference in the open air. One very detrimental form of interference is the narrowband interference which often has a very high power. In fact, this kind of interference is so detrimental that an extreme form of it, i.e., tone interference, has been commonly used as one of the worst case interference against which an anti-jam system is evaluated[8]. In commercial applications, this kind of interference may come from co-existing users such as those in PCS or ISM bands, or from various other unpredictable sources[7]. This dissertation is concerned with such kind of narrowband interference.

In wireless communication systems, spread spectrum (SS) techniques such as frequency hopping (FH) have been utilized to provide some protection against interference. Recently, there is an increasing interest in the application of SS techniques for commercial use, e.g., mobile cellular radio communications and wireless LAN, because of its inherent advantage in terms of anti-multipath, combating jamming, security, overlay communication, etc. In general, there are two classes of the spread spectrum techniques: frequency hopping and direct sequence SS techniques. For high rate transmission, there has been much interest in slow frequency hopping (SFH) which has been specified as an integral part of the advance pan-European GSM and DCS 1800 systems[7][10]. Henceforth, in this dissertation, we shall focus on slow frequency hopping systems in the presence of narrowband interference. We treat the narrowband interference as an intentional jammer. While the problem has obviously a military flavor, the solutions have great significance for commercial applications as well. For instance, the worst case analysis can equip the system designers with the knowledge about the design margin, which in turn helps them to design a robust communication system.

Over the past decade, much research work has been dedicated to analysis and cancellation of narrowband interference[8],[11]-[23]. In some of the previous works, the error performance of SFH/DPSK system under tone interference has been analyzed by ignoring the background thermal noise or restricting on some specific set of signals[11][13][14]. In [15], Wang, *et al*, presented a more general method to analyze arbi-

trary DPSK signals in both tone interference and AWGN which may model the background noise or system thermal noise. However, it seems non-trivial, if not impossible, to extend the method to the analysis of the error performance in presence of fading which is one of inherent characteristics of many wireless channels. Furthermore, in a realistic operating environment, a non-intentional or intentional (intelligent) jammer can inject one or multiple tone anywhere in each jammed band, which brings out a natural question: what is the most-effective jamming strategy? or in communicator's standpoint, what is the worst case interference? While a single tone strategy has been proven to yield the worst case scenario for FH/MFSK[8], it still remains an open issue for SFH/DPSK systems. Thus, a comprehensive study taking into account of all above impairments is indispensable.

For interference cancellation, conventionally, there are several narrowband interference rejection techniques. One is based on the use of a notch filter. The design of a notch filter calls for a careful trade-off between the degree of interference rejection and that of signal distortion. It may become quite awkward and even difficult to design a multi-notch filter if there is multiple narrowband interference. Another narrowband interference rejection technique is specific only to those applications where spread spectrum can be employed, especially with the use of direct sequence (DS) modulation in which case the interference power can be reduced in de-spreading by a factor approximately equal to the processing gain[5]. Unfortunately, in many commercial applications, due to various practical constraints, processing gains are usually between 10 to 20 dB which may often be insufficient for rejecting strong narrowband interference. In addition, in the case of frequency hopping (FH), e.g. slow FH (SFH), as considered later in the following chapters, the worst case narrowband interference can still be severely detrimental even when other anti-interference techniques such as error correction coding are used[47].

1.2 Frequency-Hop Communications

In a frequency-hopped spread spectrum communications system the available channel bandwidth is subdivided into a large number of frequency slots. In any signal interval,

the transmitted signal occupies one or more of the available frequency slots. The selection of the frequency slot(s) in each signal interval is made pseudo-randomly according the output from a PN generator. Figure 1.1 illustrates a particular frequency-hopped pattern in the time-frequency plane. Thus, in implementation of FH communications, there are two levels of modulation. The first level is the ordinary digital modulation such as M-ary frequency-shift-keying (MFSK) or differential phase-shift-keying(DPSK).

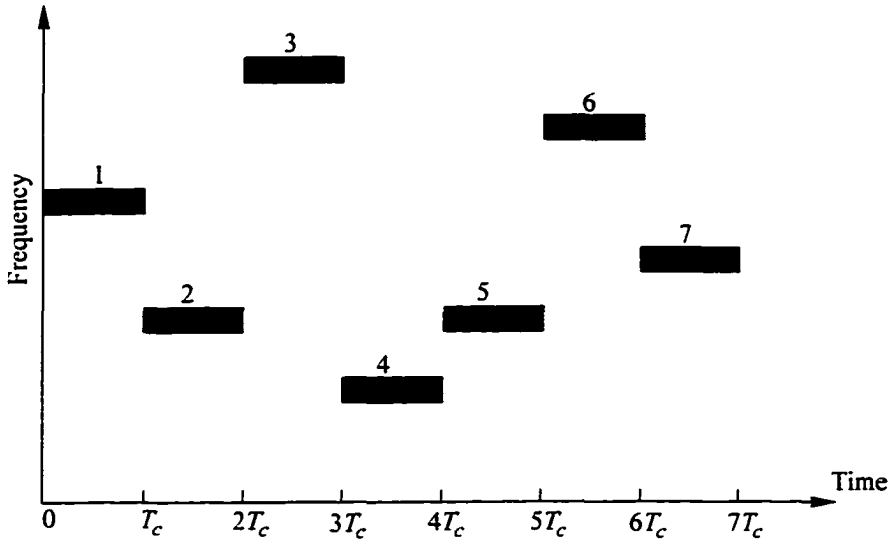

Figure 1.1 An example of a frequency-hopped pattern.

The modulating signal at this level is referred to as data symbols. The second level of modulation is the frequency hop modulation where the transmitter carrier frequency is changed every $T_c=1/R_h$ seconds within the total spread spectrum bandwidth W_{ss}. The carrier frequency changing rate R_h is called hop rate. For a system, if the hop rate is greater than symbol rate, the FH system is called a fast FH system (FFH). Otherwise, it is called a slow FH system. Generally, SFH can sustain a much higher data rate than FFH while having the same hop rate. Consequently, for a very high data rate transmission, slow frequency hopping must be used. For example, SFH at a typical R_h=20khop/s can be used to sustain transmission of information at so called T1 rate 1.544Mbit/s.

In slow frequency hopping, since there are several transmitted symbols during one

hop, the combination of differential phase encoding and phase difference detection is often used for reliable communication. One such a system is SFH/MDPSK system. A block diagram of a SFH/MDPSK system perturbed by jamming is shown in Figure 1.2. Clearly, in a jamming environment, the error performance of SFH/MDPSK is largely related to the fraction of FH slots jammed and error performances over the jammed slots.

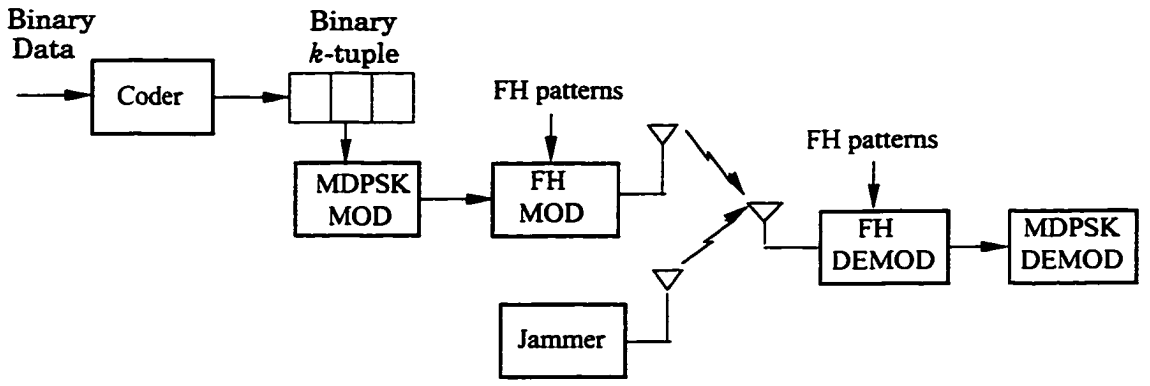

Figure 1.2 Functional block diagram of SFH/MDPSK system perturbed by jamming.

1.3 Contributions of the Dissertation

In this dissertation, we address two major issues pertaining to wireless communications systems which use slow frequency hopping spread spectrum. The first part of the dissertation deals with performance evaluation of SFH/MDPSK systems in the presence of tone interference. Based on previous work by Roberts, a rigorous mathematical theory is developed for determination of the general probability distribution of the differential phase of corrupted signals. In particular, it provides an analytical framework for studying the performance of SFH/MDPSK system in various propagation environments, as well as under different kinds of jamming, such as band multitone and frequency jitter. It is worth noting that the analytical approaches presented in much previous related work are largely based on geometric relation, and therefore restrictive (i.e., limited to a single tone interference without frequency offset and operation in non-fading channel).

Subsequently, we have derived an alternative yet simple expression for the probability distribution of differential phase perturbed by both tone interference and AWGN, which takes the previous results of Simon and Pawula, Rice and Roberts as special cases. Moreover, the expression for the desired signal corrupted by multiple tones are also presented. Our formulation of these distribution functions allows tractable analysis of SFH/MDPSK systems with an arbitrary number of interfering signals (multitone) and provides an insight into effect of frequency jitter on the overall system performance.

Finally, a comprehensive study has been carried out for SFH/DPSK systems in time non-dispersive Rayleigh and Rician fading channels. Numerical results are presented for all four combinations of the envelope fading environments: (a) desired signal and interference are Rayleigh faded; (b) both are Rician faded; (c) desired signal is Rayleigh faded and interference is Rician faded; and (d) desired signal is Rician faded and interference is Rayleigh faded. Furthermore, an evaluation of a SFH/DPSK system in a frequency selective fading channel is also presented.

The second part of this dissertation focuses on interference cancellation. A new technique for rejection of narrowband interference is proposed for systems using M-ary phase shift keying (MPSK). In our approach, a specific signalling or coding scheme is employed in conjunction with multiple symbol detection (which was first proposed by Divsalar and Simon for improving the performance of DPSK in wideband Gaussian noise). A general expression for pairwise error probability has been derived to facilitate the BER performance analysis of coherent and noncoherent MDPSK signals. It is shown that the proposed scheme can offer substantial improvement in terms of suppressing narrowband interference, and is optimum against tone interference. While the proposed signalling scheme can be viewed as a coding scheme, its implementation is significantly simpler than other error correction coding schemes which might offer the same performance with complexity that might be prohibitively high.

1.4 Outline of the Dissertation

Subsequent chapters of the dissertation are organized as follows.

In Chapter 2, preliminary theory is presented for determination of the general probability distribution of the differential phase between two complex random variables.

In Chapter 3, we analyze performance of a general uncoded SFH/DPSK under partial-band multitone jamming. A comprehensive study of jamming strategies using multitone and frequency jitter are presented.

In Chapter 4, a further study is carried out on the performance analysis of the SFH/DPSK in both partial-band multitone interference and fading. First, the channel models for both frequency non-selective and selective fading are described. Then, detailed derivation of the expressions for the bit error probability under different fading environments are presented. Effects of fading environments on the different signalling schemes are illustrated by numerical results.

Chapter 5 is concerned with the narrowband interference cancellation. First, the general multiple symbol detection of PSK in both AWGN and band pass interference (a special case is narrowband interference which is of our interest) is examined. Then, an asymptotically non-redundant coding or signalling scheme is proposed which makes the ML detection in AWGN also the ML detector in both AWGN and worst tone interference. Numerical results are presented to highlight the efficacy of the proposed signalling scheme in terms of narrowband interference suppression capability.

In Chapter 6, conclusions and suggestions for further work are provided.

Chapter 2

Preliminary Theory

2.1 Introduction

The probability distribution of the differential phase between two complex random variable is often encountered in the evaluation of the performance of a communication system where the differentially encoded phase-modulated signals such as differential shift keying (DPSK) are employed. In this chapter, the fundamental theory is provided for calculation of such probability distribution. To make the theory more self-contained, the detailed proofs and derivations are also provided.

2.2 The phase characteristic function

In this section, we start with a general presentation without referring to any specific form of signal. First, we introduce the concept of the *phase characteristic function* as follows.

Definition 2.1:

Given two complex random variables r_1 and r_2, the corresponding *phase characteristic function* is defined by

$$\Phi(u, v;\zeta) = E\left[J_0\left(\left|ur_1 + vr_2 e^{j\zeta}\right|\right)\right], \tag{2.1}$$

where u and v are real variables, and $J_o(x)$ is the *Bessel function* of the *first kind* of order zero.

When the complex random variables r_i, i=1, 2, are expressed in the exponential form as $R_i e^{j\theta_i}$, where R_i and θ_i are the amplitude and the phase of the complex random variable r_i respectively, *Definition 2.1* results in another expression of the *phase characteristic function* as follows,

$$\Phi(u, v;\zeta) = E\left[J_0\left(\sqrt{u^2R_1^2 + v^2R_2^2 + 2uvR_1R_2\cos(\theta_2 - \theta_1 + \zeta)}\right)\right], \qquad (2.2)$$

where the expectation is over random variables R_i and θ_i; i=1,2.

In a communication system, the transmitted signal is always disturbed by the background thermal noise. This background noise is often modeled as a narrowband stationary, zero-mean, *Gaussian* random variable because of the front-filter of the receiver. Thus, when using *n(t)*, the complex baseband equivalent to represent such a noise, we have that *n(t)* is a stationary complex Gaussian process with statistical properties as follows,

$$E(x(t)x(t+\tau)) = E(y(t)y(t+\tau)) = R(\tau);$$

$$E(x(t)y(t)) = 0$$

and

$$E(x(t)y(t+\tau)) = -E(x(t+\tau)y(t)) = R_{xy}(\tau), \qquad (2.3)$$

where the quantities *x(t)*, *y(t)* are real Gaussian variables related to the real and imaginary parts of *n(t)*, respectively. Since the *phase characteristic function* is particularly important and useful in our analysis, we discuss it further in the following proposition.

Proposition 2.1:

Let *n(t)* be a stationary complex Gaussian process with statistical properties as defined in (2.3), then its *phase characteristic function* can be calculated by

$$\Phi(u, v;\zeta) = \exp\left(\frac{R(0)\left(u^2 + v^2\right) + 2uv\left(R(\tau)\cos\zeta - R_{xy}(\tau)\sin\zeta\right)}{2}\right). \qquad (2.4)$$

Proof: See Section 2.5.1 for detail. ■

We now turn to characterizing the *phase characteristic function*. Generally, in a wireless communication system, in addition to the background thermal noise, the received

signal might be corrupted by various kinds of interference such as adjacent-channel interference, co-channel interference and so on. Without loss of generality, we assume the received signal has the form of

$$r(t) = s_0(t) + \sum_{i=1}^{n} s_i(t) e^{j\theta_i}, \tag{2.5}$$

where θ_i; i=1, 2,....., n, are random phases uniformly distributed in an interval of length 2π, which are introduced independently by the channel. More importantly, we desire the *phase characteristic function* defined in (2.1) to be factorable in terms of its components because such a property enables us to take a decomposition approach to the difficult analysis that will be seen later in the dissertation. In fact, the *phase characteristic function* can be guaranteed to be factorized by the following proposition:

Proposition 2.2:

Given a received signal in form of (2.5), the *phase characteristic function* of *r(t)* and *r(t+τ)* is factorable, i.e.,

$$\Phi_r(u, v;\zeta) = \prod_{i=0}^{n} \Phi_i(u, v;\zeta), \tag{2.6}$$

where $\Phi_i(u, v;\zeta)$ is the *phase characteristic function* of the *i*th component.

Proof: See Section 2.5.2 for detail. ■

2.3 Distribution of differential phase

We are now ready to explore the relation between the distribution probability of differential phase and the *phase characteristic function*. This can be drawn in the following proposition.

Proposition 2.3:

Let $r_i = A_i e^{j\theta_i}$; $i = 1, 2$ be two complex random variables, ψ is their differential

phase defined as

$$\psi = (\theta_2 - \theta_1) \, mod 2\pi .^{1} \tag{2.7}$$

Then the probability of $P\{\psi_1 \le \psi \le \psi_2\}$ given $-\pi \le \psi_1 \le \psi_1 \le \pi$ can be expressed in terms of its *phase characteristic function* $\Phi(u, v;\zeta)$ as

$$P\{\psi_1 \le \psi \le \psi_2\} = G(\psi_2) - G(\psi_1) \tag{2.8}$$

where the auxiliary function $G(\psi_i)$ has the form

$$G(\psi_i) = \frac{\psi_i}{2\pi} + \frac{1}{2\pi}\int_0^\infty \int_0^\infty \left. \frac{\partial \Phi(-u, v;\zeta)}{\partial \zeta} \right|_{\zeta = -\psi_i} \frac{1}{uv} du dv ; \; i=1,2. \tag{2.9}$$

Proof:

First we construct a random variable χ as a function of ψ as follows:

$$\chi(\psi) = \frac{1}{2\pi}[(\psi_2 - \psi_1) + \Im(\psi - \psi_2 + \pi) - \Im(\psi - \psi_1 + \pi)] , \tag{2.10}$$

where $\Im(\theta)$ is a periodic sawtooth function of period 2π defined as

$$\Im(\theta) = \theta; \qquad -\pi \le \theta \le \pi . \tag{2.11}$$

Clearly, the random variable χ is equal to 1 in $\psi_1 \le \psi \le \psi_2$ and to zero elsewhere in $-\pi \le \psi \le \pi$. Thus, we have

---

1. In general, the modulo 2π appearing in (2.7) should be understood to mean "over some 2π interval" with the assumption that the interval $[\psi_1, \psi_2]$ is contained entirely within the same 2π interval as ψ is. Without loss of generality, we here assume the modulo 2π means "over the interval of $[-\pi, \pi]$" for convenience of the presentation.

$$P\{\psi_1 \le \psi \le \psi_2\} = E[\chi(\psi)]$$

$$= \frac{\psi_2 - \psi_1}{2\pi} + \frac{1}{2\pi} E[\Im(\psi - \psi_2 + \pi) - \Im(\psi - \psi_1 + \pi)]. \tag{2.12}$$

Note the basic relation (see Section 2.5.3 for detail)

$$\Im(\theta) = \int_0^\infty \int_0^\infty \frac{\partial}{\partial\theta} J_0\left(\sqrt{x^2 + y^2 + 2xy\cos\theta}\right) \frac{dxdy}{xy}. \tag{2.13}$$

Replacing θ in (2.13) by $\psi - \psi_i + \pi$ and changing the variables of integration to u and v where $x = uR_1$, $y = vR_2$ and $R_1, R_2 > 0$, we have

$$\Im(\psi - \psi_i + \pi) =$$

$$\int_0^\infty \int_0^\infty \frac{\partial}{\partial(-\psi_i)} J_0\left(\sqrt{u^2R_1^2 + v^2R_2^2 - 2uvR_1R_2\cos(\psi - \psi_i)}\right) \frac{dudv}{uv}. \tag{2.14}$$

Taking the expected value of both sides of (2.14), we have

$$E[\Im(\psi - \psi_i + \pi)]$$

$$= E\left[\int_0^\infty \int_0^\infty \frac{\partial}{\partial(-\psi_i)} J_0\left(\sqrt{u^2R_1^2 + v^2R_2^2 - 2uvR_1R_2\cos(\psi - \psi_i)}\right) \frac{dudv}{uv}\right]$$

$$= \int_0^\infty \int_0^\infty \frac{\partial}{\partial(-\psi_i)} \left(E\left[J_0\left(\sqrt{u^2R_1^2 + v^2R_2^2 - 2uvR_1R_2\cos(\theta_2 - \theta_1 - \psi_i)}\right)\right] \right) \frac{dudv}{uv}$$

$$= \int_0^\infty \int_0^\infty \left. \frac{\partial\Phi(-u, v; \zeta)}{\partial\zeta} \right|_{\zeta = -\psi_i} \frac{dudv}{uv}. \tag{2.15}$$

Substitution of (2.15) into (2.12) leads to the desired results. ■

2.4 Summary

In this chapter, we presented a preliminary theory for determination of the probability distribution of the differential phase between two complex random variable. The *phase*

characteristic function was defined. In addition, it was also proved that the *phase characteristic* function of the received signal corrupted by additive interference can be factorized into the product of separate *phase characteristic* functions of signal and interference parts. An explicit relation was then established between the distribution of the differential phase and *phase characteristic function*. The role that the theory plays in the subsequent analysis of interference in communication systems will become clear later.

2.5 Detailed Derivation

2.5.1 Proof of *Proposition 2.1*

Consider the complex random variable $Z = u \cdot n(t) + v \cdot n(t+\tau)e^{j\zeta}$ where *n(t)* is a Gaussian process as defined in (2.3). Clearly, Z is a complex Gaussian random variable with the following statistical properties,

$$E(Z) = 0$$

$$var(Re(Z)) = var(Im(Z))$$

$$= R(0)\left(u^2 + v^2\right) + 2uv\left(R(\tau)\cos\zeta - R_{xy}(\tau)\sin\zeta\right) \tag{2.16}$$

and

$$E\{Re(Z) \cdot Im(Z)\} = 0. \tag{2.17}$$

For the sake of clarity, we denote variable σ_c^2 as

$$\sigma_c^2 = R(0)\left(u^2 + v^2\right) + 2uv\left(R(\tau)\cos\zeta - R_{xy}(\tau)\sin\zeta\right). \tag{2.18}$$

Therefore, $|Z|$ is a random variable with Rayleigh distribution given by

$$f(x) = \frac{x}{\sigma_c^2}\exp\left(-\frac{x^2}{2\sigma_c^2}\right), x \geq 0. \tag{2.19}$$

Noting the following equation[25]

$$\int_0^\infty t\exp\left(-p^2t^2/2\right)J_0(bt)\,dt = \frac{1}{p^2}\exp\left(\frac{-b^2}{2p^2}\right), \tag{2.20}$$

where $J_0(x)$ is the *Bessel function* of the *first kind* of order zero, we can easily get

$$\Phi(u, v;\zeta) = E\{J_0(|Z|)\}$$

$$= \exp\left(\frac{R(0)\left(u^2+v^2\right)+2uv\left(R(\tau)\cos\zeta - R_{xy}(\tau)\sin\zeta\right)}{2}\right). \tag{2.21}$$

2.5.2 Proof of *Proposition 2.2*

Here, we prove it by induction on *n*.

i). For n=1:

The received signal can be expressed as

$$r(t) = s_0(t) + s_1(t)e^{j\theta_1}. \tag{2.22}$$

Denote

$$A_S e^{j\alpha} = u\cdot s_0(t) + v\cdot s_0(t+\tau)e^{j\zeta} \tag{2.23}$$

and

$$A_I e^{j\beta+j\theta_1} = u\cdot s_1(t)e^{j\theta_1} + v\cdot s_2(t+\tau)e^{j\theta_1+j\zeta} \tag{2.24}$$

where the variables A_s, A_I, α and β are defined as

$$A_S = \left|u\cdot s_0(t) + v\cdot s_0(t+\tau)e^{j\zeta}\right|,\ \alpha = \arg\left(u\cdot s_0(t) + v\cdot s_0(t+\tau)e^{j\zeta}\right) \tag{2.25}$$

and

$$A_I = \left|u\cdot s_1(t) + v\cdot s_2(t+\tau)e^{j\zeta}\right|,\ \beta = \arg\left(u\cdot s_1(t) + v\cdot s_2(t+\tau)e^{j\zeta}\right). \tag{2.26}$$

Then we have

$$\left|u \cdot r(t) + v \cdot r(t+\tau) e^{j\zeta}\right| = \sqrt{A_S^2 + A_I^2 + 2A_S A_I \cos(\theta + \beta - \alpha)} . \tag{2.27}$$

Invoking Neumann's formula

$$J_0\left(\sqrt{x^2 + y^2 - 2xy\cos\theta}\right) = J_0(x) J_0(y) + 2\sum_{r=1}^{\infty} J_r(x) J_r(y) \cos(r\theta) , \tag{2.28}$$

where $J_r(x)$ is the *Bessel function* of the *first kind* of order r, we can readily obtain

$$\begin{aligned}
\Phi(u, v;\zeta) &= E\{J_0\left(\left|u \cdot r(t) + v \cdot r(t+\tau) e^{j\zeta}\right|\right)\} \\
&= E\left(\int_0^{2\pi} \frac{1}{2\pi} \cdot J_0\left(\sqrt{A_S^2 + A_I^2 + 2A_S A_I \cos(\theta + \beta - \alpha)}\right) d\theta\right) \\
&= E\left(J_0\left(\left|u \cdot s_0(t) + v \cdot s_0(t+\tau) e^{j\zeta}\right|\right)\right) \cdot E\left(J_0\left(\left|u \cdot s_1(t) + v \cdot s_1(t+\tau) e^{j\zeta}\right|\right)\right) \\
&= \Phi_0(u, v;\zeta)\, \Phi_1(u, v;\zeta) .
\end{aligned} \tag{2.29}$$

ii). As the induction hypothesis, suppose that the proposition holds for $n=k$.

Now we show it holds for $n=k+1$.

Define

$$s'_0(t) = s_0(t) + \sum_{i=1}^{k} s_i(t) e^{j\theta_i} . \tag{2.30}$$

Thus, we have

$$r(t) = s_0(t) + \sum_{i=1}^{k+1} s_i(t) e^{j\theta_i} = s'_0(t) + s_{k+1}(t) e^{j\theta_{k+1}} . \tag{2.31}$$

As shown in i), (2.31) results in

$$\Phi(u, v;\zeta) = \Phi'(u, v;\zeta)\, \Phi_{k+1}(u, v;\zeta) \tag{2.32}$$

where $\Phi'(u, v;\zeta)$ is the *phase characteristic function* which by induction assumption can be expressed as

$$\Phi'(u, v;\zeta) = \prod_{i=0}^{k} \Phi_i(u, v;\zeta) . \tag{2.33}$$

Substituting (2.33) into (2.32) leads to the desired result.

2.5.3 Derivation of (2.13)

Invoking Neumann's formula, i.e., equation (2.28), it follows that

$$\int_0^\infty \int_0^\infty \frac{\partial}{\partial\theta} J_0\left(\sqrt{x^2+y^2-2xy\cos\theta}\right)\frac{dxdy}{xy}$$

$$= \int_0^\infty \int_0^\infty \frac{\partial}{\partial\theta}\left(J_0(x)J_0(y) + 2\sum_{r=1}^{\infty} (-1)^r J_r(x)J_r(y)\cos(r\theta)\right)\frac{dxdy}{xy}$$

$$= 2\sum_{r=1}^{\infty} (-1)^{r-1}\left(\int_0^\infty \frac{J_r(x)}{x}dx\right)^2 r\sin(r\theta) , \tag{2.34}$$

where $J_r(x)$ is the *Bessel function* of the *first kind* of order r.

Note *Weber*'s infinite integral,

$$\int_0^\infty J_\nu(t)\, t^{-(\nu-\mu+1)}dt = \frac{\Gamma\left(\frac{1}{2}\mu\right)}{2^{\nu-\mu+1}\Gamma\left(\nu-\frac{1}{2}\mu+1\right)} . \tag{2.35}$$

Use of (2.35) into (2.34) leads to

$$\int_0^\infty \int_0^\infty \frac{\partial}{\partial\eta} J_0\left(\sqrt{x^2+y^2-2xy\cos\eta}\right)\frac{dxdy}{xy} = 2\sum_{r=1}^{\infty} \frac{(-1)^{r-1}}{r}\sin(r\theta) . \tag{2.36}$$

Since the right hand of (2.36) is the Fourier expansion of the function $\Im(\theta)$ defined in (2.11), the desired result then follows.

Chapter 3

Analysis of Slow Frequency Hopped Differential PSK under Tone Interference

3.1 Introduction

Differential phase shift keying (DPSK) is widely used in communications where simplicity and robustness are desired. One such a system is slow frequency hopped DPSK (SFH/DPSK) which can sustain a much higher data rate than a fast frequency hopped system while having the same hop rate. SFH/DPSK has been used for spread spectrum satellite communications[9][17] and is a strong candidate for wireless LAN (local area network) in ISM (industrial, scientific and medical) bands[5]-[7].

In the detection of SFH/DPSK, differentially coherent detection is often employed. This is because it is impossible to maintain the phase coherence between different hops[11][15][42]. Differentially coherent detection can take advantage of phase coherence within a hop and thus outperforms noncoherent detection. SFH/DPSK may often be subject and susceptible to tone interference or jamming as well as AWGN (additive white Gaussian noise). In this chapter, we present a study of the probability distribution of a received differential phase perturbed by tone jamming and Gaussian noise. The intent is to study the effects of jamming against SFH/DPSK and to provide an effective tool for the analysis of such a system. It is noted that tone jamming has been recognized as an excellent model for narrow-band interference widely found in wireless communications.

Therefore, a combination of a tone jamming and AWGN forms a theoretically interesting and practically useful interference model as it includes both narrow-band and wide-band interference.

In much previous work, the performance of SFH/DPSK has been considered. Simon[11] has analyzed the performance of SFH/DPSK under multiple continuous tone jamming for a specific set of signal phases and equally spaced decision regions. The analytical results were obtained by ignoring the system thermal noise so that the derivation relied largely on geometric relation. Gong analyzed the performance of a specific binary SFH/DPSK scheme in both tone and noise interference[14]. In [15], Wang, et al, presented a method to derive the general probability distribution for arbitrary DPSK signals in both tone interference and AWGN which may model the background noise or system thermal noise. In this chapter, we present an alternative and yet simple expression of the general probability distribution of a received differential phase corrupted by continuous tone jamming and Gaussian noise.The probability distribution of the received differential phase corrupted by either continuous tone jamming or Gaussian noise is a special form of it. Thus, our result is a generalization of the previous well known results given by Simon[11], and Pawula, Rice and Roberts[33].

Moreover, in all previous work, it has been assumed that jammer only injects one tone into each jammed band at the frequency of the signal carrier. This assumption appears too ideal. As mentioned in Chapter 1, in reality, an intelligent jammer can inject one or multiple tones anywhere (i.e., with frequency jitter) in each jammed band, which brings out a natural question: what is the most effective jamming strategy? Notice that, although the single tone strategy has been proven to be more effective against FH/MFSK than multiple tones, whether this can be extended to SFH/DPSK remains as an open question. We can raise a similar question when taking into account frequency jitter even with the use of single jamming tone. Therefore, two well known jamming strategies, i.e., frequency jitter strategy and multitone jamming strategy, are investigated in this chapter.

The remainder of the chapter is organized as follows. In Section 3.2, the probability

distribution of a differential phase perturbed by tone interference and Gaussian noise is derived. To investigate the jamming strategies, we also derive the probability distribution of a received differential phase corrupted by multitone interference. The obtained results are then applied in Section 3.3 to the evaluation of a SFH/DPSK system. Finally, the conclusions are drawn in Section 3.4.

3.2 Probability distribution of DPSK Perturbed by Tone Interference

3.2.1 With One Continuous Wave (CW) Tone Interference and Gaussian Noise

Generally, the complex baseband equivalent of the received DPSK signal corrupted by one CW tone jamming and Gaussian noise has the form

$$r(t) = Ae^{j\phi(t)+\theta_0} + A_J e^{j\theta + j\Delta\omega t} + n(t), \tag{3.1}$$

where the first term is the DPSK signal with an uncontaminated signal phase $\phi(t)$, the second term is the jamming tone with a carrier frequency offset of $\Delta\omega$, and the third term *n(t)* represents AWGN noise. In detecting M-ary DPSK, it is decided that symbol m was sent if the phase different between $r(t)$ and $r(t+\tau)$ lies between certain decision interval $\left(\psi_1^{(m)}, \psi_2^{(m)}\right)$; m=1, 2,..., M, where T is the symbol period and $T \le \tau < 2T$[1]. Therefore, the symbol error probability can be calculated as follows.

$$P_s = \sum_{m=1}^{M} p_m \left(1 - P\{\psi_1^{(m)} \le \Psi \le \psi_2^{(m)} \,|\, \phi(t+\tau) - \phi(t) = \theta_m\}\right), \tag{3.2}$$

where p_m is the probability that a differential phase θ_m was sent and

1. Usually, it is assumed that τ=T.

$$\psi = \arg\left(r(t+\tau)\, r^*(t)\right) mod 2\pi . \tag{3.3}$$

As illustrated in Chapter 2, the conditional probabilities in (3.2) can be given by

$$P\left\{\psi_1^{(m)} \le \Psi \le \psi_2^{(m)} \,\middle|\, \phi(t+\tau) - \phi(t) = \theta_m\right\} = G\left(\psi_2^{(m)}\right) - G\left(\psi_1^{(m)}\right), \tag{3.4}$$

where $G(\psi)$ has the form

$$G(\psi) = \frac{\psi}{2\pi} + \frac{1}{2\pi}\int_0^{\infty}\int_0^{\infty} \left.\frac{\partial \Phi(-u, v;\zeta)}{\partial \zeta}\right|_{\zeta = -\psi} \frac{1}{uv}\, du\, dv \tag{3.5}$$

where $\Phi(u, v;\zeta)$ is the phase characteristic function of the received signal. Thus, to calculate the probabilities in (3.2), we need the expression for $G(\psi)$. We first consider the phase characteristic function of $r(t)$ and $r(t+\tau)$. By *Proposition 2.2*, the phase characteristic function can be written as the product form,

$$\Phi(u, v;\zeta) = \Phi_S(u, v;\zeta)\, \Phi_N(u, v;\zeta)\, \Phi_J(u, v;\zeta) , \tag{3.6}$$

where the subscripts "S","J" and "N" refer to signal, jamming tone and Gaussian noise components, respectively. By definition and *Proposition 2.1*, these signal, jamming tone and noise components have the forms

$$\Phi_S(u, v;\zeta) = J_0\left(A\sqrt{u^2 + v^2 + 2uv\cos(\Delta\Phi + \zeta)}\right), \tag{3.7}$$

where $\Delta\Phi = \phi(t+T) - \phi(t)$;

$$\Phi_N(u, v;\zeta) = \exp\left(-\sigma_0^2\left(\left(u^2 + v^2\right)/2\right)\right) \tag{3.8}$$

and

$$\Phi_J(u, v;\zeta) = J_0\left[A_J\sqrt{u^2 + v^2 + 2uv\cos(\zeta + \Delta\omega\tau)}\right]. \tag{3.9}$$

Then we have

$$\Phi(-u, v;\zeta) =$$

$$J_0\left(A\sqrt{u^2+v^2-2uv\cos(\Delta\Phi+\zeta)}\right)J_0\left(A_J\sqrt{u^2+v^2-2uv\cos(\Delta\omega\tau+\zeta)}\right)e^{-\sigma_0^2\left(u^2+v^2\right)/2} \tag{3.10}$$

Making a transformation to polar coordinates by means of

$$u = \frac{R}{\sigma_0}\cos\frac{\theta'}{2} \qquad v = \frac{R}{\sigma_0}\sin\frac{\theta'}{2} \tag{3.11}$$

and then making the change $\theta' = \frac{\pi}{2} - \theta$, we can express the auxiliary function $G(\psi)$ as

$$G(\psi) = \frac{\psi}{2\pi} - \int_{-\frac{\pi}{2}}^{\frac{\pi}{2}} \frac{1}{2\pi\cos\theta} d\theta \int_0^\infty \frac{1}{R} dR \frac{\partial}{\partial\psi}\left(J_0\left(R\sqrt{\gamma_0(1-\cos\theta\cos(\Delta\Phi-\psi))}\right)\right.$$

$$\left. J_0\left(R\sqrt{\gamma_J(1-\cos\theta\cos(\Delta\omega\tau-\psi))}\right)e^{-R^2/2}\right) \tag{3.12}$$

where γ_0 and γ_J are the signal-to-noise ratios for the transmitted signal and interfering tone respectively, which are defined as

$$\gamma_0 = \frac{A^2}{\sigma^2}, \qquad \gamma_J = \frac{A_J^2}{\sigma^2} = \frac{\gamma_N}{A^2/A_J^2}. \tag{3.13}$$

It is convenient to define

$$S(\theta) = 1-\cos\theta\cos(\Delta\omega\tau-\psi); \quad T(\theta) = 1-\cos\theta\cos(\Delta\Phi-\psi). \tag{3.14}$$

Then (3.12) becomes

$$G(\psi) = \frac{\psi}{2\pi} - \frac{1}{4\pi}\int_{-\frac{\pi}{2}}^{\frac{\pi}{2}}\int_0^\infty\left(\frac{\sqrt{\gamma_0}\sin(\Delta\Phi-\psi)}{\sqrt{T(\theta)}}J_1\left(R\sqrt{\gamma_0 T(\theta)}\right)J_0\left(R\sqrt{\gamma_J S(\theta)}\right)+\right.$$

$$\frac{\sqrt{\gamma_J}\sin(\Delta\omega\tau-\psi)}{\sqrt{S(\theta)}}J_0\left(R\sqrt{\gamma_0 T(\theta)}\right)J_1\left(R\sqrt{\gamma_J S(\theta)}\right)\Big)e^{-R^2/2}dRd\theta, \tag{3.15}$$

where $J_1(x)$ is the Bessel function of the first kind of order one.

Invoking the following equation proven in Section 3.5,

$$\int_0^\infty \exp\left(-p^2x^2/2\right)J_0(bx)J_1(ax)\,dx = \frac{1}{a}\left[1-Q\left(\frac{b}{p},\frac{a}{p}\right)\right]$$

$$= \frac{1}{a}q\left(\frac{b}{p},\frac{a}{p}\right), \tag{3.16}$$

where $Q(x,y)$ is Marcum's Q-function, and $q(x,y)$ is complimentary Marcum's Q-function, we can obtain

$$G(\psi) = \frac{\psi}{2\pi}-\frac{1}{4\pi}\int_{-\frac{\pi}{2}}^{\frac{\pi}{2}}\left[\frac{\sin(\Delta\Phi-\psi)}{T(\theta)}q\left(\sqrt{\gamma_J S(\theta)},\sqrt{\gamma_0 T(\theta)}\right)+\right.$$

$$\left.\frac{\sin(\Delta\omega\tau-\psi)}{S(\theta)}q\left(\sqrt{\gamma_0 T(\theta)},\sqrt{\gamma_J S(\theta)}\right)\right]d\theta. \tag{3.17}$$

3.2.2 Special forms of G(ψ)

In this section, two important special cases are considered. Although some of these results have been given in previous papers, we herein include them as special cases to demonstrate the generality of our results. To some extent, the previously known results offer a verification of our new results.

Case I: the signal is perturbed by Gaussian noise only.

Let $\gamma_J = 0$ in (3.17), it follows that

$$G(\psi) = F(\psi)+g(\psi), \tag{3.18}$$

where $F(\psi)$ and $g(\psi)$ can be calculated as

$$F(\psi) = \frac{\sin(\Delta\Phi-\psi)}{4\pi}\int_{-\frac{\pi}{2}}^{\frac{\pi}{2}} \frac{\exp-(\gamma_N(1-\cos(\Delta\Phi-\psi)\cos\theta)/2)}{1-\cos(\Delta\Phi-\psi)\cos\theta}d\theta \qquad (3.19)$$

and

$$g(\psi) = \frac{\psi}{2\pi} - \frac{\sin(\Delta\Phi-\psi)}{4\pi}\int_{-\frac{\pi}{2}}^{\frac{\pi}{2}} \frac{1}{1-\cos\theta\cos(\Delta\Phi-\psi)}d\theta$$

$$= \begin{cases} \dfrac{\Delta\Phi+\pi}{2\pi} & if\ \Delta\Phi < \psi \le \Delta\Phi + 2\pi \\ \dfrac{\Delta\Phi-\pi}{2\pi} & if\ \Delta\Phi - 2\pi \le \psi < \Delta\Phi \end{cases}. \qquad (3.20)$$

Hence, for $\psi_1 < \psi_2$, we have

$$P\{\psi_1 \le \psi \le \psi_2\} = \begin{cases} F(\psi_2) - F(\psi_1) + 1; & \psi_1 < \Delta\Phi < \psi_2 \\ F(\psi_2) - F(\psi_1); & else \end{cases}, \qquad (3.21)$$

which is a result given by Pawula, Rice and Roberts in [33].

Case II: the Gaussian noise is ignored--tone jamming only.

This is the case often considered in much previous work[11]. While the ignorance of AWGN may or may not be reasonable in practice, we here include this case as a special case of our results.

Let $\sigma_0 = 0$ in (3.10), similarly we can have

$$G(\psi) = \frac{\psi}{2\pi} - \frac{1}{4\pi}\int_{-\frac{\pi}{2}}^{\frac{\pi}{2}}\int_0^{\infty}\left(\frac{\sin(\Delta\Phi-\psi)}{\sqrt{T}}J_1(R\sqrt{T})J_0\left(R\sqrt{\rho_J S}\right) + \right.$$

$$\left.\frac{\sqrt{\rho_J}\sin(\Delta\omega\tau-\psi)}{\sqrt{S}}J_0(R\sqrt{S})J_1\left(R\sqrt{\rho_J S}\right)\right)dRd\theta, \qquad (3.22)$$

where ρ_J is defined as

$$\rho_J = \frac{A_J^2}{A^2}. \tag{3.23}$$

Note the following equation

$$\int_0^\infty J_1(ap) J_0(rp)\, dp = \begin{cases} \frac{1}{a}, & 0 < r < a; \\ \frac{1}{2a}, & r = a; \\ 0, & r > a \end{cases} . \tag{3.24}$$

Then, (3.22) can be expressed as

$$G(\psi) = \frac{\psi_i}{2\pi} - \frac{1}{4\pi}\int_{-\frac{\pi}{2}}^{\frac{\pi}{2}} \left(\frac{\sin(\Delta\Phi - \psi)\, 1(-\mu(\theta))}{1 - \cos\theta\cos(\Delta\Phi - \psi)} + \frac{\sin(\Delta\omega\tau - \psi)\, 1(\mu(\theta))}{(1 - \cos\theta\cos\Delta\omega\tau - \psi)} \right) d\theta, \tag{3.25}$$

where

$$\mu(\theta) = \rho_J(1 - \cos\theta\cos(\Delta\omega\tau - \psi)) - (1 - \cos\theta\cos(\Delta\Phi - \psi)) \tag{3.26}$$

and 1(x) is the unite-step function.

In [11], Simon derived the probability of the following error event

$$Q_{2\pi n/M} = Pr\left\{ \left| \arg\left((r_2 - r_1) - \frac{2\pi n}{M} \right) \right| > \frac{\pi}{M} \right\}. \tag{3.27}$$

His derivation relied largely on geometric relations and is therefore applicable to a specific set of signal phases with equally spaced decision regions. As shown in Section 3.5, from (3.25)-(3.26), we can get the same result as Simon's. Thus, (3.25) is a generalization of Simon's result.

3.2.3 With Multiple Continuous Wave (CW) Tone Interference

As mentioned early in this chapter, an intelligent jammer might insert multiple tone interference into every jammed band as its jamming strategy. For simplicity, we neglect the background noise and only consider the signal corrupted by two jamming tones, although

this analysis can be extended to the more general case with the background noise and more than two jamming tones. Assume the received signal is given as follows,

$$r(t) = Ae^{j\phi(t)+\theta_0} + A_J^{(1)} e^{j\theta_1 + j\Delta\omega_1 t} + A_J^{(2)} e^{j\theta_2 + j\Delta\omega_2 t}, \tag{3.28}$$

where the second and the third term are two independent jamming tones with carrier frequency offsets of $\Delta\omega_1$ and $\Delta\omega_2$ respectively.

Similarly, by the factorization characterization, the *phase characteristic function* can be written as follows,

$$\Phi(u, v;\zeta) =$$

$$J_0\left(A\sqrt{u^2+v^2+2uv\cos(\Delta\Phi+\zeta)}\right)\prod_{i=1}^{2} J_0\left(A_J^{(i)}\sqrt{u^2+v^2+2uv\cos(\Delta\omega_i\tau+\zeta)}\right). \tag{3.29}$$

Similar to the derivation of (3.15), the auxiliary function $G(\psi)$ can be expressed as

$$G(\psi) = \frac{\psi}{2\pi} - \frac{1}{4\pi}\int_{-\frac{\pi}{2}}^{\frac{\pi}{2}}\int_0^{\infty}\left(\frac{\sin(\Delta\Phi-\psi)}{\sqrt{T(\theta)}}J_1(R\sqrt{T(\theta)})\prod_{i=1}^{2}J_0\left(R\sqrt{\rho_J^{(i)}S_i(\theta)}\right)+\right.$$

$$\left.\sum_{\substack{i=1\\k\neq i}}^{2}\frac{\sqrt{\rho_J^{(i)}}\sin(\Delta\omega_i\tau-\psi)}{\sqrt{S_i(\theta)}}J_1\left(R\sqrt{\rho_J^{(i)}S_i(\theta)}\right)J_0(R\sqrt{T(\theta)})J_0\left(R\sqrt{\rho_J^{(k)}S_k(\theta)}\right)\right)dRd\theta, \tag{3.30}$$

where $\rho_J^{(i)}$ and $S_i(\theta)$; i=1, 2, are defined as

$$\rho_J^{(i)} = \frac{A_J^{(i)2}}{A^2}; \; i=1,2, \tag{3.31}$$

$$S_i(\theta) = 1-\cos\theta\cos(\Delta\omega_i\tau-\psi); \; i=1,2. \tag{3.32}$$

Noting the following equation[25],

$$\int_0^\infty J_1(at)J_0(bt)J_0(ct)\,dt = \begin{cases} 0; & a^2 < (b \pm c)^2 \\ \frac{1}{a}; & a^2 > (b \pm c)^2 \\ \frac{1}{\pi a}\arccos\frac{b^2+c^2-a^2}{2bc}; & otherwise \end{cases} \tag{3.33}$$

and the fact that when a, b and c are positive,

$$|b-c| < a < b+c \Leftrightarrow |a-c| < b < a+c \Leftrightarrow |b-a| < c < b+a;$$

$$a > |b \pm c| \Leftrightarrow c < |a \pm b| \quad and \quad b < |c \pm a|,$$

it follows that

1. when $\left|\sqrt{\rho_J^{(1)} S_1(\theta)} - \sqrt{\rho_J^{(2)} S_2(\theta)}\right| \le \sqrt{T(\theta)} \le \sqrt{\rho_J^{(1)} S_1(\theta)} + \sqrt{\rho_J^{(2)} S_2(\theta)}$,

$$G(\psi) = \frac{\psi}{2\pi} - \frac{1}{4\pi}\int_{-\frac{\pi}{2}}^{\frac{\pi}{2}} \left(\frac{\sin(\Delta\Phi - \psi)}{T(\theta)} \cdot \frac{\eta_0}{\pi} + \sum_{i=1}^{2} \frac{\sin(\Delta\omega_i \tau - \psi)}{S_i(\theta)} \cdot \frac{\eta_i}{\pi} \right) d\theta; \tag{3.34}$$

2. otherwise,

$$G(\psi) = \frac{\psi}{2\pi} - \frac{1}{4\pi}\int_{-\frac{\pi}{2}}^{\frac{\pi}{2}} \left(\frac{\sin(\Delta\Phi - \psi)}{T(\theta)} \cdot 1\left(\sqrt{T(\theta)} - \sum_{i=1}^{2} \sqrt{\rho_J^{(i)} S_i(\theta)} \right) + \right.$$

$$\left. \sum_{\substack{i=1 \\ j \ne i}}^{2} \frac{\sqrt{\rho_J^{(i)}}\sin(\Delta\omega_i \tau - \psi)}{S_i(\theta)} \cdot 1\left(\sqrt{\rho_J^{(i)} S_i(\theta)} - \sqrt{T(\theta)} - \sqrt{\rho_J^{(j)} S_j(\theta)} \right) \right) d\theta, \tag{3.35}$$

where η_i; i=0, 1, 2, are defined as

$$\eta_0 = \arccos\frac{\sum_{i=1}^{2} \rho_J^{(i)} S_i(\theta) - T(\theta)}{2\sqrt{\rho_J^{(1)} \rho_J^{(2)} S_1(\theta) S_2(\theta)}} \tag{3.36}$$

and

$$\eta_i = arc\cos\frac{\rho_J^{(k)} S_k(\theta) + T(\theta) - \rho_J^{(i)} S_i(\theta)}{2\sqrt{\rho_J^{(k)} S_k(\theta)\, T(\theta)}};\ i,k = 1,2;\ i \neq k. \tag{3.37}$$

3.3 Performance of SFH/MDPSK under Multi-tone Interference

3.3.1 The Worst Case Performance

In this section, we apply the result derived in the Section 3.2 to evaluating the performance of uncoded SFH/DPSK under partial-band multitone jamming. To gain critical insight to the effect of tone jamming on SFH/DPSK, the error performance under worst case tone jamming should be considered. We assume the system model is the same as that in [8][15]. Suppose the transmitted *M-ary* DPSK signal has M possible differential phase θ_i for $i=1,\ldots\ldots, M$, with equal probability of transmission. The signal is hopped over N frequencies and is jammed with probability ρ. When the signal is jammed, it has the probability distribution as calculated in Section 3.2. If the signal is not jammed, it is subject to the background noise modeled by AWGN with a two-side spectral density of $N_0/2$. Thus, for a correlation receiver, $\sigma^2 = N_0/T_s$, where T_s is the DPSK symbol period. We assume that all jamming tones have equal power $A_J^2/2$ and there are m independent tones in each jammed band. With a total jamming power J available, the number of jammed frequency slots is

$$Q = \frac{J}{m\left(A_J^2/2\right)} = \frac{J\beta}{m\left(A^2/2\right)} \tag{3.38}$$

where $A^2/2$ is the signal power and $\beta = A^2/A_J^2$.

Then we have

$$\rho = \frac{Q}{N} = \frac{J\beta}{A^2/2} \cdot \frac{1}{mN} = \frac{\beta}{mT_s \frac{A^2}{2} \cdot \frac{N}{JT_s}} = \frac{\beta}{m \log M E_b/N_J} \tag{3.39}$$

where N is the total number of hop frequency slots, E_b is the signal energy per bit and N_J is the equivalent broadband jamming power spectral density defined by

$$N_J = T_s \cdot \frac{J}{N} \tag{3.40}$$

so that, if the total jamming power J is uniformly distributed over all N frequencies, then at any frequency $N_J/T_s = J/N$ is the jamming power which is parallel to AWGN power $\sigma^2 = N_0/T_s$. Note that the above derivation of ρ is more general than those in [15][17][47] because it needs not assume the hopping channel bandwidth or spacing.

The average symbol error probability over the entire frequency band is

$$P_s = (1-\rho) \times P_{AWGN}(E_b/N_0) + \rho \times P_J(E_b/N_o, \rho E_b/N_J) \tag{3.41}$$

where P_{AWGN} is the symbol error probability when a hop is free of jamming[2] and P_J is the symbol error probability when a hop is jammed. For simplicity, we follow [11][15] to assume that ρ is continuous. Then the best strategy for jammer (worst case for communicator) is choosing ρ_{max} to maximize (3.41).

To compare system performance for different M, we must convert P_s into an equivalent bit error rate (BER) P_b. In this dissertation, we use the following conversion,

2. when background Gaussian noise is ignored, the item is simply zero.

$$P_b \approx \frac{M}{2(M-1)} P_s. \tag{3.42}$$

This conversion is exact for M=2 but is approximate for larger M unless the signal sets are orthogonal. The conversion yields a convenient, usually very accurate, upper bound to the bit error probability[13]. A more precise evaluation requires knowledge of the mapping of bits to symbols. For simplicity, precise evaluation is not done in this chapter.

3.3.2 Computational Results

In this section selected numerical results are presented for DPSK and 4-ary DPSK based on the above analysis. Figure 3.1 plots the worst case BER performance of binary DPSK with the signaling scheme $\theta_1 = 0$ and $\theta_2 = \pi$ (called BDPSK) as a function of E_b/N_J under different E_b/N_o. The performance of another signaling scheme with $\theta_1 = \pi/2$ and $\theta_2 = 3\pi/2$ for binary DPSK is shown in Figure 3.2. Comparing Figure 3.1 with Figure 3.2 shows that using signalling scheme with $\theta_1 = 0$ and $\theta_2 = \pi$ results in a degradation in performance of approximately 2.4 dB at a BER of 10^{-3} and $E_b/N_o = 30dB$. Hence, for a system employing binary DPSK, appropriate selection of signalling scheme is crucial to maximize the system performance. For a system employing 4-ary DPSK, two signaling schemes are considered in Figure 3.3. One has $\theta_1 = 0$, $\theta_2 = \frac{\pi}{2}$, $\theta_3 = \pi$, $\theta_2 = \frac{3\pi}{2}$ (called QDPSK) and another has $\theta_1 = \frac{\pi}{4}$, $\theta_2 = \frac{3\pi}{4}$, $\theta_3 = \frac{5\pi}{4}$, $\theta_4 = \frac{7\pi}{4}$. In contrast to the binary DPSK case, it is evident from Figure 3.3 that variations in signalling schemes for 4-ary DPSK have little impact on the system performance. In all these cases, we have assumed equal and symmetric decision regions. Thus we can conclude that the signaling schemes may affect the performance of SFH/DPSK under tone jamming and the choice of the best signaling scheme is dependent upon M.

Moreover, comparing Figure 3.1 with Figure 3.3, we can find that when E_b/N_o is

small, the performance of BDPSK is better than QDPSK, but worse when E_b/N_o is large. This is interesting because, in AGWN the performance of BDPSK is superior to QDPSK, which is in contrast to what is shown here, namely, when tone jamming is predominant, QDPSK is superior to BDPSK.

As mentioned early in this chapter, an intelligent jammer can inject one or several tones anywhere in each jammed band. We now investigate these strategies in details. First, the multitone effects are studied. For simplicity and clarity, we only consider the band multitone interference with at most two CW tones in each jammed band. Figure 3.4 demonstrates the worst case BER of SFH/MDPSK under band multitone interference. It is clear that single tone jamming[3] is always more effective against SFH/DPSK system employing BDPSK. However, the conclusion for QDPSK is quite different and multitone jamming is more effective at large E_b/N_J. Figure 3.5 presents BER performance as a function of jamming probability for BDPSK under band multitone interference, which examines the band multitone jamming from a different angle. It can be seen that single tone jamming curve cuts off much earlier than multitone. This suggest that at some large jamming probabilities, band multitone is more harmful.

After the above comparisons, we now consider the frequency jitter jamming strategy. First, we focus on the case with single tone in each jammed band. The variation of the performances due to the frequency offset between the signal carrier and tone interference is shown in Figure 3.6 and Figure 3.7 for binary DPSK and 4-ary DPSK with different signalling schemes, respectively. Since the average bit error rate is periodic with respect to the normalized frequency offset $\Delta\omega T_S$ with a period $2\pi/M$ for MDPSK (see Section 3.5.3 for detail), the results in those figures are given for one period. It is interesting to see from these two figures that for a given signalling scheme, the BER performance can be degraded drastically due to the frequency offset at some jamming probability ρ, while improved at other ρ. In addition, these figures suggest that some signalling schemes are

3. Here, the term of "single tone jamming" means that there is only one tone in each jammed band.

more robust than others with respect to the frequency offset. For example, the frequency offset does not degrade the performances of binary DPSK with $\theta_1 = \pi/2$ and 4-ary DPSK with $\theta_1 = \pi/4$, although slight degradation may occur at some ρ. Furthermore, they also suggest that the communicator can increase its number of hopping frequencies, i.e., decreasing the jammed probability ρ, to overcome the degradation caused by the frequency jitter. Comparing Figure 3.6 and Figure 3.7, we can observe that binary DPSK is more vulnerable to the frequency offset than 4-ary DPSK.

Binary DPSK		**4-ary DPSK**	
θ_1=0	θ_1=π/2	θ_1=0	θ_1=π/4
		(-1/2, 0)	
	(-1/2, 0)	(0, 1/2)	(-3/8, 1/8)
(-1/4, 1/4)	(0, -1/2)	(1/4, -1/4)	(1/8, -3/8)
(1/4, -1/4)	(1/2, 0)	(1/2, 0)	(3/8, -1/8)
	(0, 1/2)	(0, 1/2)	(-1/8, 3/8)
		(-1/4, 1/4)	

Table 3.1. The effective jamming frequency pair (E_b/N_J=10dB, ρ=0.01).

Finally, we consider the frequency jitter strategy for the band multitone jamming with two tones in each jammed band. Again, for simplicity, we ignore the background thermal noise and focus on the non-fading case. Figure 3.8 through Figure 3.11 illustrate the effects of frequency offsets between the signal carrier and tone interferences for binary and 4-ary DPSK with different signalling schemes. For clarity, the contours of BER performance are also given. From these figures, we can observe that it is always the least effective strategy for jammer to inject two tone in each jammed band at the same frequency. To maximize degradation, the best way is to put the tones at the frequencies which at least satisfy $\left|f_J^{(1)} - f_J^{(2)}\right| = \frac{1}{2T_s}$. For different signalling schemes, the most effective jamming frequency pairs are different. For example, Table 3.1 lists all effective jamming

frequency pairs at E_b/N_J=10dB and ρ=0.01[4].

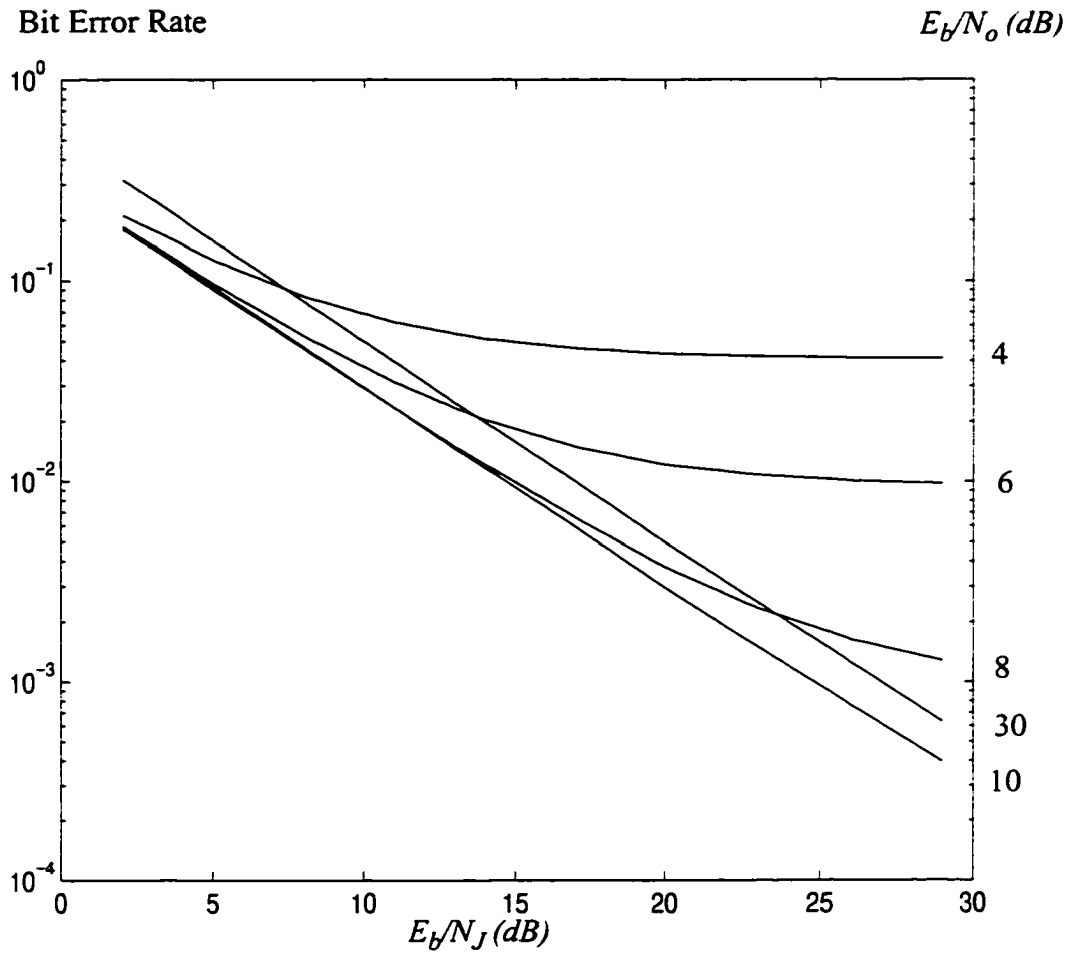

Figure 3.1 Worst case BER versus E_b/N_J for different E_b/N_o for binary DPSK with $\theta_1=0$ and $\theta_2=\pi$. Decision regions are equal and symmetric.

4. In Table 3.1, frequency is expressed in term of normalized carrier frequency offset between jammer and signal.

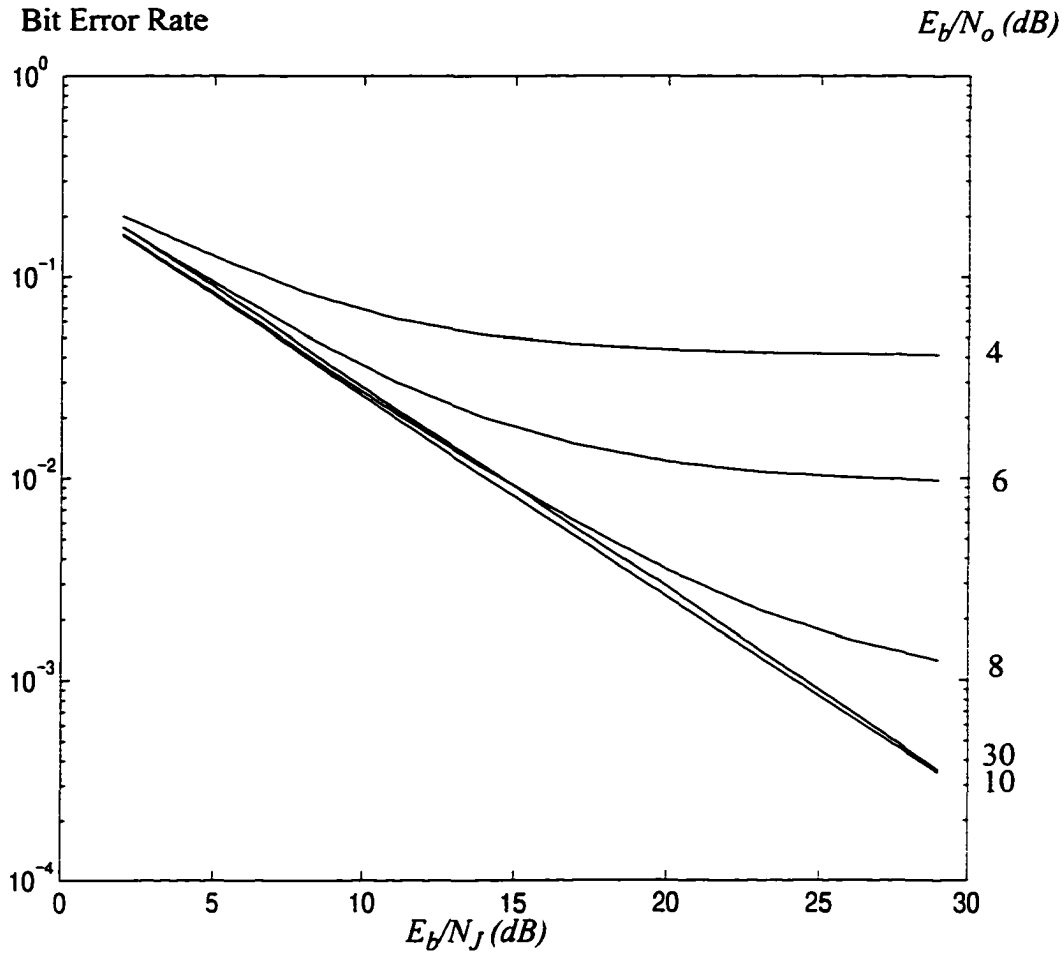

Figure 3.2 Worst case BER versus E_b/N_J for different E_b/N_o for binary DPSK with $\theta_1=\pi/2$ and $\theta_2=3\pi/2$. Decision regions are equal and symmetric.

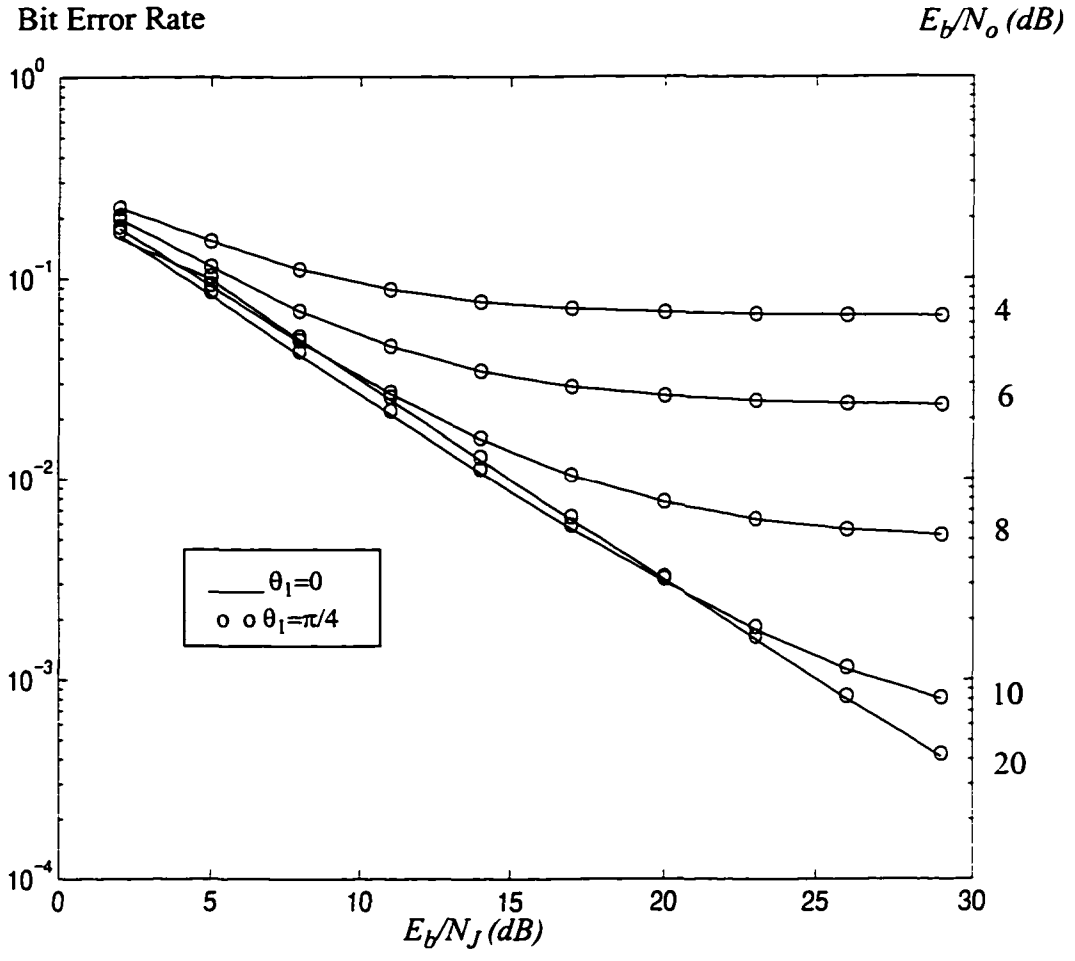

Figure 3.3 Worst case BER versus E_b/N_J for different E_b/N_o for 4-ary DPSK with different signalling schemes. Decision regions are equal and symmetric.

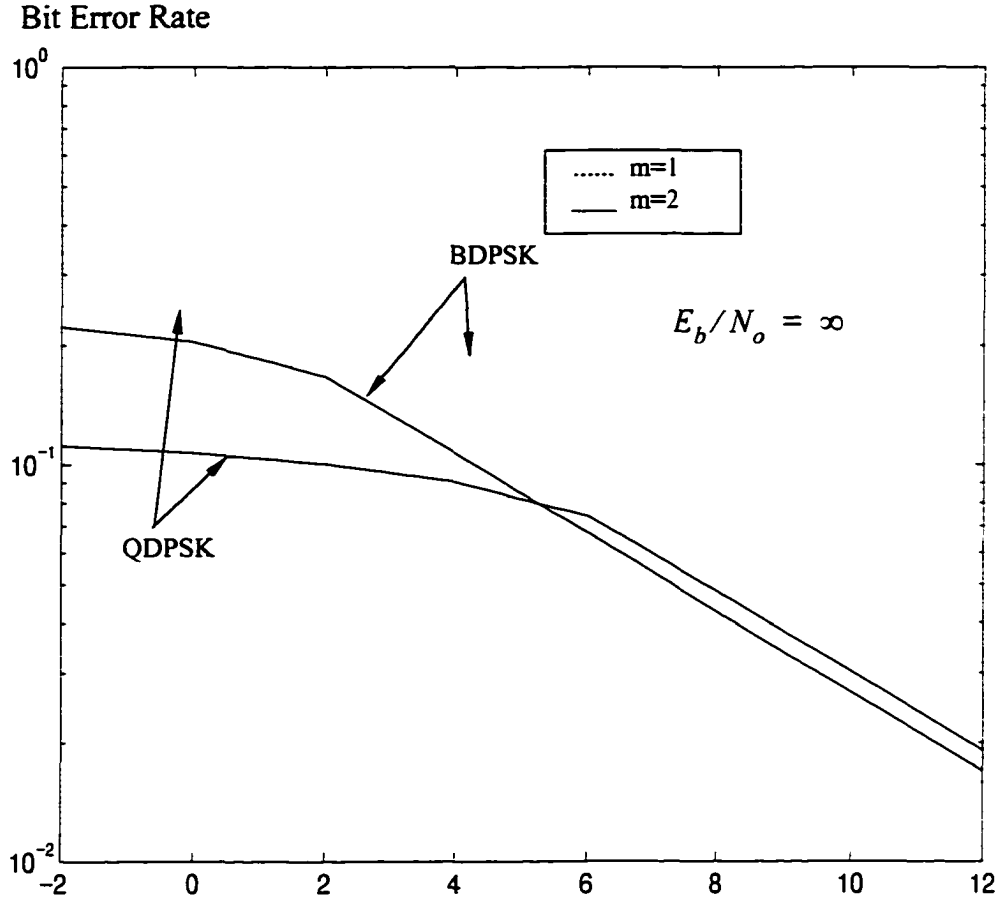

Figure 3.4 Worst case BER of SFH/MDPSK under band multitone jamming.

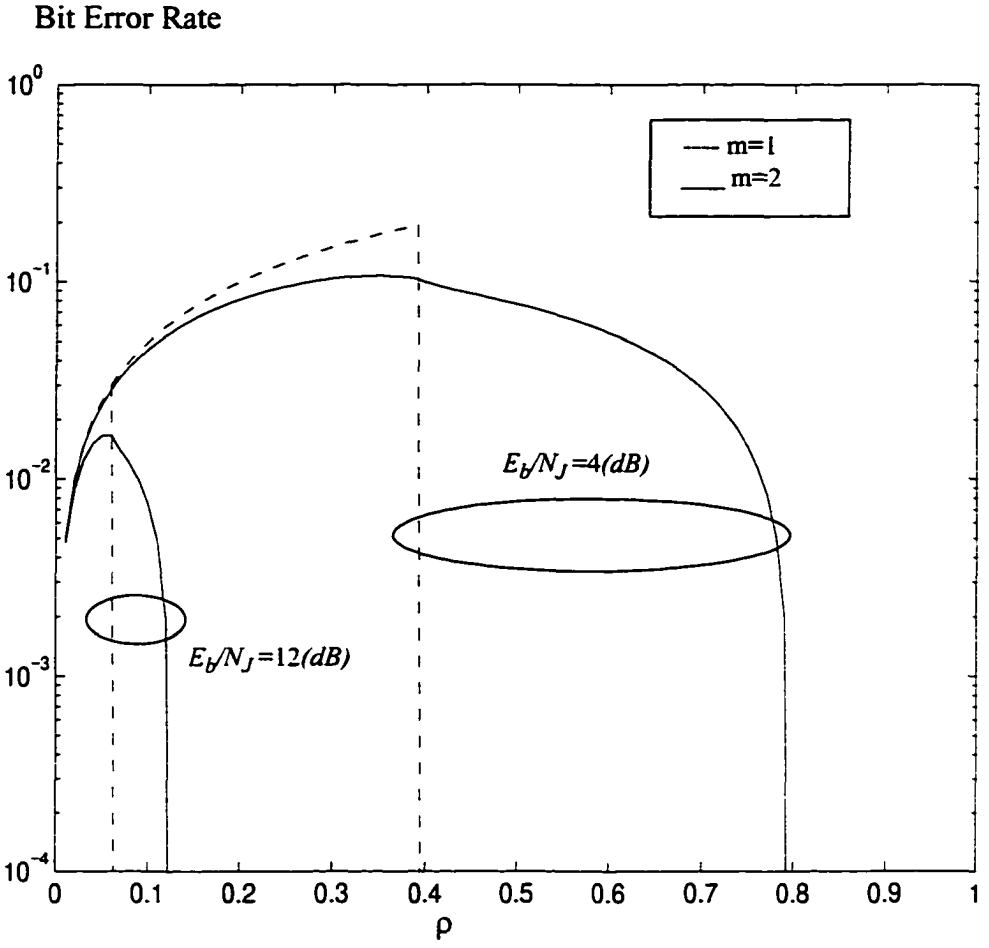

Figure 3.5 BER versus jamming probability for SFH/BDPSK under band multitone jamming.

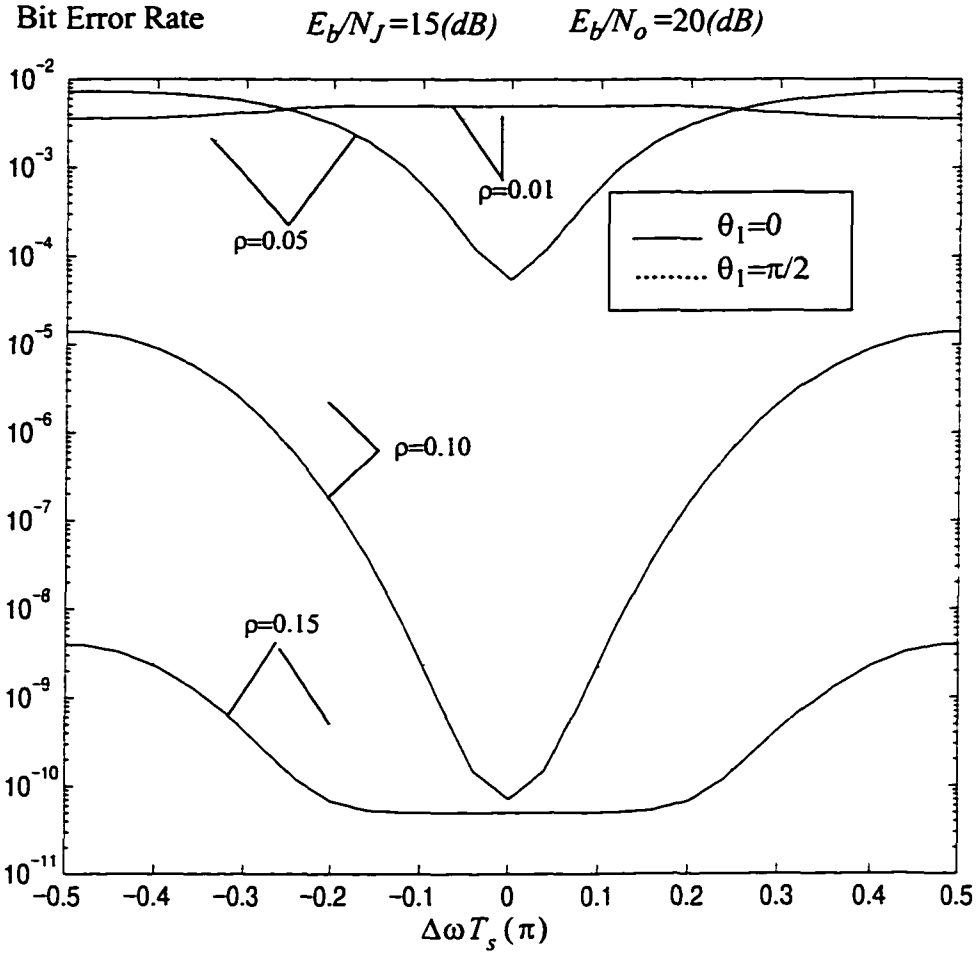

Figure 3.6 BER versus frequency offset for binary DPSK with different signalling schemes.

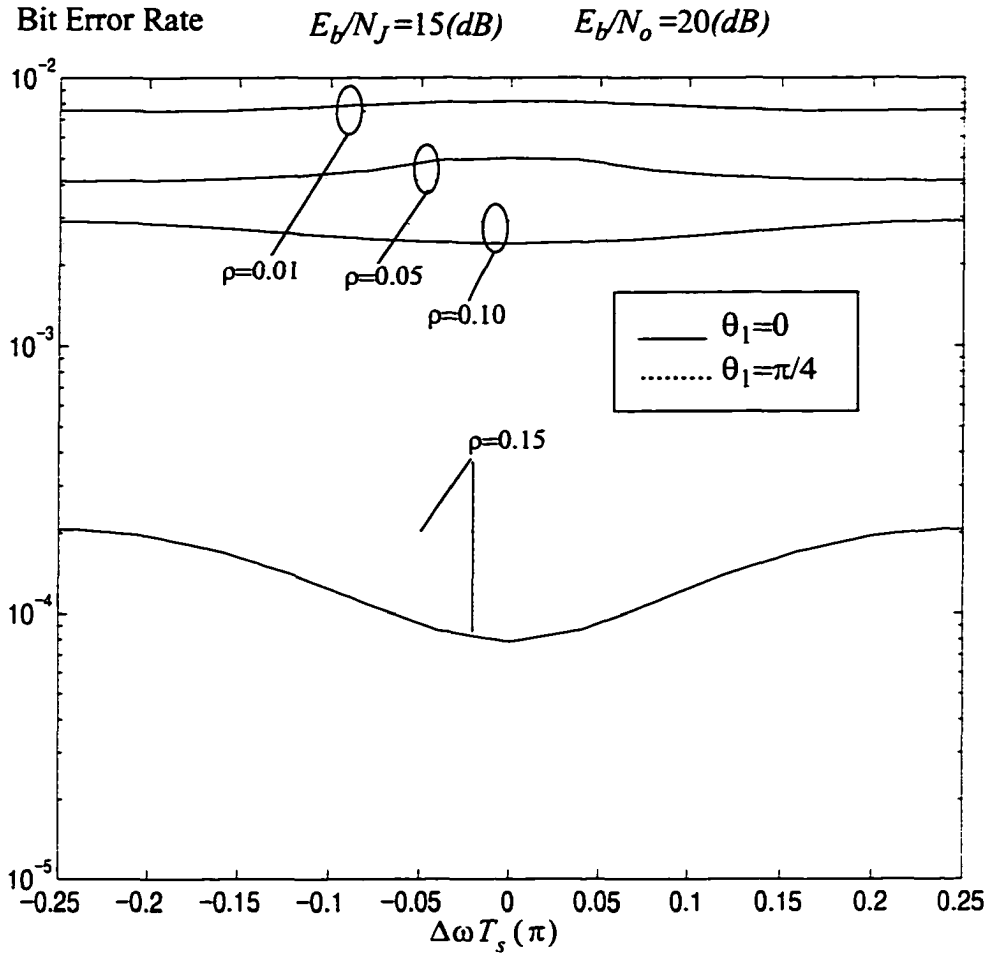

Figure 3.7 BER versus frequency offset for 4-ary DPSK with different signalling schemes.

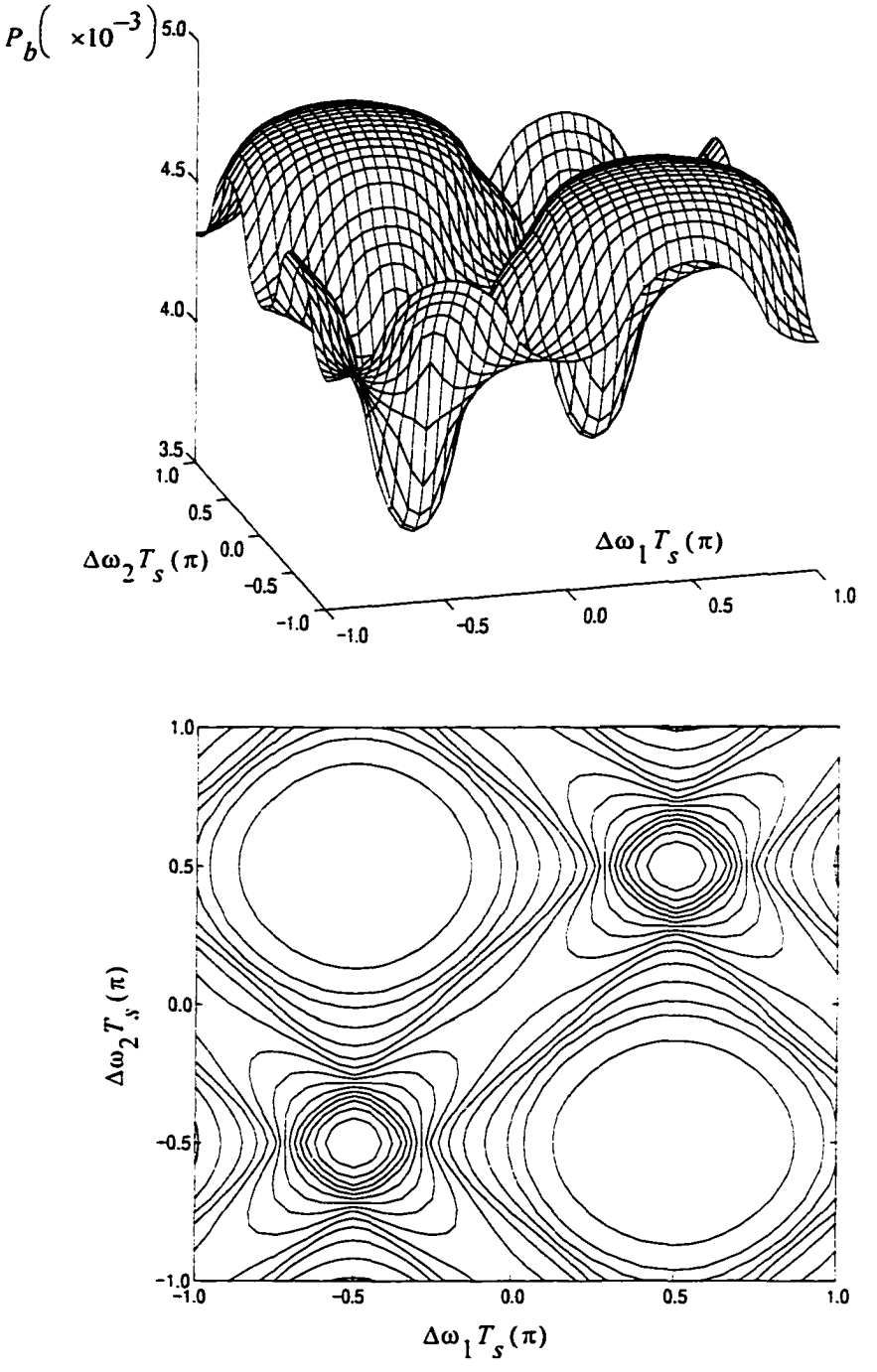

Figure 3.8 BER performance of BDPSK (with θ_1=0 and θ_2=π) against band multitone jamming. E_b/N_J=10dB and ρ=0.01.

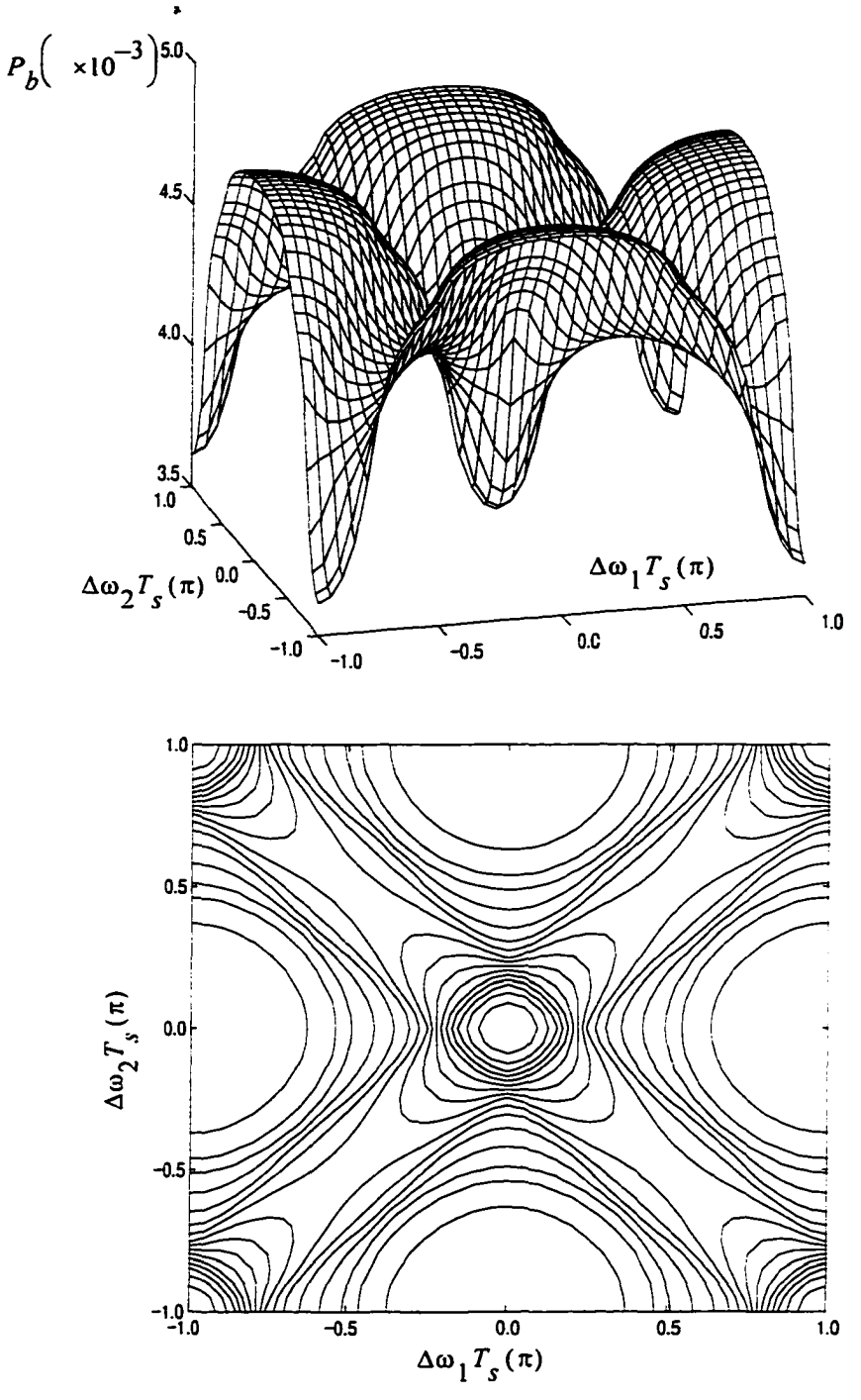

Figure 3.9 The effect of frequency jitters on BER performance of binary DPSK (with $\theta_1=\pi/2$ and $\theta_2=3\pi/2$) against band multitone jamming. E_b/N_J=10dB and ρ=0.01.

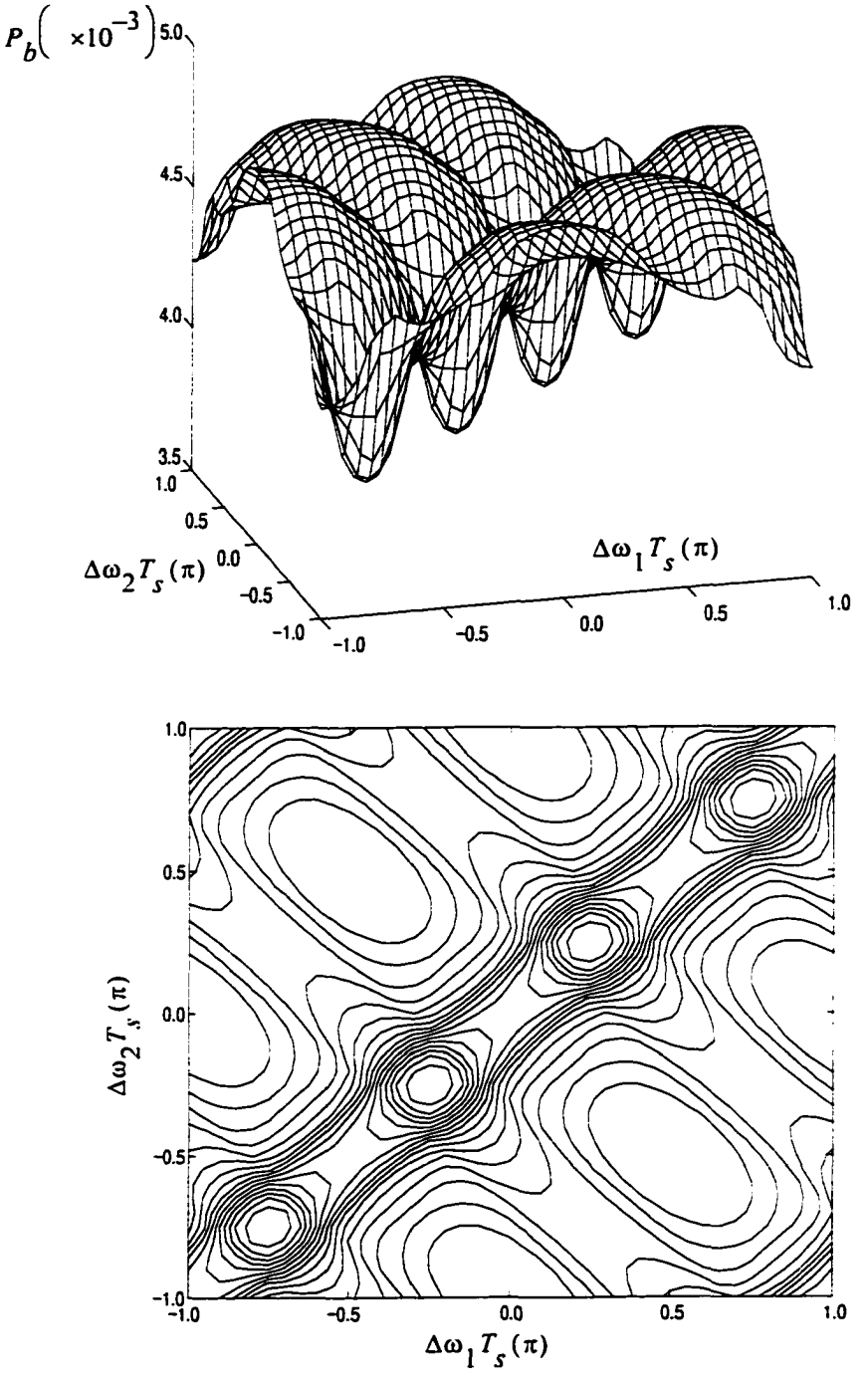

Figure 3.10 The effect of frequency jitters on BER performance of 4-ary DPSK (with $\theta_1=0$, $\theta_2=\pi/2$, $\theta_3=\pi$ and $\theta_4=3\pi/2$) against band multitone jamming. E_b/N_J=10dB and ρ=0.01.

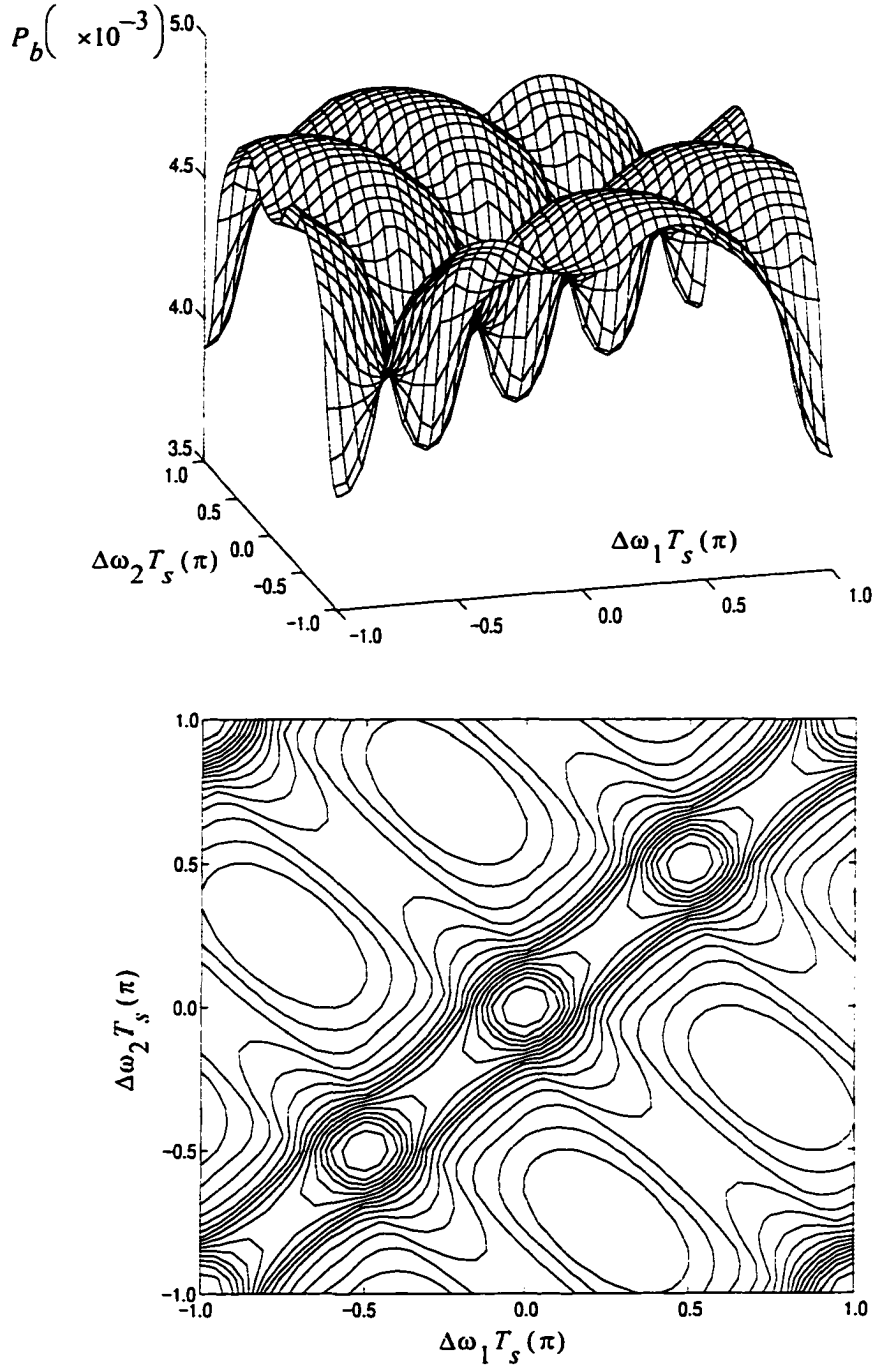

Figure 3.11 The effect of frequency jitters on BER performance of 4-ary DPSK (with $\theta_1=\pi/4$, $\theta_2=3\pi/4$, $\theta_3=5\pi/4$ and $\theta_4=7\pi/4$) against band multitone jamming. E_b/N_J=10dB and ρ=0.01.

3.4 Summary

A method for evaluation of error performance of DPSK under tone jamming and Gaussian noise has been presented in this chapter. A general and yet simple expression is given for the probability distribution of perturbed differential phase. It takes the previous results of Simon[11] and Pawula, Rice and Roberts[33] as special cases. Then we have analyzed the performance of SFH/DPSK under both tone jamming and system thermal noise for M-ary DPSK. Furthermore, the jamming strategies using band multitone and frequency jitter have also been investigated. The numerical results indicate that, without fading, a significant improvement can be gained through a proper signalling design for the systems where binary DPSK is employed. Moreover, the signalling design is also important for a system against jamming tone with a deliberate frequency offset. The numerical results also demonstrate that single tone jamming is the most harmful against SFH employing BDPSK but not necessarily so against that employing non-binary DPSK.

3.5 Detailed Derivations

3.5.1 Derivation of (3.16)

Considering Weber's second exponential integral, we have

$$\int_0^\infty e^{-p^2t^2/2} J_0(at) J_0(bt)\, t dt = \frac{1}{p^2} \exp\left(\frac{a^2+b^2}{2p^2} \right) I_0\left(\frac{ab}{p^2} \right), \tag{3.43}$$

where $J_0(x)$ is the *Bessel function* of the *first kind* of order zero.

Then we have

$$\int_0^\infty e^{-\lambda t^2} J_0(atv) J_0(bt)\, at dt = \frac{av}{p^2} \exp\left(\frac{a^2v^2+b^2}{2p^2} \right) I_0\left(\frac{abv}{p^2} \right). \tag{3.44}$$

Integrating both sides of (3.44) with respect to v over [0,1], and interchanging the order of integrations on the left-hand side, we have

$$\int_0^\infty e^{-p^2t^2/2} J_0(bt) J_1(at)\, dt = \int_0^1 \frac{av}{p^2} \exp\left(-\frac{a^2v^2+b^2}{2p^2}\right) I_0\left(\frac{abv}{p^2}\right) dv, \tag{3.45}$$

where we have made use of the following basic relation

$$\frac{J_1(x)}{x} = \int_0^1 v J_0(vx)\, dv. \tag{3.46}$$

Through the transformation $x = \frac{av}{p}$, (3.45) results in

$$\int_0^\infty e^{-p^2t^2/2} J_0(bt) J_1(at)\, dt = \frac{1}{a}\left[1 - \int_{\frac{a}{p}}^\infty x \exp\left(-\frac{x^2 + (b/p)^2}{2}\right) I_0\left(\frac{b}{p}x\right) dx\right]$$

$$= \frac{1}{a}\left[1 - Q\left(\frac{b}{p}, \frac{a}{p}\right)\right], \tag{3.47}$$

which is (3.16).

3.5.2 Calculation of (3.27)

In the derivation below, we follow the assumption $\Delta\omega\tau = 0$ as made in [11] in order to derive comparable results. For convenience, we denote variables $\Delta\Phi$, ψ_1 and ψ_2 as

$$\Delta\Phi = 2n\alpha;\ \psi_2 = (2n+1)\alpha;\ \psi_1 = (2n-1)\alpha, \text{ where } \alpha = \frac{\pi}{M}. \tag{3.48}$$

a). $\rho_J < 1$

Now we calculate $G(\psi_1)$.

Define

$$\kappa_1 = \frac{1-\rho_J}{\cos\alpha - \rho_J \cos(2n-1)\alpha}. \tag{3.49}$$

If

$$\sqrt{\rho_J} < \sqrt{\frac{1-\cos\alpha}{1-\cos(2n-1)\alpha}} = \frac{\sin n\alpha - \sin(n-1)\alpha}{\sin(2n-1)\alpha} = \beta_1, \tag{3.50}$$

then we have

$$\kappa_1 \geq 1. \tag{3.51}$$

Hence

$$\rho_J(1-\cos\theta\cos(2n-1)\alpha) < 1-\cos\theta\cos\alpha; \qquad \forall\theta \in \left[0, \frac{\pi}{2}\right]. \tag{3.52}$$

Then (3.25) becomes

$$G(\psi_1) = \frac{\psi_1}{2\pi} \frac{1}{2\pi}\int_0^{\frac{\pi}{2}} \frac{\sin\alpha}{1-\cos\theta\cos\alpha} d\theta$$

$$= \frac{\psi_1}{2\pi} - \frac{1}{2\pi} 2arctg\sqrt{\frac{1+\cos\alpha}{1-\cos\alpha}} = \frac{n\alpha}{\pi} - \frac{1}{2}. \tag{3.53}$$

If $\sqrt{\rho_J} > \beta_1$, then we have $\kappa_1 < 1$.

Define

$$\theta_0 = arc\cos\kappa_1. \tag{3.54}$$

Calculating (3.25),we have

$$G(\psi_1) = \frac{\psi_1}{2\pi} + \frac{1}{2\pi}\int_0^{\theta_0} \frac{\sin\psi_1}{1-\cos\theta cso\psi_1} d\theta + \frac{1}{2\pi}\int_{\theta_0}^{\frac{\pi}{2}} \frac{\sin(\psi_1-\Delta\Phi)}{1-\cos\theta\cos(\psi_1-\Delta\Phi)} d\theta$$

$$= \frac{n\alpha}{\pi} - \frac{1}{2} + \frac{1}{\pi}\left(arctg\sqrt{\frac{1+\cos(2n-1)\alpha}{1-\cos(2n-1)\alpha}\frac{1-\cos\theta_0}{1+\cos\theta_0}} + arctg\sqrt{\frac{1+\cos\alpha}{1-\cos\alpha}\frac{1-\cos\theta_0}{1+\cos\theta_0}} \right)$$

$$= \frac{n\alpha}{\pi} - \frac{1}{2} + \frac{1}{\pi} arc\cos\left[\frac{\sin\alpha - \rho_J\sin(2n-1)\alpha}{2\sqrt{\rho_J}\sin(n-1)\alpha} \right]. \tag{3.55}$$

Thus, from (3.50) through (3.55), $G(\psi_1)$ can be expressed as

$$G(\psi_1) = \frac{n\alpha}{\pi} - \frac{1}{2} + \frac{1}{\pi} arc\cos\left[\frac{\sin\alpha - \rho_J \sin(2n-1)\alpha}{2\sqrt{\rho_J}\sin(n-1)\alpha}\right] 1\left(\sqrt{\rho_J} - \beta_1\right), \tag{3.56}$$

where 1(.) is the unit-step function.

Similarly, we can get

$$G(\psi_2) = \frac{n\alpha}{\pi} + \frac{1}{2} - \frac{1}{\pi} arc\cos\left[\frac{\sin\alpha + \rho_J \sin(2n+1)\alpha}{2\sqrt{\rho_J}\sin(n+1)\alpha}\right] 1\left(\sqrt{\rho_J} - \beta_2\right). \tag{3.57}$$

Therefore

$$\begin{aligned} Q_{2n\alpha} &= 1 - G(\psi_2) + G(\psi_1) \\ &= \frac{1}{\pi} arc\cos\left[\frac{\sin\alpha + \rho_J \sin(2n+1)\alpha}{2\sqrt{\rho_J}\sin(n+1)\alpha}\right] 1\left(\sqrt{\rho_J} - \beta_2\right) + \\ &\quad \frac{1}{\pi} arc\cos\left[\frac{\sin\alpha - \rho_J \sin(2n-1)\alpha}{2\sqrt{\rho_J}\sin(n-1)\alpha}\right] 1\left(\sqrt{\rho_J} - \beta_1\right). \end{aligned} \tag{3.58}$$

b). If $\rho_J \geq 1$,

then we have

$$1 - \cos\theta\cos\alpha < \rho_J(1 - \cos\theta\cos\psi_i) \qquad \forall\theta \in \left[-\frac{\pi}{2}, \frac{\pi}{2}\right],$$

$$\begin{aligned} G(\psi_i) &= \frac{\psi_i}{2\pi} + \frac{1}{4\pi}\int_{-\frac{\pi}{2}}^{\frac{\pi}{2}} \frac{\sin\psi_i}{1 - \cos\theta\cos\psi_i} d\theta \\ &= \frac{\psi_i}{2\pi} + \frac{1}{2\pi}\left(2 arctg\sqrt{\frac{1+\cos\psi_i}{1-\cos\psi_i}}\right) = \frac{1}{2}. \end{aligned} \tag{3.59}$$

Thus

$$Q_{2n\alpha} = 1 \quad , \tag{3.60}$$

which is the same as the conclusion in [11].

3.5.3 Proof of the periodicity of BER with respect to $\Delta\omega T_s$

Clearly, to show that the average BER of MDPSK has a period of $2\pi/M$, we only need to show that the symbol error probability conditional on that a hop is jammed is periodic with respect to $\Delta\omega T_s$ with the period of $2\pi/M$, i.e.,$P_J\left(\Delta\omega T_S + 2\frac{\pi}{M}\right) = P_J(\Delta\omega T_S)$.

We start with the following conditional probability

$$P\{\psi_1^{(m)} \le \Psi \le \psi_2^{(m)} \left| \phi(t+\tau) - \phi(t) = \theta_m \right.\}.$$

Denote

$$f_m(\Delta\omega T_S) = P\{\psi_1^{(m)} \le \Psi \le \psi_2^{(m)} \left| \Delta\Phi = \theta_m \right.\} = G\left(\psi_2^{(m)}\right) - G\left(\psi_1^{(m)}\right). \quad (3.61)$$

For MDPSK, we suppose that the transmitted differential phases satisfy

$$\theta_{m+1} = \theta_m + \frac{2\pi}{M};\ 1 \le m < M; \quad (3.62)$$

$$\theta_1 = \theta_M + \frac{2\pi}{M} - 2\pi, \quad (3.63)$$

and the equal decision intervals are employed, i.e.,

$$\psi_i^{(m+1)} = \psi_i^{(m)} + \frac{2\pi}{M},\ 1 \le m < M, \quad (3.64)$$

$$\psi_i^{(1)} = \psi_i^{(M)} + \frac{2\pi}{M} - 2\pi;\ \text{i=1, 2.} \quad (3.65)$$

Thus, using (3.62) - (3.65) in (3.17), we can readily get

$$f_{(m+1)\,mod M}\left(\Delta\omega T_S + \frac{2\pi}{M}\right) = f_m(\Delta\omega T_S)\ ;\ 1 \le m \le M \quad (3.66)$$

When all symbols are transmitted equally likely, using (3.66) in (3.2) leads to the desired result.

Chapter 4

Performance of SFH/DPSK System in Fading Environments

4.1 Introduction

In general, wireless communication channels experience multipath fading due to reflection, diffraction and scattering phenomena in propagation of radio signals. Multipath fading can result in rapid variations in the envelope of the received signal. Typically, the received envelope can vary by as much as 30 to 40 dB over a fraction of a wavelength due to constructive and destructive addition. Multipath also causes time dispersion, because the multiple replicas of the transmitted signal propagate over different transmission paths and reach the receiver antenna with different time delays. In this chapter we consider the performance of SFH/DPSK system over such a randomly time-variant channel.

4.2 Characterization of Fading Multipath Channels

The statistical model for the fading of the received signal level is based on a physical propagation environment consisting of a large number of isolated scatters with unknown locations and reflection properties. Consider the transmission of the band-pass signal

$$s(t) = Re\{u(t)e^{j2\pi f_c t}\}, \tag{4.1}$$

where $u(t)$ is the complex low-pass signal with bandwidth W, f_c is the carrier frequency, and $\mathrm{Re}\{z\}$ denotes the real part of z. When there are multiple propagation paths, the

received band-pass signal, exclusive of additive noise, can be expressed in the form of [28][29]

$$x(t) = \sum_n \alpha_n(t)\, s[t-\tau_n(t)]\, e^{jf_{D,n}(t)\,(t-\tau_n(t))}, \tag{4.2}$$

where $\alpha_n(t)$, $\tau_n(t)$ and $f_{D,n}(t)$ are the attenuation factor, the propagation delay and the Doppler shift, respectively, associated with the *n*th path. The Doppler shift is caused by the mobility of either transmitter or receiver. Thus, the received complex low-pass signal *r(t)* can be written as

$$r(t) = \sum_n \alpha_n(t)\, e^{-j\phi_n(t)}\, u(t-\tau_n(t)) \tag{4.3}$$

where

$$\phi_n(t) = 2\pi\{(f_c + f_{D,n}(t))\,\tau_n(t) - f_{D,n}(t)\} \tag{4.4}$$

is the phase associated with *n*th path.

One of the important parameters to model the effect of the channel on the transmitted signal *u(t)* is the multipath delay spread defined as

$$T_m = max_n(\tau_n(t)) - min_n(\tau_n(t)), \tag{4.5}$$

which is related to the coherent bandwidth Δf_c of the channel, i.e.,

$$\Delta f_c \approx \frac{1}{T_m}. \tag{4.6}$$

When the signal bandwidth is much less than the coherent bandwidth of the channel ($W \ll \Delta f_c$), the channel is said to be *frequency-nonselective* in the sense that all of the frequency components in the transmitted signal undergo the same attenuation and phase shift while traversing through the channel. In this case, we have that $u(t-\tau_n(t)) \approx u(t-\tau_o)$ where $\tau_o \in [\min_n(\tau_n(t)), \max_n(\tau_n(t))]$ [28]. Then, we can rewrite (4.3) as follows.

$$r(t) \approx \left(\sum_n \alpha_n(t) e^{-j\phi_n(t)} \right) u(t-\tau_o) , \tag{4.7}$$

where the phase $\phi_n(t)$ modulo 2π can be modeled as i.i.d. random variables uniformly distributed over [0, 2π][44].

We can observe that, in addition to the time delay, the received signal in (4.7) differs from the original transmitted signal by the complex scale factor in the parentheses. For convenience, let

$$c(t) = \sum_n \alpha_n(t) e^{-j\phi_n(t)} = \alpha(t) e^{j\Theta(t)} . \tag{4.8}$$

It follows that the equivalent lowpass channel can be described by the time-variant impulse response as[41]

$$h(t;\tau) = \alpha(t) e^{j\Theta(t)} \delta(\tau-\tau_o) . \tag{4.9}$$

If we assume that $\alpha_n(t)$ are i.i.d and have bounded variance, then by central limit theorem, $c(t)$ will approach a complex Gaussian random variable as the number of scatters becomes large. In the absence of a line-of-sight (LOS) or specular component, $c(t)$ has zero-mean. Therefore, the received envelope $\alpha(t)$ has a Rayleigh distribution at any time, i.e.,

$$p(\alpha) = \frac{\alpha}{\sigma^2} \exp\left(-\frac{\alpha^2}{2\sigma^2} \right), \alpha \geq 0 \tag{4.10}$$

and $\Theta(t)$ is uniformly distributed over [0, 2π]. This type of fading is called Rayleigh fading and is often observed in macrocellular applications. For a Rayleigh distribution envelope, the average power denoted as Ω_p is

$$\Omega_p = E[\alpha^2(t)] = 2\sigma^2 . \tag{4.11}$$

For a multipath-fading channel containing a specular or LOS component, $c(t)$ has non-zero mean and the complex envelop has a Rician distribution at any time, i.e.,

$$p(\alpha) = \frac{\alpha}{\sigma^2}\exp\left(-\frac{\alpha^2+s^2}{2\sigma^2}\right)I_0\left(\frac{xs}{\sigma^2}\right), \tag{4.12}$$

where s^2 is the average power in the direct LOS and $I_0(.)$ is the modified Bessel function of the zeroth order. This type of fading is called Rician fading and is very often observed in microcellular applications. The Rician factor κ is defined as the ratio of the power in the specular and scattered components, i.e., $\kappa = s^2/2\sigma^2$, which reflects the relative depth of the fading and has been found to vary between 6 and 12 dB in value depending on the characteristics of the surroundings along the propagation path [39][40][37]. When $\kappa = 0$ the channel exhibits Rayleigh fading, and when $\kappa = \infty$ the channel does not exhibit fading. For a Rician distribution envelope, the average power denoted as Ω_p is

$$\Omega_p = E[z^2] = s^2 + 2\sigma^2. \tag{4.13}$$

Clearly, we have the following relations

$$s^2 = \frac{\kappa\Omega_p}{\kappa+1}, \; 2\sigma^2 = \frac{\Omega_p}{\kappa+1}. \tag{4.14}$$

Thus, a Rician distribution can be fully decided by its average power Ω_p and Rician factor κ.

As the signal bandwidth W increases so that $W \approx \Delta f_c$, the approximation $u(t-\tau_n(t)) \approx u(t-\tau_o)$ for $\tau_o \in [\min_n(\tau_n(t)), \max_n(\tau_n(t))]$ is no longer valid. Then, the received signal is sum of copies of the original signal, each is delayed in time by $\tau_n(t)$ and phase shifted by $\phi_n(t)$. For wideband signals (i.e., $W \gg \Delta f_c$), the channel becomes *frequency-selective* and its response can be approximated using Turin's model[32] if the incoming paths forms subpath clusters. In this model, paths that have approximately the same length ($|\tau_n(t) - \tau_i(t)| < W^{-1}$) are not resolvable at the receiver. Thus, they are combined into a single path. If we assume a finite number of resolvable paths, then the received signal can be written as

$$r(t) = \sum_{l=1}^{L} \alpha_l(t) e^{j\phi_l(t)} u(t-\tau_l) , \tag{4.15}$$

where L represents the number of resolvable paths or subpath clusters, and $\alpha_l(t)$, $\phi_l(t)$ and τ_l are the amplitude, phase and delay of each resolvable path. The complex gains $\alpha_l(t)\, e^{j\phi_l(t)}$ can be modeled as independent complex Gaussian processes. Again, the equivalent lowpass channel can be described by the time-variant impulse response[41]

$$h(t;\tau) = \sum_{l=1}^{L} \alpha_l(t) e^{j\phi_l(t)} \delta(t-\tau_l) , \tag{4.16}$$

which illustrates that the frequency-selective channel can be modeled as tapped delay line (transversal) filter with time-variant tap coefficients.

4.3 Performance Analysis in Frequency Non-selective fading Channel

We consider the situation where the signal and tone interference are subject to frequency non-selective fading. As illustrated in the section 4.2, over frequency non-selective fading channel, the faded signal is the product of a complex scale factor and the original signal perhaps delayed in time. Without loss of generality, we assume the time delay is zero. Then, when the tone interference is also considered, the received complex low-pass signal can be expressed as

$$r(t) = \alpha_s(t) A e^{j(\phi(t)+\Theta_s(t))} + \alpha_J(t) A_J e^{j(\Delta\omega t+\theta+\Theta_J(t))} + n(t) , \tag{4.17}$$

where $\Delta\omega$ is the difference between the carrier frequencies of the signal and tone interference, i.e., $\Delta\omega = \omega_J - \omega$. The first term in (4.17) represents the faded signal component, the second term models the faded component of the interfering tone, and *n(t)* is the background noise. $\alpha_s(t) e^{j\Theta_s(t)}$ and $\alpha_J(t) e^{j\Theta_J(t)}$ are the complex gains introduced by the

fading channel independently. We assume that fading is slow enough to be roughly constant over two successively received signal symbols used in DPSK decision. Thus, complex gains $\alpha_s(t)e^{j\Theta_s(t)}$ and $\alpha_J(t)e^{j\Theta_J(t)}$ are considered to be time-invariant in our analysis. As shown in Chapter 3, to evaluate the symbol error probability, it is necessary to calculate the following probability

$$P\{\psi_1 \le \arg(r(t+\tau)r^*(t)) \bmod 2\pi \le \psi_2\},$$

which can be expressed in terms of the auxiliary function $G(\psi_i)$ defined in Chapter 2. Therefore, similar to what was done in Chapter 3, we start from the calculation of G(ψ) for fading channel. When fading is considered, the *phase characteristic function* of r(t) and r(t+τ) can be expressed as

$$\Phi(u, v;\zeta) = E_{\alpha_s, \alpha_J}[\Phi(u, v;\zeta|\alpha_s, \alpha_J)],^1 \tag{4.18}$$

where $\Phi(u, v;\zeta|\alpha_s, \alpha_J)$ is the conditional *phase characteristic function* with fixed α_s and α_J. Therefore, the auxiliary function $G(\psi_i)$ can be calculated as

$$\begin{aligned} G(\psi_i) &= \frac{\psi_i}{2\pi} + \frac{1}{2\pi}\int_0^\infty\int_0^\infty \frac{\partial E_{\alpha_s, \alpha_J}[\Phi(-u, v;\zeta|\alpha_s, \alpha_J)]}{\partial\zeta}\bigg|_{\zeta=-\psi_i} \frac{1}{uv}dudv \\ &= \frac{\psi_i}{2\pi} + \frac{1}{2\pi}E_{\alpha_s, \alpha_J}\left(\int_0^\infty\int_0^\infty \frac{\partial\Phi(-u, v;\zeta|\alpha_s, \alpha_J)}{\partial\zeta}\bigg|_{\zeta=-\psi_i} \frac{1}{uv}dudv\right) \\ &= \iint G(\psi|\alpha_s, \alpha_J)p_s(\alpha_s)p_J(\alpha_J)\,d\alpha_s d\alpha_J, \end{aligned} \tag{4.19}$$

where $p_s(\alpha_s)$ and $p_J(\alpha_J)$ are the probability density functions of α_s and α_J, and the conditional auxiliary function $G(\psi|\alpha_s, \alpha_J)$, as illustrated in Chapter 3, can be calculated

1. Equation (4.18) can be easily verified by factorizing the *phase characteristic function*. Since the *phase characteristic functions* of the signal and tone interference components are not related to random variables Θ_s and Θ_J, the expectation is only taken with respect to α_s and α_J.

by

$$G(\psi|\alpha_s,\alpha_J) = \frac{\psi}{2\pi} - \frac{1}{4\pi}\int_{-\frac{\pi}{2}}^{\frac{\pi}{2}}\left(\frac{\sin(\Delta\Phi-\psi)}{\sqrt{T(\theta)}}q\left(\alpha_J\sqrt{\gamma_J S(\theta)},\alpha_s\sqrt{\gamma_N T(\theta)}\right)+\right.$$

$$\left.\frac{\sin(\Delta\omega\tau-\psi)}{S(\theta)}q\left(\alpha_s\sqrt{\gamma_N T(\theta)},\alpha_J\sqrt{\gamma_J S(\theta)}\right)\right)d\theta, \tag{4.20}$$

where γ_N, γ_J, $S(\theta)$ and $T(\theta)$ are defined in Chapter 3.

Because the signal and tone interference are independently faded and can each follow either Rayleigh or Rician distribution, we consider four different fading cases. We start from the case that the signal and interference tone are both Rician faded since the other cases can be viewed as its special cases from the mathematical viewpoint.

Case I. Both Rician faded

In this case, there exist LOS paths for both transmitted signal and tone interference. Thus, α_s and α_s are two independent random variables with Rician distribution defined in (4.12). As derived in Section 4.7, the following equation can be obtained for the Rician fading case,

$$\int_0^\infty\int_0^\infty Q(ax,by)\frac{x}{\sigma_1^2}\exp\left(\frac{x^2+s_1^2}{2\sigma_1^2}\right)I_0\left(\frac{s_1x}{\sigma_1^2}\right)\cdot\frac{y}{\sigma_2^2}\exp\left(\frac{y^2+s_2^2}{2\sigma_2^2}\right)I_0\left(\frac{s_2y}{\sigma_2^2}\right)dxdy$$

$$= \frac{1+a^2\sigma_1^2}{1+a^2\sigma_1^2+b^2\sigma_2^2}Q\left(\frac{as_1}{\sqrt{1+a^2\sigma_1^2+b^2\sigma_2^2}},\frac{bs_2}{\sqrt{1+a^2\sigma_1^2+b^2\sigma_2^2}}\right)+$$

$$\frac{b^2\sigma_2^2}{1+a^2\sigma_1^2+b^2\sigma_2^2}\left(1-Q\left(\frac{bs_2}{\sqrt{1+a^2\sigma_1^2+b^2\sigma_2^2}},\frac{as_1}{\sqrt{1+a^2\sigma_1^2+b^2\sigma_2^2}}\right)\right). \tag{4.21}$$

Define the average ratio of the transmitted signal and interference tone, respectively, to noise as

$$\bar{\gamma}_o = \frac{A^2}{\sigma_0^2} E\left(\alpha_s^2\right); \bar{\gamma}_J = \frac{A_J^2}{\sigma_0^2} E\left(\alpha_J^2\right), \tag{4.22}$$

where σ_0^2 is the variance of the background Gaussian noise, and A and A_J are the amplitude of the transmitted DPSK signal and interference tone respectively.

Therefore, given (4.21) and (4.20), (4.19) becomes

$$G(\psi) = \frac{\psi - \theta_0}{2\pi} - \frac{1}{4\pi}\int_{-\frac{\pi}{2}}^{\frac{\pi}{2}}$$

$$\left(C_1(\theta) q\left(\sqrt{\frac{2\kappa_J \bar{\gamma}_J S(\theta)/(\kappa_J+1)}{2 + \frac{\bar{\gamma}_J}{\kappa_J+1} S(\theta) + \frac{\bar{\gamma}_o}{\kappa_o+1} T(\theta)}}, \sqrt{\frac{2\kappa_o \bar{\gamma}_o T(\theta)/(\kappa_o+1)}{2 + \frac{\bar{\gamma}_J}{\kappa_J+1} S(\theta) + \frac{\bar{\gamma}_o}{\kappa_o+1} T(\theta)}} \right) + \right.$$

$$\left. C_2(\theta) q\left(\sqrt{\frac{2\kappa_o \bar{\gamma}_o T(\theta)/(\kappa_o+1)}{2 + \frac{\bar{\gamma}_J}{\kappa_J+1} S(\theta) + \frac{\bar{\gamma}_o}{\kappa_o+1} T(\theta)}}, \sqrt{\frac{2\kappa_J \bar{\gamma}_J S(\theta)/(\kappa_J+1)}{2 + \frac{\bar{\gamma}_J}{\kappa_J+1} S(\theta) + \frac{\bar{\gamma}_o}{\kappa_o+1} T(\theta)}} \right) \right) d\theta,$$

where κ_o and κ_J are the Rician factors for transmitted DPSK signal and interference tone components respectively, and $C_1(\theta)$, $C_2(\theta)$ and θ_0 can be calculated as follows:

$$C_1(\theta) = \frac{\bar{\gamma}_J [\sin(\Delta\Phi - \psi) - \sin(\Delta\omega\tau - \psi) - \sin(\Delta\Phi - \Delta\omega\tau)\cos\theta]}{T(\theta)\left[2(\kappa_J+1) + \bar{\gamma}_J S(\theta) + \bar{\gamma}_o T(\theta)(\kappa_J+1)/(\kappa_o+1)\right]}$$

$$+ \frac{2(\kappa_J+1)\sin(\Delta\Phi - \psi)}{T(\theta)\left[2(\kappa_J+1) + \bar{\gamma}_J S(\theta) + \bar{\gamma}_o T(\theta)(\kappa_J+1)/(\kappa_o+1)\right]}$$

$$C_2(\theta) = \frac{\bar{\gamma}_o [\sin(\Delta\omega\tau - \psi) - \sin(\Delta\Phi - \psi) + \sin(\Delta\Phi - \Delta\omega\tau)\cos\theta]}{S(\theta)\left[2(\kappa_o+1) + \bar{\gamma}_J S(\theta)(\kappa_o+1)/(\kappa_J+1) + \bar{\gamma}_o T(\theta)\right]}$$

$$+ \frac{2(\kappa_o+1)\sin(\Delta\omega\tau - \psi)}{S(\theta)\left[2(\kappa_o+1) + \bar{\gamma}_J S(\theta)(\kappa_o+1)/(\kappa_J+1) + \bar{\gamma}_o T(\theta)\right]}$$

and

$$\theta_0 = 2\frac{\bar{\gamma}_o \sin(\Delta\Phi-\psi)/(\kappa_o+1) + \bar{\gamma}_J \sin(\Delta\omega\tau-\psi)/(\kappa_J+1)}{\sqrt{\left(2+\frac{\bar{\gamma}_o}{\kappa_o+1}+\frac{\bar{\gamma}_J}{\kappa_J+1}\right)^2 - \left[\frac{\bar{\gamma}_J}{\kappa_J+1}\cos(\Delta\omega\tau-\psi)+\frac{\bar{\gamma}_o}{\kappa_o+1}\cos(\Delta\Phi-\psi)\right]^2}}$$

$$\times arctg\left(\sqrt{\frac{1+\frac{\bar{\gamma}_o}{\kappa_o+1}\cos^2\left(\frac{\Delta\Phi-\psi}{2}\right)+\frac{\bar{\gamma}_J}{\kappa_J+1}\cos^2\left(\frac{\Delta\omega\tau-\psi}{2}\right)}{1+\frac{\bar{\gamma}_o}{\kappa_o+1}\sin^2\left(\frac{\Delta\Phi-\psi}{2}\right)+\frac{\bar{\gamma}_J}{\kappa_J+1}\sin^2\left(\frac{\Delta\omega\tau-\psi}{2}\right)}}\right). \qquad (4.23)$$

Case II. Both Rayleigh faded

In this case, there is no LOS path for either transmitted signal or tone interference. Thus, α_s and α_s are two independent random variables with Rayleigh distribution defined in (4.10). Let $\kappa_o = \kappa_J = 0$ in equation (4.23). Consequently, we can get the auxiliary function $G(\psi)$ for this case as

$$G(\psi) = \frac{\psi}{2\pi} - \frac{\bar{\gamma}_o \sin(\Delta\Phi-\psi)+\bar{\gamma}_J \sin(\Delta\omega\tau-\psi)}{\pi\sqrt{U^2-V^2}} arctg\left(\sqrt{\frac{U+V}{U-V}}\right) \qquad (4.24)$$

where $U = 2+\bar{\gamma}_o+\bar{\gamma}_J$ and $V = \bar{\gamma}_o\cos(\Delta\Phi-\psi)+\bar{\gamma}_J\cos(\Delta\omega\tau-\psi)$.

Case III. Differently faded

First we consider there is LOS path only for the transmitted signal, i.e., the transmitted DPSK signal is Rician faded and the interference tone is Rayleigh faded.

Let $\kappa_J = 0$ in (4.23), we can get the expression for $G(\psi)$ as

$$G(\psi) = \frac{\psi-\theta_0}{2\pi} - \frac{1}{4\pi}\int_{-\frac{\pi}{2}}^{\frac{\pi}{2}} \exp\left(\frac{-\kappa_o\bar{\gamma}_o T(\theta)/(\kappa_o+1)}{2+\bar{\gamma}_J S(\theta)+\bar{\gamma}_o T(\theta)/(\kappa_o+1)}\right)\times$$

$$\frac{\bar{\gamma}_J[\sin(\Delta\Phi-\psi)-\sin(\Delta\omega\tau-\psi)-\sin(\Delta\Phi-\Delta\omega\tau)\cos\theta]+2\sin(\Delta\Phi-\psi)}{T(\theta)\left[2+\bar{\gamma}_J S(\theta)+\bar{\gamma}_o T(\theta)/(\kappa_o+1)\right]}d\theta,$$

where θ_0 can be calculated as

$$\theta_0 = 2\frac{\bar{\gamma}_o\sin(\Delta\Phi-\psi)/(\kappa_o+1)+\bar{\gamma}_J\sin(\Delta\omega\tau-\psi)}{\sqrt{\left(2+\frac{\bar{\gamma}_o}{\kappa_o+1}+\bar{\gamma}_J\right)^2-\left[\bar{\gamma}_J\cos(\Delta\omega\tau-\psi)+\frac{\bar{\gamma}_o}{\kappa_o+1}\cos(\Delta\Phi-\psi)\right]^2}}$$

$$\times arctg\left(\sqrt{\frac{1+\bar{\gamma}_o\cos^2\left(\frac{\Delta\Phi-\psi}{2}\right)/(\kappa_o+1)+\bar{\gamma}_J\cos^2\left(\frac{\Delta\omega\tau-\psi}{2}\right)}{1+\bar{\gamma}_o\sin^2\left(\frac{\Delta\Phi-\psi}{2}\right)/(\kappa_o+1)+\bar{\gamma}_J\sin^2\left(\frac{\Delta\omega\tau-\psi}{2}\right)}}\right). \quad (4.25)$$

For the case where transmitted DPSK signal is Rayleigh faded and the interference tone is Rician faded, a similar expression for $G(\psi)$ can be obtained from (4.25) by interchanging the subscript "o" and $\Delta\Phi$ with subscript "J" and $\Delta\omega$, respectively.

4.4 Performance Analysis in Frequency Selective fading Channel

In the presence of frequency selective fading, as demonstrated in Section 4.2, the channels can be modeled as a tapped delay line (transversal) filter. We assume the channel for the transmitted DPSK signal has impulse response as

$$h(t;\tau) = \sum_{l=0}^{L-1}\alpha_l e^{j\Theta_l}\delta(t-\tau_l), \quad (4.26)$$

where the time delays are assumed to be integer multiple of the symbol period of the signal. Without loss of generality, we assume that the time delay for the zeroth path is zero, i.e., $\tau_0 = 0$. Thus the received complex low-pass signal can be expressed as [2]

$$r(t) = \alpha_0 A e^{j(\phi(t)+\Theta_0)} + \sum_{l=1}^{L-1} \alpha_l A e^{j(\phi(t)+\Theta_l)} + \alpha_J(t) A_J e^{j(\Delta\omega t+\theta+\Theta_J(t))} + n(t), \tag{4.27}$$

where the first term represents the faded signal component, the second term is so called inter-symbol interference(ISI) caused by multipath, the third term models the faded component of the interfering tone and *n(t)* is the background noise. We assume that $\alpha_l; l=0, 2,\ldots, L-1$ and α_J are independently Rayleigh distributed.

Noting *Hankel Exponential integral*, i.e.,

$$\int_0^\infty t\exp\left(-p^2t^2/2\right)J_0(at)\,dt = \frac{1}{p^2}\exp\left(\frac{-a^2}{2p^2}\right) \tag{4.28}$$

then, we can express the *phase characteristic function* of $r(t)$ and $r(t+\tau)$ as

$$\Phi(u, v;\zeta) = E\left[\prod_{l=0}^{L} J_0\left(\alpha_l A\sqrt{u^2+v^2+2uv\cos(\Delta\Phi_l+\zeta)}\right)\right.$$

$$\left. J_0\left(\alpha_J A_J\sqrt{u^2+v^2+2uv\cos(\Delta\omega\tau+\zeta)}\right)e^{-\sigma_0^2\left(u^2+v^2\right)/2}\right]$$

$$= \exp\left(\frac{A^2}{4}\sum_{l=0}^{L}\Omega_l\left(u^2+v^2+2uv\cos(\Delta\Phi_l+\zeta)\right)\right)\times$$

$$\exp\left(\frac{A_J^2\Omega_J}{4}\left(u^2+v^2+2uv\cos(\Delta\omega\tau+\zeta)\right)\right)\exp\left(\frac{-\sigma_0^2\left(u^2+v^2\right)}{2}\right) \tag{4.29}$$

where $\Delta\Phi_l = \phi(t+\tau-\tau_l)-\phi(t-\tau_l)$, and $\Omega_l; l=0, 2,\ldots, L-1$ and Ω_J are the average power of $\alpha_l; l=0, 2,\ldots, L-1$ and α_J respectively.

Therefore, the auxiliary function $G(\psi_i)$ can be calculated as

---

2. Here, the channel for tone interference is modeled as frequency non-selective fading channel. This is because that the bandwidth of tone interference is zero.

$$G(\psi_i) = \frac{\psi_i}{2\pi} + \frac{1}{2\pi}\int_0^\infty\int_0^\infty \frac{\partial\Phi(-u, v, \zeta)}{\partial\zeta}\bigg|_{\zeta=-\psi_i} \frac{1}{uv}dudv$$

$$= \frac{\psi_i}{2\pi} - \frac{1}{4\pi}\int_0^\infty\int_0^\infty \left(\exp\left(-\frac{A^2}{4}\sum_{l=0}^{L}\Omega_l\left(u^2+v^2-2uv\cos(\Delta\Phi_l-\psi_i)\right)\right)\right) \times$$

$$\exp\left(-\frac{A_J^2\Omega_J}{4}\left(u^2+v^2-2uv\cos(\Delta\omega\tau-\psi_i)\right)\right)\exp\left(\frac{-\sigma_0^2\left(u^2+v^2\right)}{2}\right)\times$$

$$\left(\sum_{n=0}^{L-1} A^2\Omega_n\sin(\Delta\Phi_n-\psi_i) + A_J^2\Omega_J\sin(\Delta\omega\tau-\psi_i)\right)\Bigg]dudv \qquad (4.30)$$

Similarly, making a transformation to polar coordinates by means of

$$u = \frac{R}{\sigma_0}\cos\frac{\theta'}{2} \qquad v = \frac{R}{\sigma_0}\sin\frac{\theta'}{2} \qquad (4.31)$$

and then making the change $\theta' = \frac{\pi}{2} - \theta$, we can express the auxiliary function $G(\psi)$ as

$$G(\psi_i) = \frac{\psi_i}{2\pi} -$$

$$\frac{1}{4\pi}\int_{-\frac{\pi}{2}}^{\frac{\pi}{2}} \frac{\sum_{n=0}^{L-1}\bar{\gamma}_n\sin(\Delta\Phi_n-\psi_i) + \bar{\gamma}_J\sin(\Delta\omega\tau-\psi_i)}{2+\sum_{l=0}^{L-1}\bar{\gamma}_l(1-\cos\theta\cos(\Delta\Phi_l-\psi_i)) + \bar{\gamma}_J(1-\cos\theta\cos(\Delta\omega\tau-\psi_i))}d\theta$$

$$= \frac{\psi_i}{2\pi} - \frac{\sum_{n=0}^{L-1}\bar{\gamma}_n\sin(\Delta\Phi_n-\psi_i) + \bar{\gamma}_J\sin(\Delta\omega\tau-\psi_i)}{\pi\sqrt{U^2-V^2}}arctg\left(\sqrt{\frac{U+V}{U-V}}\right), \qquad (4.32)$$

where U and V are defined as

$$U = 2 + \sum_{l=0}^{L-1} \bar{\gamma}_l + \gamma_J,\ V = \sum_{l=0}^{L-1} \bar{\gamma}_l \cos(\Delta\Phi_l - \psi_i) + \bar{\gamma}_J \cos(\Delta\omega\tau - \psi_i)\ .$$

and $\bar{\gamma}_l$; l=0, 2,..., L-1 and $\bar{\gamma}_J$ are defined as the average signal-to-noise ratios and average interference-to-noise ratio, respectively. Clearly, when L=1, (4.32) leads to the result for frequency non-selective Rayleigh fading channel, i.e., (4.24).

Based on the above results, the symbol error probability can be obtained given $\Delta\Phi_i$; i=1, 2,..., L-1. Denote this conditional probability as $P_s(e|\Delta\Phi_1, \Delta\Phi_2, ..., \Delta\Phi_{L-1})$. Then, the average symbol error probability can be calculated as

$$P_s = \frac{1}{M^{L-1}} \sum_{\Delta\Phi_1, \ldots \Delta\Phi_{L-1}} P_s(e|\Delta\Phi_1, \ldots \Delta\Phi_{L-1})\ , \tag{4.33}$$

where we assume M symbols of MDPSK are equally likely transmitted every time.

4.5 Numerical Results

In this section, numerical results are presented for SFH/DPSK in fading and tone interference based on the above analyses. Since the system under study involves a number of parameters such as E_b/N_o, E_b/N_J, κ_0 and κ_J, only selected results are given to offer key insight. The ranges of these parameters are chosen so as to illustrate in a general way, their influence on system performance. No attempt is made to provide an exhaustive study of all possible combinations of values. Similar to what was done in Chapter 3, binary DPSK and 4-ary are investigated in combination with two signalling schemes.

Figure 4.1-Figure 4.4 plot the BER performances of binary and 4-ary DPSK over frequency non-selective fading channels. These performances are measured by the worst case BER for given E_b/N_J and E_b/N_o. When the transmitted signal and the tone interference are both Rician faded, we assume the signal and the tone are subject to the same depth of fading, i.e., they have the same Rician factors. The following conclusions can be drawn from these figures. First, binary DPSK is always superior to 4-ary DPSK regardless of E_b/N_o, and the difference becomes most significant when the transmitted

signal is subject to Rician fading and the tone interference is subject to Rayleigh fading. This conclusion is quite different from that drawn on non-fading channel, where the performance of BDPSK are better only for small E_b/N_o. Second, the signalling schemes almost have no effect on the performance of either binary or 4-ary DPSK. In the non-fading case, different signalling schemes result in a performance difference of $2.4dB$ in E_b/N_J at BER of 10^{-3} and $E_b/N_o = 28dB$ for binary DPSK and none for 4-ary DPSK. Third, Rayleigh fading is the worst fading case for signals. Comparing Figure 4.1 with Figure 4.4 shows that when the transmitted signal is Rayleigh faded, fading on the tone interference has little effect on performance. This result was found to be true for values of κ_J as high as 20 dB. On the contrary, when the transmitted signal is Rician faded, the performance is largely decided by the fading on the tone interference. This observation can be readily made from Figure 4.2 and Figure 4.3.

Figure 4.5 and Figure 4.6 plot the effect of the frequency offset when the transmitted signal and interference are both Rayleigh faded and both Rician faded, respectively. In Figure 4.6, the results are shown for different depth of fading κ. From these figures, we observe that, when the signal channel approaches Rayleigh fading channel, the effect of the jamming frequency offset on the BER performance diminishes. When the signal is Rician faded, whether the frequency offset degrades or improves the BER performance depends on ρ and the fading depth (see curves for ρ=0.05 in Figure 4.6).

The BER performances of binary and 4-ary DPSK over frequency selective fading channels is shown in Figure 4.7. In our computation, we choose the number of the resolvable paths to be 2 and the relative path strengths to be (0, -10dB) for simplicity. From this figure, it can be clearly seen that binary DPSK is superior to 4-ary DPSK. Furthermore, Figure 4.7 shows much higher error floors for the bit error probability than the corresponding ones in frequency non-selective fading channels. These floors are caused by the large value of the bit error probability when the hop is free of jamming. Frequency selective fading channels result in inter-symbol interference which can drastically degrade the BER performance. The effect of the frequency offset in frequency selective fading channel is shown in Figure 4.8. Same as what was observed for frequency non-

selective fading case, the frequency offset has very little effect on the BER performance.

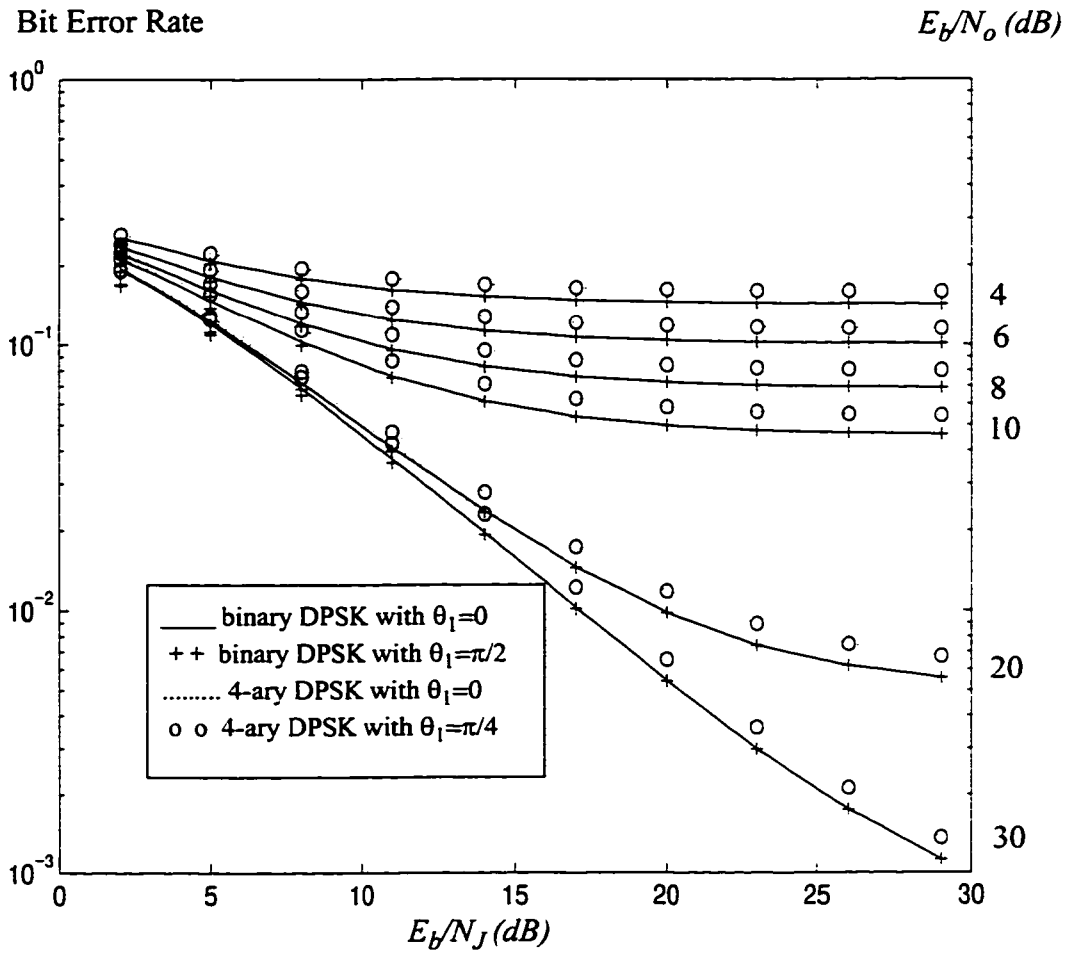

Figure 4.1 Worst case BER versus E_b/N_J for different E_b/N_o for binary DPSK and 4-ary DPSK in frequency non-selective fading (both signal and interference are Rayleigh faded).

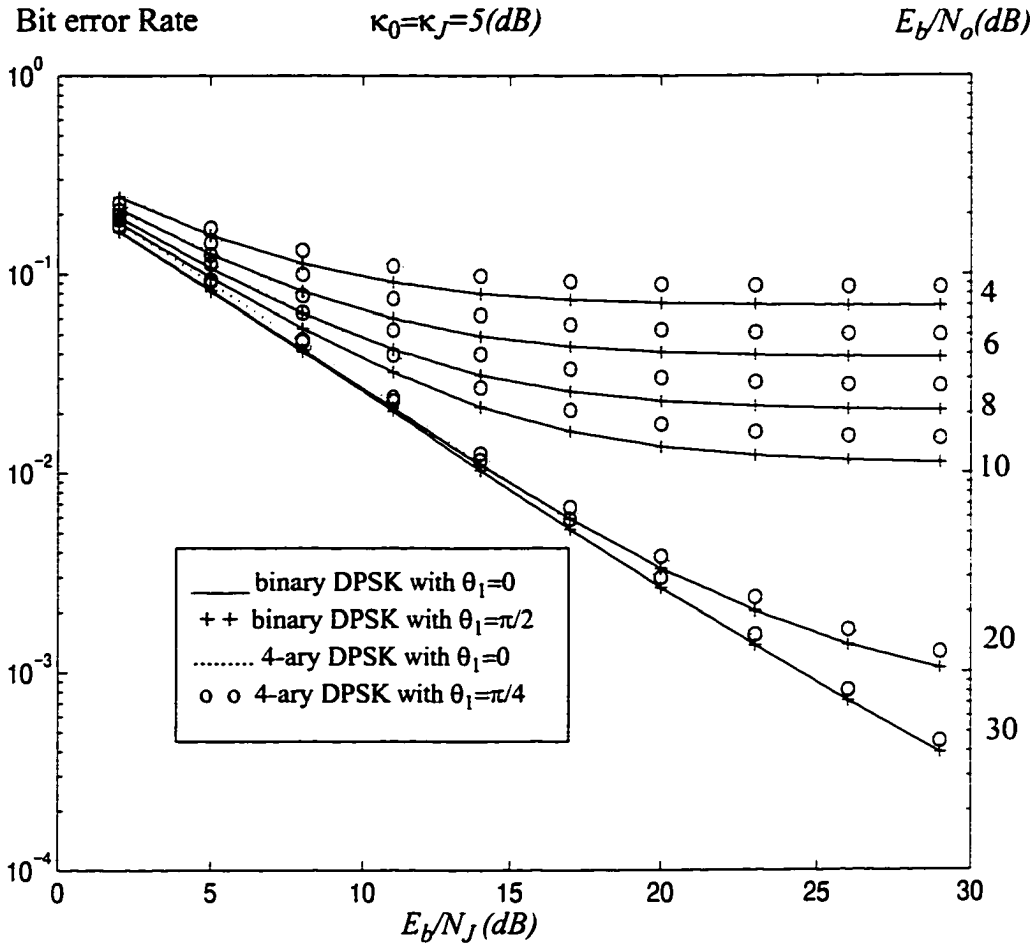

Figure 4.2 Worst case BER versus E_b/N_J for different E_b/N_o for binary DPS and 4-ary DPSK in frequency non-selective fading (both signal and interference are Rician faded).

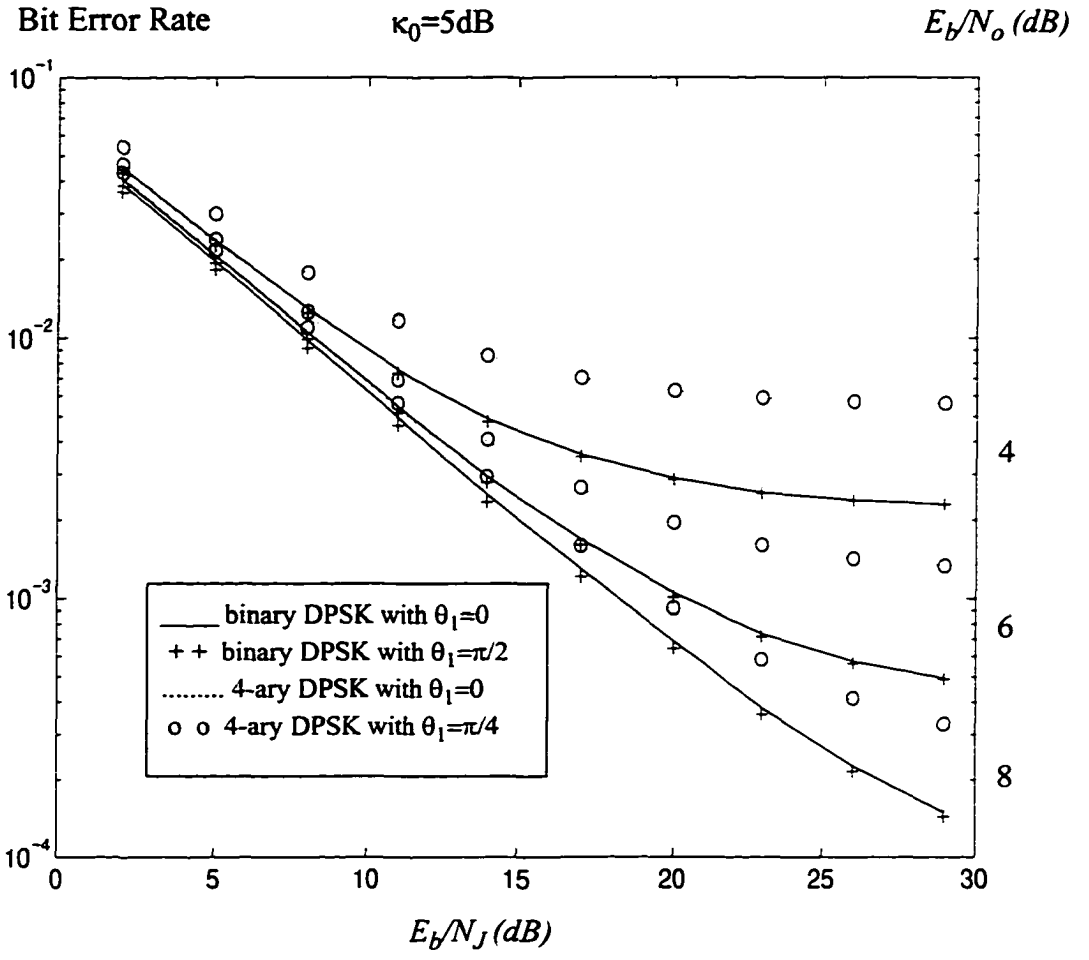

Figure 4.3 Worst case BER versus E_b/N_J for different E_b/N_o for binary DPS and 4-ary DPSK in frequency non-selective fading (with Rician faded signal and Rayleigh faded tone interference).

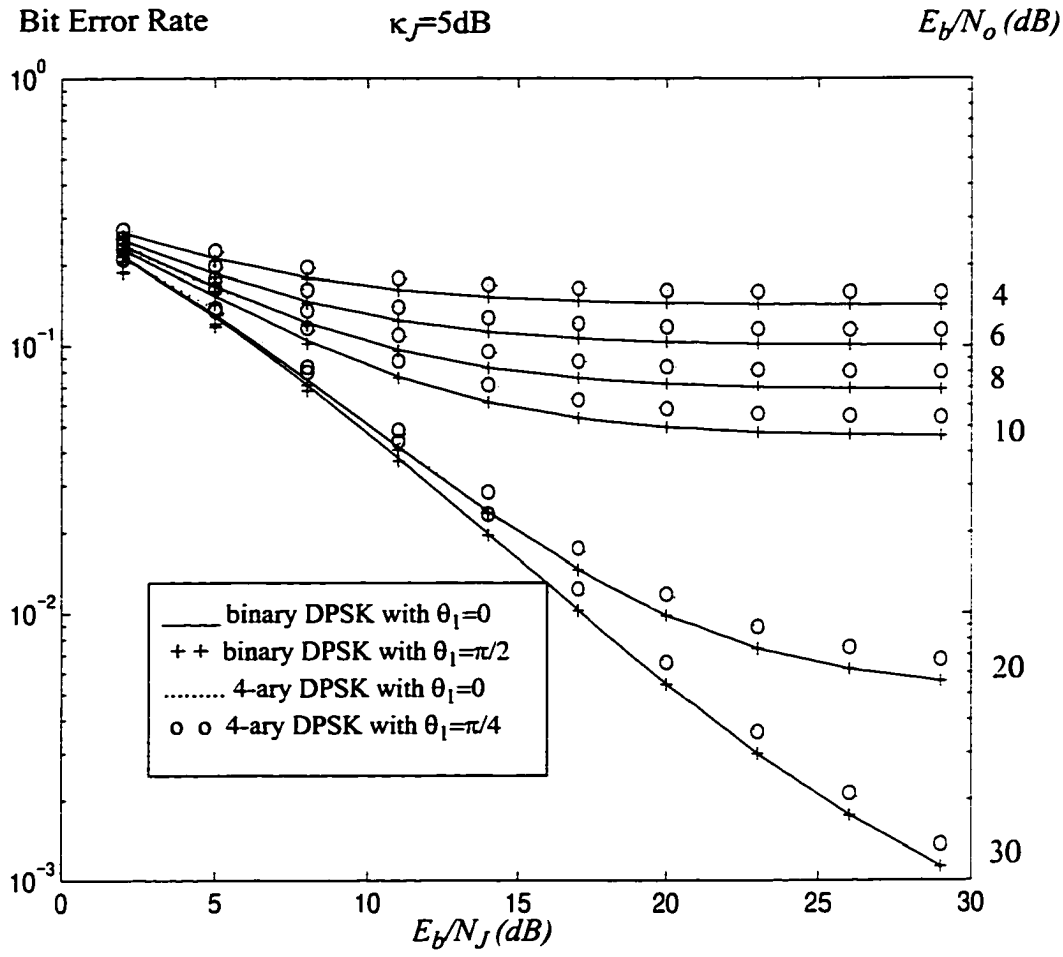

Figure 4.4 Worst case BER versus E_b/N_J for different E_b/N_o for binary DPS and 4-ary DPSK in frequency non-selective fading (with Rayleigh faded signal and Rician faded tone interference).

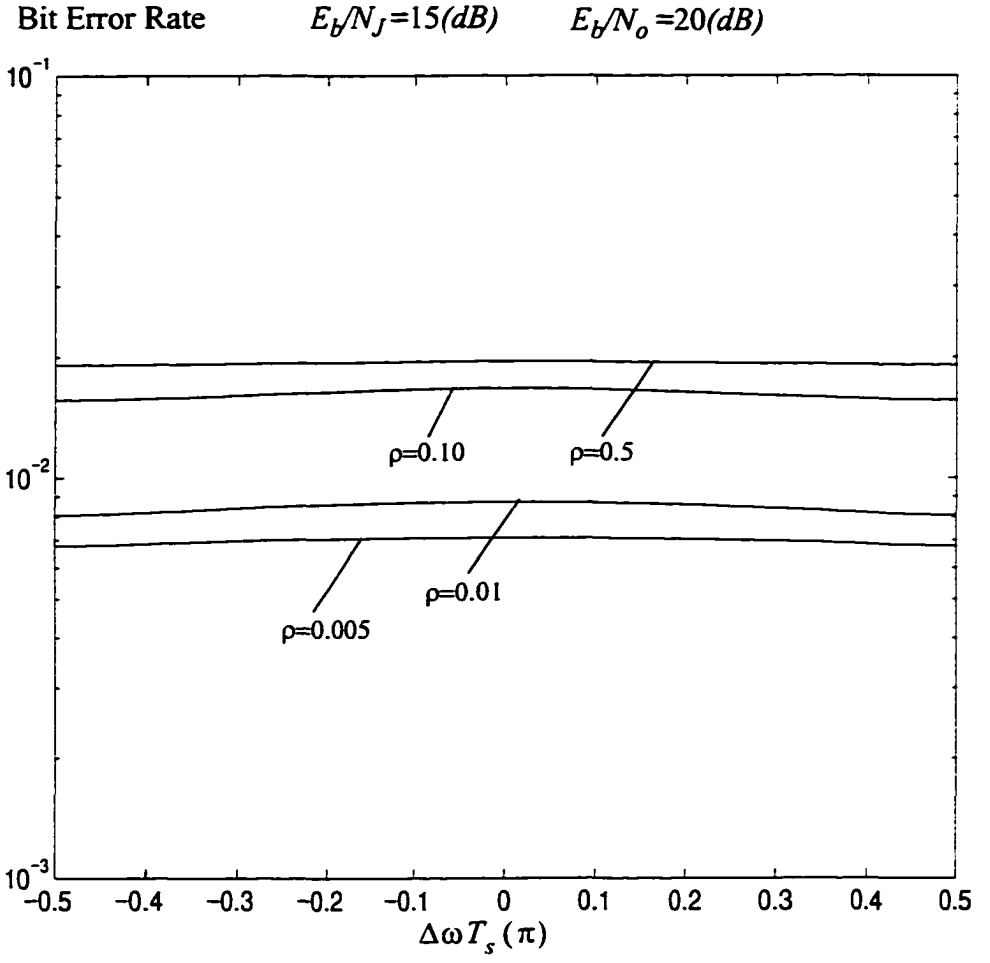

Figure 4.5 BER versus frequency offset for BDPSK in frequency non-selective fading (both signal and interference are Rayleigh faded)[3].

3. For the case where the transmitted signal is Rayleigh faded and the tone interference is Rician faded, results are almost the same as those shown in Figure 4.5.

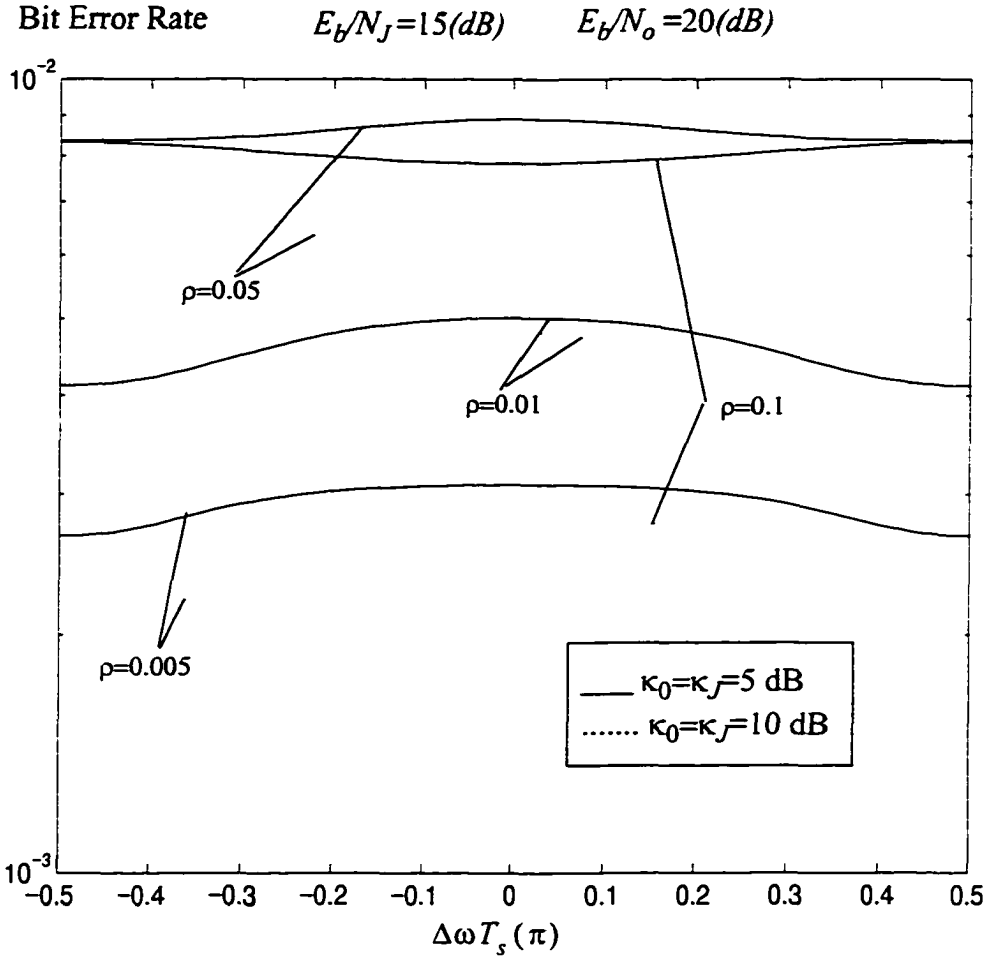

Figure 4.6 BER versus frequency offset for BDPSK in frequency non-selective fading (both signal and interference are Rician faded).

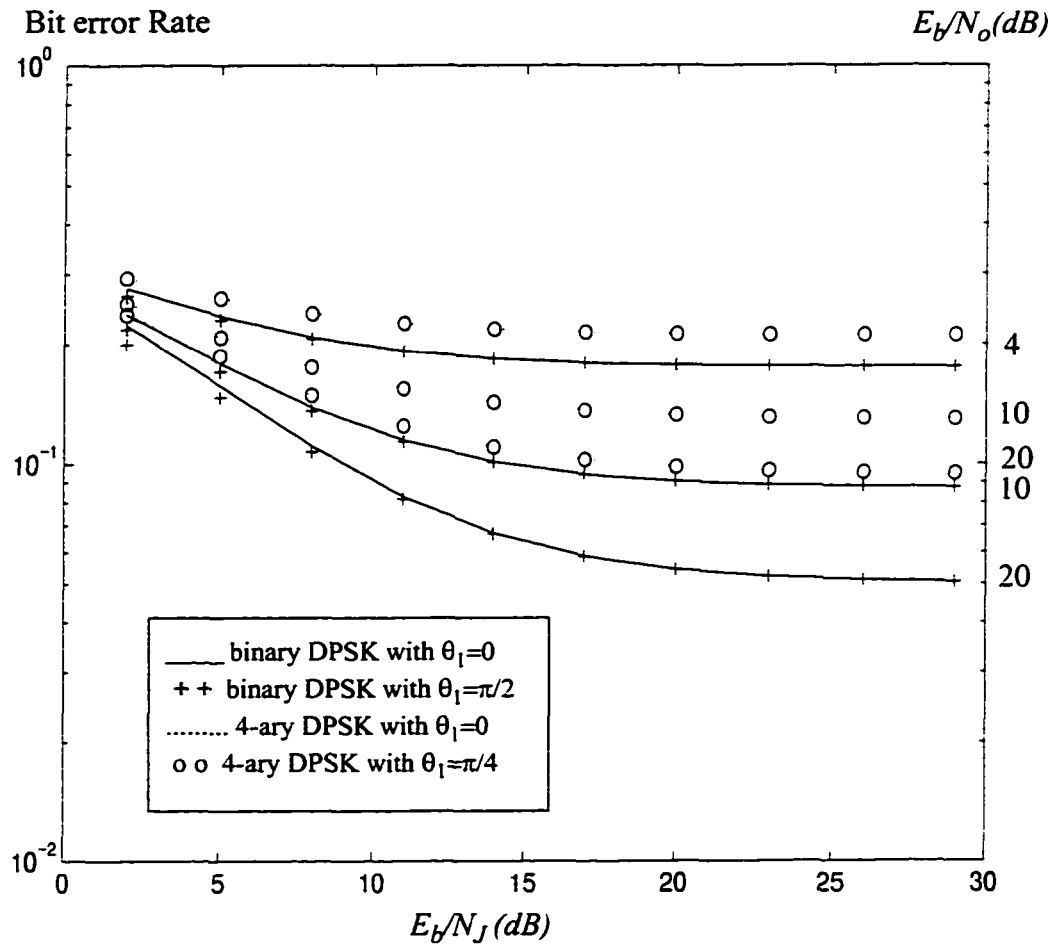

Figure 4.7 Worst case BER versus E_b/N_J for different E_b/N_o for binary DPSK and 4-ary DPSK in frequency selective fading with relative path strengths (0, -10dB).

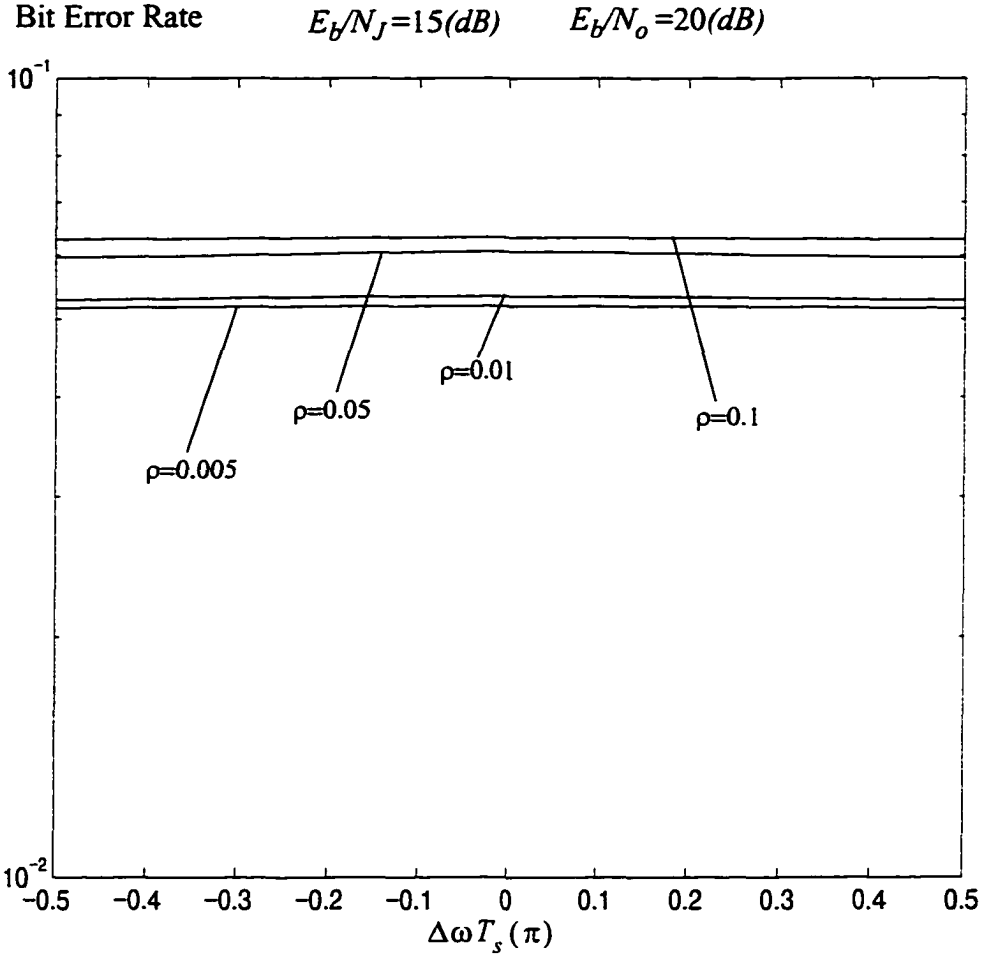

Figure 4.8 BER versus frequency offset for BDPSK in frequency selective fading with relative path strengths (0, -10dB).

4.6 Summary

In this chapter, we have evaluated the performance of SFH/MDPSK in fading and tone interference. Both frequency non-selective and selective fading channels have been investigated. The presented results indicate that, in fading, binary DPSK results a better performance than 4-ary DPSK. However, the choice of different signaling schemes of both binary and non-binary DPSK has little effects on performance improvement. To make the system robust against jamming tone with a deliberate frequency offset, (i.e., frequency jitter), a careful signalling design is required when the transmitted signal is subject to light fading (i.e., Rician fading). However, in the presence of deep fading, we have shown that DPSK becomes insensitive to the frequency offset between the signal and the jamming carrier frequencies.

4.7 Detailed Derivation

4.7.1 Derivation of (4.21)

We start with the following integral

$$\int_0^\infty Q(ax, c)\,\frac{x}{\sigma^2}\exp\left(-\frac{x^2+s^2}{2\sigma^2}\right)I_0\left(\frac{sx}{\sigma^2}\right)dx$$

$$= \int_0^\infty \frac{x}{\sigma^2}\exp\left(-\frac{x^2+s^2}{2\sigma^2}\right)I_0\left(\frac{sx}{\sigma^2}\right)dx\int_c^\infty z\exp\left(-\frac{z^2+(ax)^2}{2}\right)I_0(axz)\,dz$$

$$= \int_0^\infty \frac{z}{\sigma^2}\exp\left(-\frac{s^2}{2\sigma^2}-\frac{z^2}{2}\right)dz\int_c^\infty x\exp\left(-\frac{1+a^2\sigma^2}{2\sigma^2}x^2\right)I_0\left(\frac{sx}{\sigma^2}\right)I_0(azx)\,dx \qquad (4.34)$$

If we change the order of integration and make use of the following equation[25]

$$\int_0^\infty t\exp\left(-p^2t^2/2\right)I_0(at)\,I_0(bt)\,dt = \frac{1}{p^2}\exp\left(\frac{a^2+b^2}{2p^2}\right)I_0\left(\frac{ab}{p^2}\right), \qquad (4.35)$$

integral (4.34) becomes

$$\int_0^\infty Q(ax, c)\frac{x}{\sigma^2}\exp\left(-\frac{x^2+s^2}{2\sigma^2}\right)I_0\left(\frac{sx}{\sigma^2}\right)dx$$

$$= \frac{1}{1+a^2\sigma^2}\int_c^\infty z\exp\left(-\frac{a^2s^2+z^2}{2\left(1+a^2\sigma^2\right)}\right)I_0\left(\frac{asz}{1+a^2\sigma^2}\right)dz$$

$$= Q\left(\frac{as}{\sqrt{1+a^2\sigma^2}}, \frac{c}{\sqrt{1+a^2\sigma^2}}\right). \tag{4.36}$$

Hence, using equation (4.36), we have

$$\int_0^\infty\int_0^\infty Q(ax, by)\frac{x}{\sigma_1^2}\exp\left(-\frac{x^2+s_1^2}{2\sigma_1^2}\right)I_0\left(\frac{s_1x}{\sigma_1^2}\right)\frac{y}{\sigma_2^2}\exp\left(-\frac{y^2+s_2^2}{2\sigma_2^2}\right)I_0\left(\frac{s_2y}{\sigma_2^2}\right)dxdy$$

$$= \int_0^\infty Q\left(\frac{as_1}{\sqrt{1+a^2\sigma_1^2}}, \frac{by}{\sqrt{1+a^2\sigma_1^2}}\right)\cdot\frac{y}{\sigma_2^2}\exp\left(-\frac{y^2+s_2^2}{2\sigma_2^2}\right)I_0\left(\frac{s_2y}{\sigma_2^2}\right)dy \tag{4.37}$$

Invoking the following relation in (4.37)

$$Q(\alpha, \beta) + Q(\beta, \alpha) = 1 + \exp\left(-\frac{\alpha^2+\beta^2}{2}\right)I_0(\alpha\beta) \tag{4.38}$$

it follows that

$$\int_0^\infty\int_0^\infty Q(ax, by)\frac{x}{\sigma_1^2}\exp\left(-\frac{x^2+s_1^2}{2\sigma_1^2}\right)I_0\left(\frac{s_1x}{\sigma_1^2}\right)\frac{y}{\sigma_2^2}\exp\left(-\frac{y^2+s_2^2}{2\sigma_2^2}\right)I_0\left(\frac{s_2y}{\sigma_2^2}\right)dxdy$$

$$= 1 + \int_0^\infty \exp\left(-\frac{b^2y^2+a^2s_1^2}{2\left(1+a^2\sigma_1^2\right)}\right)I_0\left(\frac{abs_1}{1+a^2\sigma_1^2}y\right)\cdot\frac{y}{\sigma_2^2}\exp\left(-\frac{y^2+s_2^2}{2\sigma_2^2}\right)I_0\left(\frac{s_2y}{\sigma_2^2}\right)dy.$$

$$-\int_0^\infty Q\left(\frac{by}{\sqrt{1+a^2\sigma_1^2}}, \frac{as_1}{\sqrt{1+a^2\sigma_1^2}}\right)\cdot\frac{y}{\sigma_2^2}\exp\left(-\frac{y^2+s_2^2}{2\sigma_2^2}\right)I_0\left(\frac{s_2y}{\sigma_2^2}\right)dy \tag{4.39}$$

Then the equations (4.35), (4.36) and (4.38) can be used to yield (4.21).

Chapter 5

Multiple Symbol Detection of MPSK in Narrowband Interference and AWGN

5.1 Introduction

In this chapter, we propose an alternative method for narrowband interference rejection for systems using M-ary phase shift keying (MPSK). It is based on multiple symbol detection scheme which was first proposed by Divsalar and Simon for improving the performance of DPSK (differential PSK) in wideband Gaussian noise[43]. Their motivation was to create a better phase reference for differential detection through multiple symbols. Indeed, a performance close to that of coherent detection can be achieved this way. In this chapter, our motivation is different in the following sense. Although we also involve multiple symbols in detection as in [43], we try to take advantage of them to cancel the narrowband interference. As we will show, unfortunately, the direct use of multiple symbol detection can not improve the performance if the narrowband interference is dominant (in the coherent case, it will actually degrade the performance). Therefore, we propose a new PSK multi-symbol signalling scheme or coding scheme with which narrowband interference can be significantly reduced. This scheme is optimum under certain conditions as explained later. To maintain the generality of our work, we have considered both coherent and noncoherent or differential MPSK for any M. To facilitate the evaluation of BER performance in all cases, we have derived a general formula for pairwise error probability which generalizes a formula given earlier in [43].

Since both narrowband interference and wideband interference (e.g., additive white

Gaussian noise, AWGN) are considered in this chapter, it offers an insight to an interesting and yet difficult general problem, i.e., how to devise a detection scheme that is nearly optimum in both kinds of interference which represent two extremes in bandwidth.

This chapter is organized as follows. In Section 5.2, we consider the general multi-symbol maximum-likelihood (ML) detection of PSK in both AWGN and bandpass interference (a special case is narrowband interference which is of our interest). We identify the ML detector in AWGN (one for DPSK is what was used in [43]). However, the direct use of this ML detector leads to a poor performance in the presence of narrowband interference and background AWGN. This is shown in Section 5.3 where we also show that tone interference is the worst case narrowband interference against the "ML" detector in both coherent and differential cases. Therefore, in Section 5.4, we propose a signalling or coding scheme that makes the ML detector in AWGN also the ML detector in both AWGN (used to model the background noise) and the worst case tone interference. We prove that the coding scheme is asymptotically non-redundant and evaluate the BER performance which shows a dramatic improvement against narrowband interference. In Section 5.5, as an example of application, we apply the proposed signalling technique to the popular SFH/DPSK. The system has been used for high speed spread spectrum communications and is a strong candidate for wireless LAN over ISM bands in addition to its anti-jam use[15][8]. It, however, has been known to suffer severely from the worst case tone interference or jamming. We show that, with the use of our proposed technique, the performance can be drastically improved even in the worst case narrowband interference which is more general than tone jamming and takes tone jamming as a special case. Section 5.6 contains conclusions.

5.2 Maximum-likelihood Detection of PSK

To introduce our new signalling scheme, we start with the maximum-likehood (ML) detection of MPSK. First, we consider the transmission of MPSK signal in unknown narrowband interference and AWGN. The transmitted signal in the interval $kT \le t < (k+1)T$ has the complex form

$$s_k = \sqrt{2A}e^{j\theta_k}, \tag{5.1}$$

where A denotes the constant signal power, T the MPSK symbol interval and θ_k the transmitted phase in the kth signaling interval which normally takes on one of M values $2\pi m/M$ for m=0,1,.....M-1 around the unit circle. Then the corresponding received signal is

$$r_k = s_k e^{j\phi} + J_k + n_k, \tag{5.2}$$

where n_k is zero-mean uncorrelated complex Gaussian noise with variance $\sigma^2 = \frac{2N_0}{T}$, ϕ is a phase introduced by the channel and J_k denotes the narrowband interference.

Without loss of generality, we consider a received sequence of MPSK symbols with length N in the time interval $0 \le t \le NT$. Similar to (5.2), the received sequence $\boldsymbol{r}$ is expressed as

$$\boldsymbol{r} = \boldsymbol{S}e^{j\phi} + \boldsymbol{J} + \boldsymbol{n} \tag{5.3}$$

where r_k, s_k, J_k and n_k are the kth components of the length-N sequences $\boldsymbol{r}$, $\boldsymbol{S}$, $\boldsymbol{J}$ and $\boldsymbol{n}$ respectively, where k=0, 1,....., N-1.

5.2.1 Noncoherent Detection

For the assumed AWGN model, a *posteriori* probability density of $\boldsymbol{r}$ given $\boldsymbol{S}$, ϕ and $\boldsymbol{J}$ is

$$P(\boldsymbol{r}|\boldsymbol{S}, \boldsymbol{J}, \phi) = \frac{1}{\left(2\pi\sigma^2\right)^N}\exp\left\{\frac{\left\|\boldsymbol{r}-\boldsymbol{S}e^{j\phi}-\boldsymbol{J}\right\|^2}{2\sigma^2}\right\}, \tag{5.4}$$

where

$$\left\|\boldsymbol{r}-\boldsymbol{S}e^{j\phi}-\boldsymbol{J}\right\|^2 = \sum_{k=0}^{N-1}\left|r_k - s_k e^{j\phi} - J_k\right|^2. \tag{5.5}$$

Expanding the right-hand side of (5.5), we have

$$\|\boldsymbol{r}-\boldsymbol{S}e^{j\phi}-\boldsymbol{J}\|^2 = \sum_{k=0}^{N-1}\left(|r_k-J_k|^2+|s_k|^2\right)-2Re\left\{\sum_{k=0}^{N-1}(r_k-J_k)\,s^*_k\right\}\cos\phi$$

$$-2Im\left\{\sum_{k=0}^{N-1}(r_k-J_k)\,s^*_k\right\}\sin\phi$$

$$= \sum_{k=0}^{N-1}\left(|r_k-J_k|^2+|s_k|^2\right)-2\left|\sum_{k=0}^{N-1}(r_k-J_k)\,s^*_k\right|\cos(\phi-\beta)\,, \tag{5.6}$$

where

$$\beta = arctg\frac{Im\left\{\sum_k (r_k-J_k)\,s^*_k\right\}}{Re\left\{\sum_k (r_k-J_k)\,s^*_k\right\}}. \tag{5.7}$$

For noncoherent detection, we assume that ϕ is uniformly distributed over $(-\pi, \pi]$, a *posteriori* probability density of $\boldsymbol{r}$ given $\boldsymbol{S}$ and $\boldsymbol{J}$ is simply

$$P(\boldsymbol{r}|\boldsymbol{S},\boldsymbol{J}) = \int_{-\pi}^{\pi} p(\boldsymbol{r}|\boldsymbol{S},\boldsymbol{J},\phi)\,d\phi$$

$$= \frac{1}{\left(2\pi\sigma^2\right)^N}\exp\left\{\frac{1}{2\sigma^2}\sum_{k=0}^{N-1}|r_k-J_k|^2+|s_k|^2\right\} I_o\left(\frac{1}{\sigma^2}\left|\sum_{k=0}^{N-1}(r_k-J_k)\,s^*_k\right|\right), \tag{5.8}$$

where $I_o(x)$ is the zeroth order modified Bessel function of the first kind.

Because $I_o(x)$ is a monotonically increasing function of its argument, $|r_k-J_k|^2$ and $|s_k|^2$ are constant for all transmitted signal phases, we have

$$P(\boldsymbol{r}|\boldsymbol{S},\boldsymbol{J}) \propto I_o\left(\frac{1}{\sigma^2}\left|\sum_{k=0}^{N-1}(r_k-J_k)\,s^*_k\right|\right). \tag{5.9}$$

Without narrowband interference, i.e. $J_k = 0$, maximizing the *posteriori* probability $p(\boldsymbol{r}|\boldsymbol{S})$ over $\boldsymbol{S}$ is equivalent to

$$\max_{\boldsymbol{S}} \left| \sum_{k=0}^{N-1} r_k s^*_k \right| \tag{5.10}$$

which is the scheme proposed by D. Divsalar and M. K. Simon for multiple symbol differential detection of MPSK signal transmitted over AWGN[43]. If DPSK is employed, and vector $\hat{\Omega} = (\alpha_1, \ldots\ldots, \alpha_{N-1})$ denotes the differential phases transmitted in the interval $T \le t \le NT$, (5.10) results in the decision rule,

$$\max_{\hat{\Omega}} \Lambda(\boldsymbol{r}, \hat{\Omega}) = \left| r_0 + \sum_{k=1}^{N-1} r_k e^{-j\sum_{i \le k} \alpha_i} \right| . \tag{5.11}$$

Intuitively, since the detector based on (5.11) is the ML detector in AWGN, it might be expected to outperform conventional differential detector even when it is used straightforwardly in narrowband interference. In Section 5.3, we will show whether this is true through an evaluation of the error performance of the multiple symbol detector.

Figure 5.1 is a simple serial implementation of the decision rule of (5.11).

5.2.2 Coherent Detection

In coherent detection, since the reference phase is known to the detector, we have

$$\ln P(\boldsymbol{r}|\boldsymbol{S}, \boldsymbol{J}) \propto Re\left\{ \sum_{k=0}^{N-1} (r_k - J_k) s_k^* e^{-j\phi} \right\} . \tag{5.12}$$

Without narrowband interference, i.e. $J_k = 0$, maximizing the *posteriori* probability $p(\boldsymbol{r}|\boldsymbol{S})$ over $\hat{\Omega}$ is then equivalent to

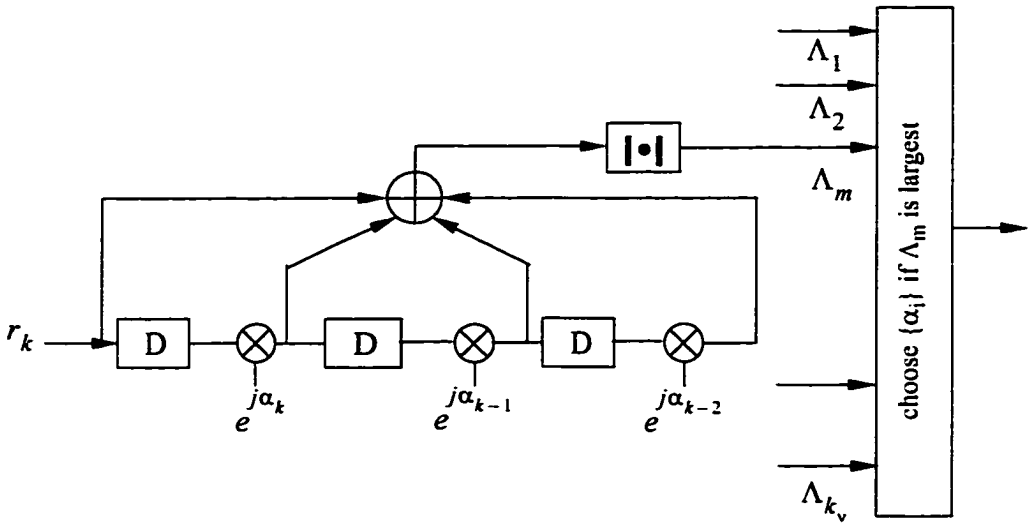

a). Serial implementation of multiple bit differential detector;

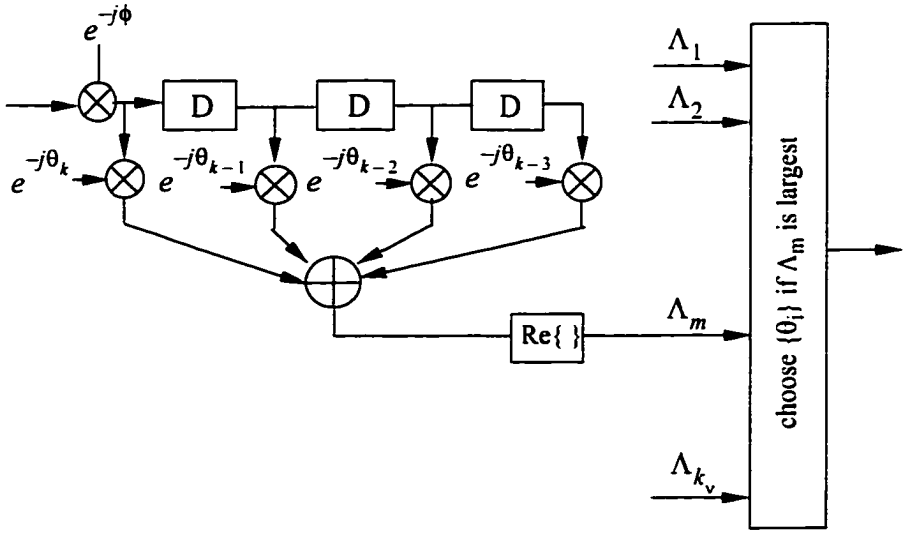

b). Implementation of multiple bit coherent detector;.

Figure 5.1 Implementation of multiple bit detection; N=4.

$$\max_{\hat{\Omega}} \Lambda(r, \hat{\Omega}) = Re\left\{\sum_{k=0}^{N-1} r_k s_k^* e^{-j\phi}\right\}, \tag{5.13}$$

where we re-define the vector $\hat{\Omega}$ slightly differently as $\hat{\Omega} = (\theta_1, \ldots\ldots, \theta_N)$, which denotes the phases transmitted in the interval $0 \le t \le NT$. The implementation of coherent detection is illustrated in Figure 5.1.

5.3 Bit Error Performance

Since we assume that the narrowband interference is unknown to the communicator which may often be the case in practice, a ML detector can not be obtained in the presence of the narrowband interference. Here we assume the rule (5.11) and (5.13), which correspond to the ML detection in AWGN only, are used even when the narrowband interference exists.

To obtain the upper bound on the average bit error probability of a multiple symbol detection scheme, we first evaluate the pairwise error probability. The pairwise error probability is an important fundamental measure of the error performance. Using a union bound analogous to that used for upper bounding the error performance of an error correction coded system, we can have a simple upper bound on the average bit error probability of the multiple symbol detection scheme in terms of the sum of the pairwise error probabilities weighted by the number of information bit errors due to a pairwise error in sequence detection as follows

$$P_b \le \frac{1}{\log k_v} \sum_{\Omega} p(\Omega) \sum_{\Omega \ne \tilde{\Omega}} w(\Omega, \tilde{\Omega}) Pr(\Omega \to \tilde{\Omega} | \Omega) \tag{5.14}$$

where $p(\Omega)$ denotes the probability of Ω being transmitted, $Pr(\Omega \to \tilde{\Omega}|\Omega)$ denotes the pairwise probability that $\tilde{\Omega}$ is incorrectly chosen when Ω was actually sent, $w(\Omega, \tilde{\Omega})$ is the number of information bit errors caused by the pairwise error event $\Xi = \{\Omega \to \tilde{\Omega}|\Omega\}$, and k_v is the number of M-ary information vectors corresponding to

a length-N sequence which is equal to MN for coherent MPSK and $M(N-1)$ for differential PSK.

5.3.1 Evaluation of Pairwise Error Probability in Narrowband Interference

a) Noncoherent detection

To compute $Pr(\Omega \rightarrow \tilde{\Omega}|\Omega)$ for multiple symbol differential detection, it is convenient to define

$$Z_1 = \sum_{k=0}^{N-1} r_k z_k^* = \left(\sum_{k=0}^{N-1} r_k s_k^* \right) s_0 \tag{5.15}$$

and

$$Z_2 = \sum_{k=0}^{N-1} r_k \tilde{z}_k^* = \left(\sum_{k=0}^{N-1} r_k \tilde{s}_k^* \right) \tilde{s}_0, \tag{5.16}$$

where $z_0 = 1$ and $z_k = e^{j\sum_{i \le k} \alpha_i}$, $k = 1, \ldots N-1$, (i.e., $s_k = s_0 z_k$). $\tilde{s}_k$ and $\tilde{z}_k$ are corresponding parameters for $\tilde{\Omega}$.

In accordance with the decision rule (5.11), the pairwise probability that $\tilde{\Omega}$ is incorrectly chosen when Ω was actually sent can be expressed as

$$\begin{aligned} P(\Omega \rightarrow \tilde{\Omega}|\Omega) &= Pr(\Lambda(\boldsymbol{r}, \Omega) < \Lambda(\boldsymbol{r}, \tilde{\Omega})|\Omega) \\ &= Pr(\Lambda(\boldsymbol{r}, \Omega) - \Lambda(\boldsymbol{r}, \tilde{\Omega}) < 0|\Omega) \\ &= Pr(f < 0|\Omega), \end{aligned} \tag{5.17}$$

where

$$f = |Z_1|^2 - |Z_2|^2. \tag{5.18}$$

If the narrowband interference is assumed to be Gaussian which is an assumption

most often made, then Z_1 and Z_2 are Gaussian random variables. Using the characteristic function of f, we can express the probability (5.17) in terms of its characteristic function $G_f(t)$ as[24]

$$Pr(f<0) = \frac{-1}{2\pi j}\int_{-\infty+j\varepsilon}^{\infty+j\varepsilon} \frac{G_f(t)}{t}dt, \tag{5.19}$$

where ε is a small positive number. In Section 5.7.1, we derive the following results which is a generalization of a result in [43]

$$Pr(f<0) = \frac{t_1}{t_1+t_2}Q(a,b) + \frac{t_2}{t_1+t_2}(1-Q(b,a)), \tag{5.20}$$

where

$$\begin{bmatrix} a^2 \\ b^2 \end{bmatrix} = \frac{2\left(\sigma_2^2|E(Z_1)|^2 + \sigma_1^2|E(Z_2)|^2 - 2Re(\gamma E(Z_1)(E(Z_2))^*)\right)}{\left(\sigma_1^2+\sigma_2^2\right)^2 - 4|\gamma|^2} \mp$$

$$\frac{\sqrt{\left(\sigma_1^2+\sigma_2^2\right)^2 - 4|\gamma|^2} \mp \left(\sigma_1^2-\sigma_2^2\right)}{\left(\sigma_1^2+\sigma_2^2\right)^2 - 4|\gamma|^2}\left(|E(Z_1)|^2 - |E(Z_2)|^2\right) \tag{5.21}$$

and

$$\begin{bmatrix} t_1 \\ t_2 \end{bmatrix} = \frac{\sqrt{\left(\sigma_1^2+\sigma_2^2\right)^2 - 4|\gamma|^2} \mp \left(\sigma_1^2-\sigma_2^2\right)}{2\left(\sigma_1^2\sigma_2^2 - |\gamma|^2\right)}, \tag{5.22}$$

where $\sigma_i^2 = var(Z_i), i = 1, 2$, and $\gamma = E((Z_1 - E(Z_1))^*(Z_2 - E(Z_2)))$.

By use of (5.2) and (5.15)-(5.16), we have the following parameters for the signal transmitted in narrowband interference and AWGN.

$$E(Z_1) = \sum_{k=0}^{N-1} \sqrt{2A}e^{j\phi}s_k z_k^* + E\left\{\sum_{k=0}^{N-1} z_k^*(J_k + n_k)\right\}$$

$$= N\sqrt{2A}e^{j\phi}s_0, \tag{5.23}$$

$$E(Z_2) = \sum_{k=0}^{N-1} \sqrt{2A}e^{j\phi}s_k\tilde{z}_k^* + E\left\{\sum_{k=0}^{N-1} \tilde{z}_k^*(J_k + n_k)\right\}$$

$$= \delta\sqrt{2A}e^{j\phi}s_0 \tag{5.24}$$

$$\sigma_1^2 = E\left\{\left(\sum_{i=0}^{N-1} z_i^*(n_i + J_i)\right)^*\left(\sum_{j=0}^{N-1} z_j^*(n_j + J_j)\right)\right\}$$

$$= N\sigma_0^2 + Z^T\Re Z^*\sigma_J^2, \tag{5.25}$$

$$\sigma_2^2 = E\left\{\left(\sum_{i=0}^{N-1} \tilde{z}_i^*(n_i + J_i)\right)^*\left(\sum_{j=0}^{N-1} \tilde{z}_j^*(n_j + J_j)\right)\right\}$$

$$= N\sigma_0^2 + \tilde{Z}^T\Re\tilde{Z}^*\sigma_J^2, \tag{5.26}$$

and

$$\gamma = E\left\{\left(\sum_{i=0}^{N-1} z_i^*(n_i + J_i)\right)^*\left(\sum_{j=0}^{N-1} \tilde{z}_j^*(n_j + J_j)\right)\right\}$$

$$= \delta\sigma_0^2 + Z^T\Re\tilde{Z}^*\sigma_J^2, \tag{5.27}$$

where

$$Z^T = \left[z_0\ z_1 \cdots z_{N-1}\right],$$

$$\tilde{Z}^T = \left[\tilde{z}_0\ \tilde{z}_1 \cdots \tilde{z}_{N-1}\right],$$

$$\delta = \sum_{k=0}^{N-1} z_k\tilde{z}_k^*,$$

and

$$\Re = \begin{bmatrix} \rho_J(0) & \rho_J(T) & \dots & \rho_J((N-1)T) \\ \rho_J(-T) & \rho_J(0) & \dots & \rho_J((N-2)T) \\ \dots & \dots & \dots & \dots \\ \rho_J((1-N)T) & \rho_J((2-N)T) & \dots & \rho_J(0) \end{bmatrix}_{N \times N} \tag{5.28}$$

In (5.28), $\rho_J(\tau)$ is the normalized autocorrelation function of narrowband interference.

b). Coherent detection

From the decision rule (5.13), we have

$$\begin{aligned} P(\Omega \to \tilde{\Omega}|\Omega) &= Pr(\Lambda(\vec{r}, \Omega) < \Lambda(\vec{r}, \tilde{\Omega})|\Omega) \\ &= Pr(V < 0|\Omega), \end{aligned} \tag{5.29}$$

where

$$V = Re\left\{\sum_{k=0}^{N-1} r_k (s_k^* - \tilde{s}_k^*) e^{-j\phi}\right\}. \tag{5.30}$$

Since V is a Gaussian random variable when J_k is assumed to be Gaussian, then the probability (5.29) can be expressed as

$$P(\Omega \to \tilde{\Omega}|\Omega) = \frac{1}{2} erfc\left(\frac{E(V))}{\sqrt{2var(V)}}\right), \tag{5.31}$$

where by using (5.2) and (5.30), the expected value and variance of V can be calculated as

$$E(V) = \sqrt{2A}\left(N - Re\left(\sum_{k=0}^{N-1} s_k \tilde{s}_k^*\right)\right) \tag{5.32}$$

and

$$var(V) = \frac{1}{2}\xi^T\left(\sigma_0^2 I + \sigma_J^2 \Re\right)\xi^*, \tag{5.33}$$

where $\xi_R^T = (s_0 - \tilde{s}_0, \dots\dots, s_{N-1} - \tilde{s}_{N-1})$ and σ_J^2 is the variance of J_k.

5.3.2 Numerical Results and Remarks

To demonstrate performance variation due to extending the observation interval for detection from the conventional case to multiple symbol case, some numerical results based on the analysis in the preceding section are presented here. In computing these results, we have assumed that the narrowband interference is bandpass Gaussian with a power spectral density *S(f)* given by

$$S(f) = \begin{cases} \dfrac{\sigma_J^2}{2f_J} & |f| \le f_J/2 \\ 0 & else \end{cases}, \tag{5.34}$$

where f_J is the bandwidth of the narrowband interference.

Figure 5.2 shows the bit error rate versus E_b/N_J for binary DPSK (BDPSK) with different levels of background thermal noise characterized by E_b/N_o, where E_b is the energy per information bit and N_J is an equivalent interference spectral density defined so that the variance of J_k in (5.2) has a form of $\sigma_J^2 = \dfrac{2N_J}{T}$ that is in parallel to $\sigma^2 = \dfrac{2N_0}{T}$ for AWGN. That is, $N_J = \sigma_J^2 T/2$. Note that, due to the equivalent lowpass notation used in (3.2.2), the actual narrowband interference power is $\sigma_J^2/2$. This implies that $\dfrac{E_s}{N_J} = \dfrac{E_s/T}{N_J/T}$ $= \dfrac{signal\ power}{interference\ power}$, where E_s is the energy per PSK symbol. For 4-ary DPSK (QDPSK), BER results are given in Figure 5.3. In these two figures, the normalized bandwidth of narrowband interference is set to 0.1. At the first sight, one may observe that as N increases, BER performance improves due to a longer observation interval used in detection. For example, for BDPSK, extending the observation interval from N=2 to N=4, we have a gain (in E_b/N_J) against narrowband interference of approximately 8 dB at BER

10^{-3} with $E_b/N_o = 8dB$. The corresponding gain at $E_b/N_o = 10dB$ is about 1 dB. With the same $E_b/N_o = 10dB$ for QDPSK, the corresponding gain in E_b/N_J is more than 2 dB which is higher than that for BDPSK. A closer look at these BER curves suggests that multiple symbol differential detection offers a larger gain in E_b/N_J near error floors of BER curves. This is because multiple symbol differential detection can effectively reduce the effect of background noise which causes the error floors. Nevertheless, when the narrowband interference is dominant, the improvement offered by the straightforward use of multiple symbol detection is somewhat disappointing. This calls for alternative techniques one of which is proposed below and shows nearly complete rejection of narrowband interference under certain conditions.

The BER results for N-symbol coherent detection of binary PSK (BPSK) are given in Figure 5.4. It can be seen that in the coherent case, the direct use of N-symbol detection can NOT improve the BER performance. In fact, when the narrowband interference is dominant, the multiple symbol detection actually degrades the BER performance. Nevertheless, in the next section, we will show that the use of our proposed signalling scheme can drastically reduce the effect of narrowband interference and, therefore, significantly improve the BER performance.

Figure 5.5 and Figure 5.6 show the BER performance of multiple symbol detection as a function of the bandwidth of the narrowband interference for BDPSK and QDPSK, respectively. For coherent detection, the results are give in Figure 5.7. It can be clearly seen from all these three figures that the BER performance degrades as the bandwidth decreases, or as $f_J T \to 0$, namely, when narrowband interference approaches tone interference which is shown to be the worst interference. Figure 5.6 also shows that multiple symbol detection of QDPSK is more vulnerable to narrowband interference than that of BDPSK.

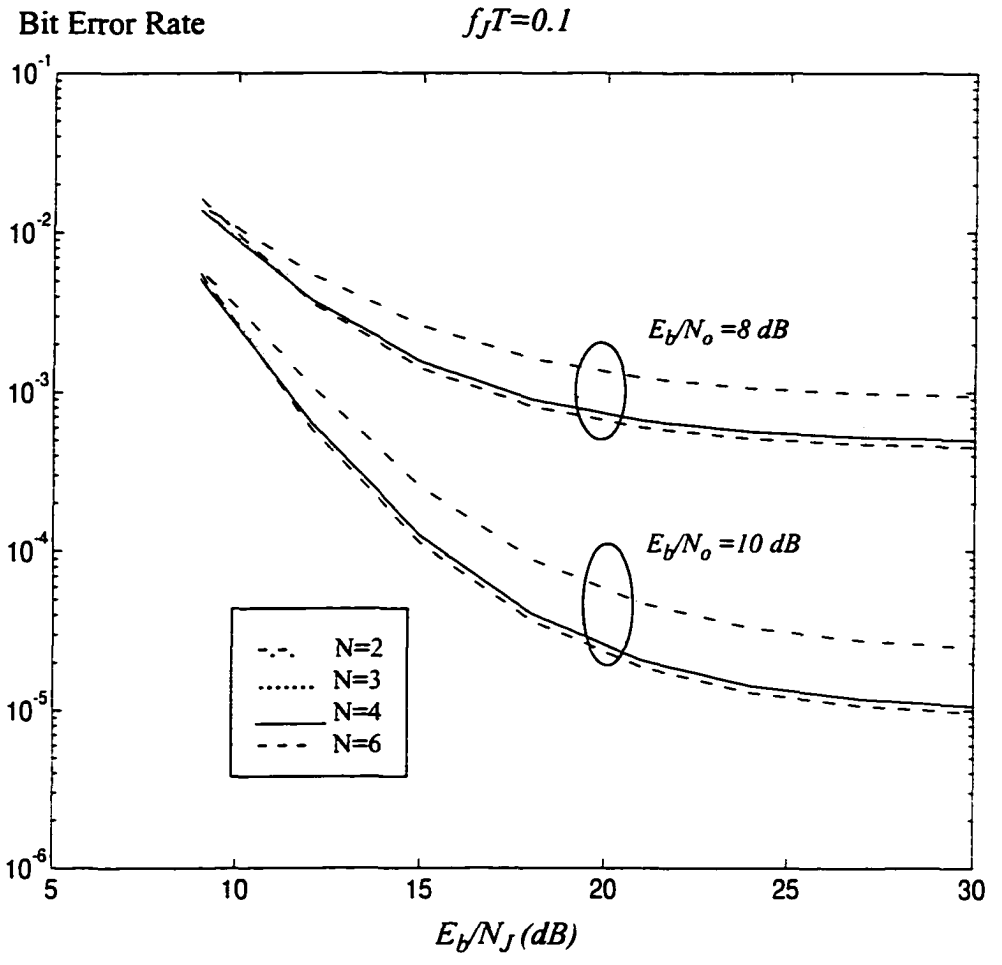

Figure 5.2 BER versus E_b/N_J for N-symbol differential detection of BDPSK with E_b/N_o =8, 10 *dB*

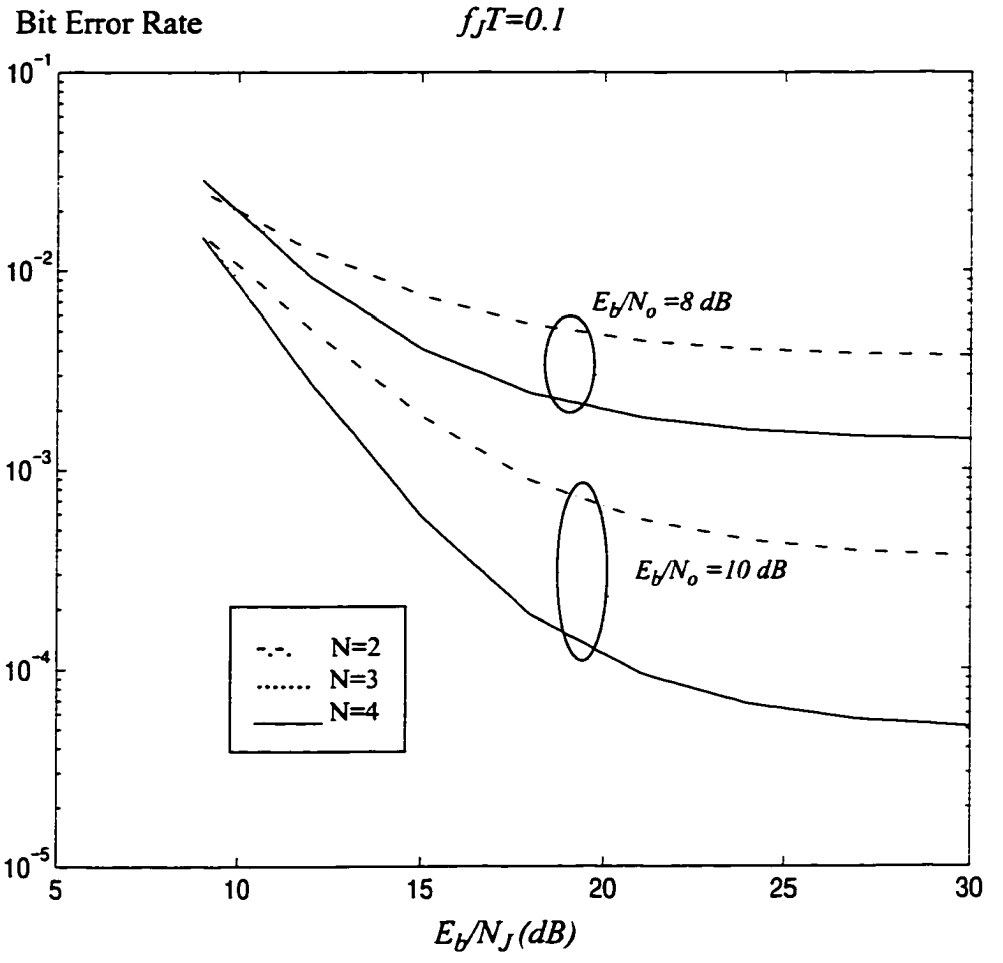

Figure 5.3 BER versus E_b/N_J for N-symbol differential detection of QDPSK with E_b/N_o =8, 10 *dB*

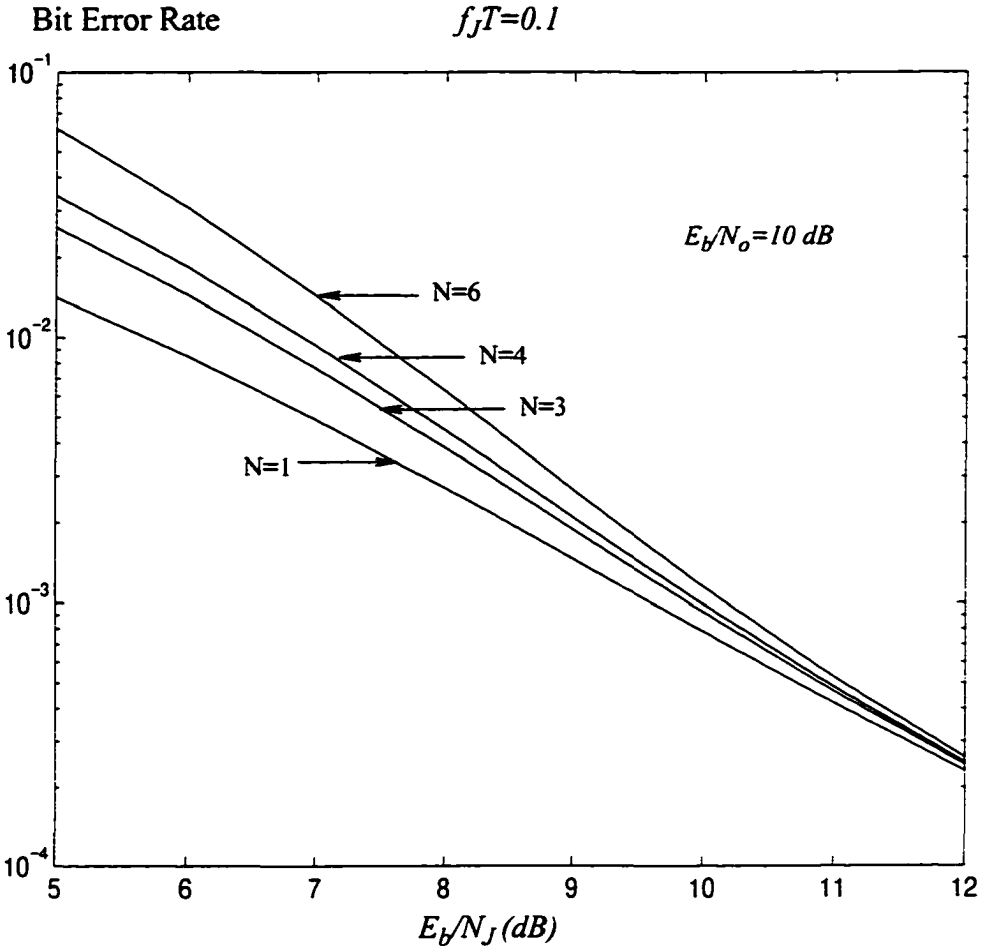

Figure 5.4 BER versus E_b/N_J for N-symbol coherent detection of BPSK

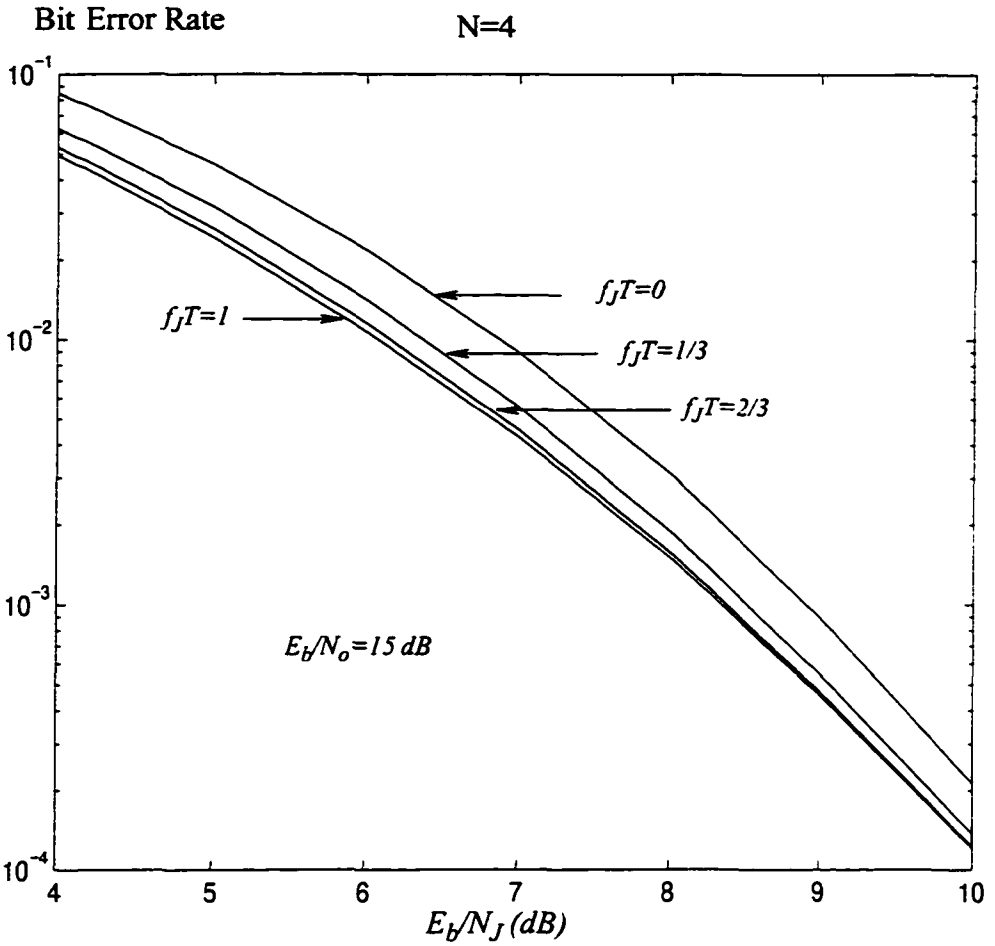

Figure 5.5 BER versus E_b/N_J for multiple symbol differential detection of BDPSK in narrowband interference of different bandwidth: $f_JT=0, 1/3, 2/3, 1$.

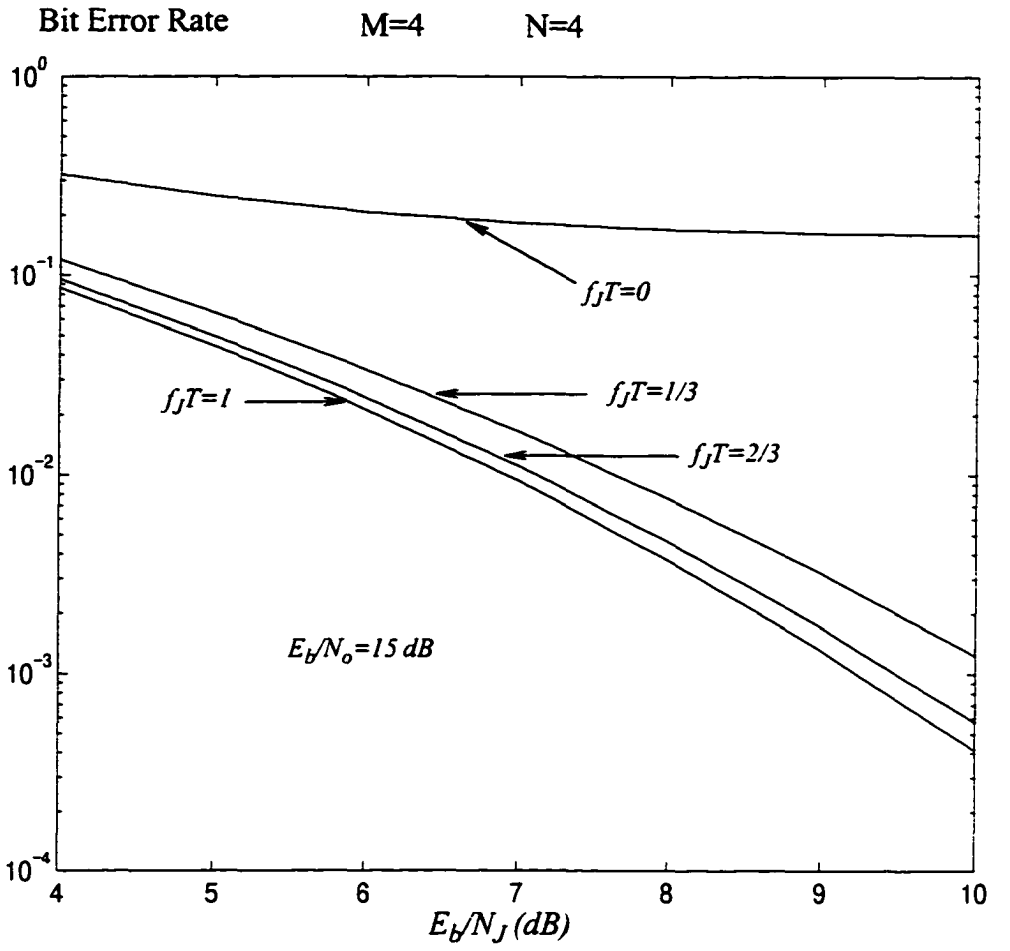

Figure 5.6 BER versus E_b/N_J for multiple symbol differential detection of QDPSK in narrowband interference of different bandwidth: $f_JT=0,\ 1/3,\ 2/3,\ 1$.

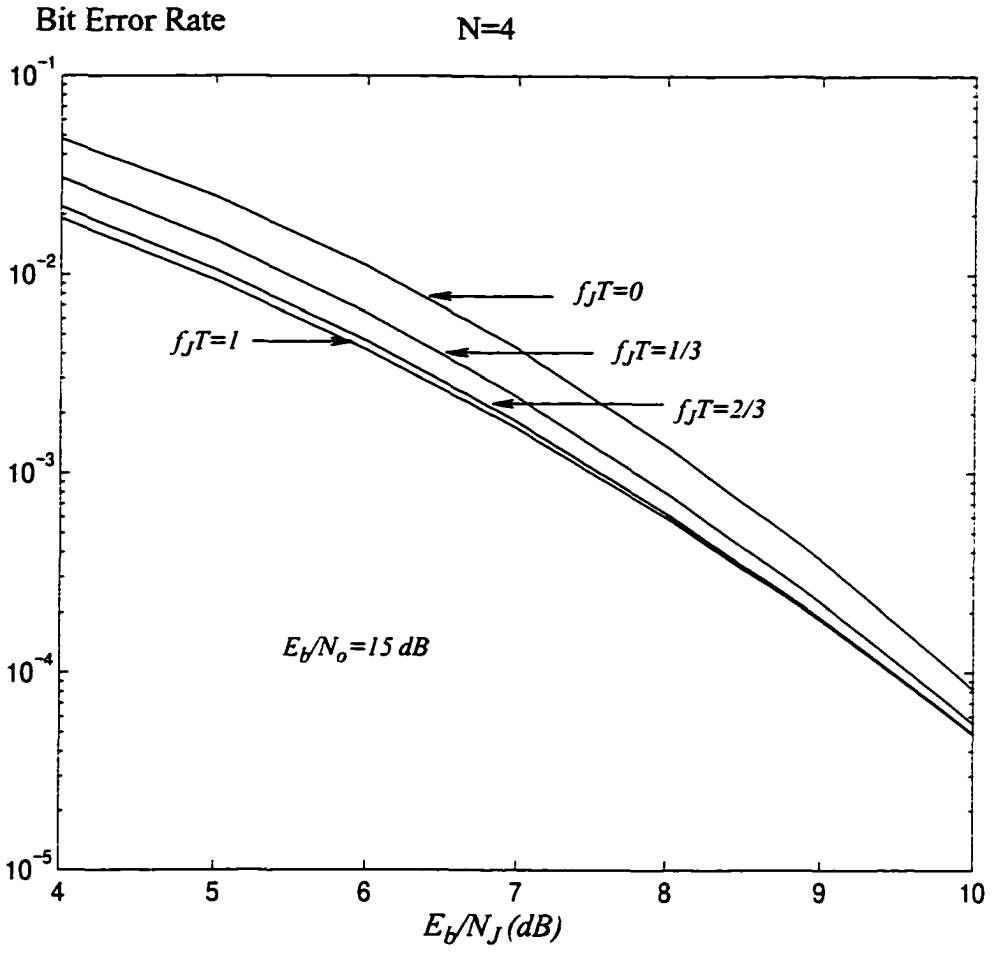

Figure 5.7 BER versus E_b/N_J for N-symbol coherent detection of BPSK in narrowband interference with different bandwidth f_JT.

5.4 New Signalling Scheme

In this section, a new signalling scheme is proposed to improve the effectiveness of multiple symbol detection against narrowband interference. As shown above, the tone interference is the worst case narrowband interference. Therefore, we start with this asymptotic case. Note that tone interference is random interference due to its random initial phase. But the interference parameters (initial phase value and tone amplitude) are constant over a period of time. This indeed represents a typical kind of interference whose parameters can be considered to be invariant over a relatively short period of time of interest, e.g., a small detection window, a hop in a slow frequency hop (SFH) system (refer to the next section for more details), etc. Our motivation here is to devise a signalling scheme so as to eliminate tone interference completely by taking advantage of its special characteristics, meanwhile, it can also offer strong resistance to narrowband interference.

5.4.1 Noncoherent MDPSK

If transmitted differential phases, $\Omega = (\alpha_1,\ldots\ldots,\alpha_{N-1})$, are all selected from a "good" signalling set as follows

$$C = \left\{ \Omega = (\alpha_1,\ldots\ldots,\alpha_{N-1}) \left| 1 + \sum_{k=1}^{N-1} e^{j \sum_{0<i\le k} \alpha_i} = 0 \right. \right\}, \tag{5.35}$$

then, noting J_k is invariant with k for tone interference, we have

$$\sum_{k=0}^{N-1} s_k^* J_k = 0. \tag{5.36}$$

Therefore from (5.8) we have,

$$P(\boldsymbol{r}|\boldsymbol{S}) = \int_{\boldsymbol{J}} p(\boldsymbol{r}|\boldsymbol{S},\boldsymbol{J})\, d\boldsymbol{J}$$

$$\propto I_o\left(\frac{1}{\sigma^2}\left|\sum_{i=0}^{N-1} r_k s^*_k\right|\right). \tag{5.37}$$

This means that the detection based on rule (5.11) is the maximum-likelihood detection in this case.

5.4.2 Coherent MPSK

Similarly, we can choose signals from the following "good" signalling set

$$C = \left\{\Omega = (\theta_0,\ldots\ldots,\theta_{N-1}) \,\middle|\, \sum_{k=0}^{N-1} e^{j\theta_k} = 0\right\}. \tag{5.38}$$

Then the detection based on the rule (5.13) is the maximum-likelihood detection.

Now Ω should be chosen from the set of signal patterns which satisfy (5.35) and (5.38) for noncoherent and coherent case respectively. This is equivalent to employing a coding scheme which spans over multiple symbol intervals with objective of generating a spectral null at frequency of the signal carrier for suppression of the narrowband interference. We define the code rate R=$\log_2$(the number of such signal patterns)/(K$\log_2$M), where K is the number of M-ary information symbols corresponding to a length-N sequence which is equal to N for coherent MPSK and N-1 for non-coherent MDPSK. For M=2, Table 5.1[1] lists the number of such signal patterns and corresponding code rates for various N. From Table 5.1, we can see that when N is too small, there is a significant coding rate loss. Therefore, N>4 is preferred for binary PSK. In general, for M>2, let A_{2n}(M) and B_{2n}(M) denote the numbers of such signal patterns for MDPSK and MPSK with length 2n respectively, then as shown in Section 5.7.2, they can be obtained from the iteration

1. As shown in Section 5.7.3, for M=4, it has the same code rates as M=2. Thus the table can also be used for M=4.

N	Noncoherent BDPSK		Coherent BPSK	
	Number. of signal patterns	code rate	Number of signal patterns	code rate
odd	0	0	0	0
2	1	0	2	= 1/2
4	3	≈ 1/3	6	≈ 1/2
6	10	≈ 3/5	20	≈ 2/3
8	35	≈ 5/7	70	≈ 3/4
2n	C_{2n-1}^{n}	$\frac{\log_2 C_{2n-1}^{n}}{2n-1}$	C_{2n-1}^{n}	$\frac{\log_2 C_{2n}^{n}}{2n}$

Table 5.1. Coding for binary PSK.

$$\left.\begin{aligned} A_{2n}\left(2^k\right) &= \sum_i C_{2n-1}^{2i} B_{2i}\left(2^{k-1}\right) A_{2(n-i)}\left(2^{k-1}\right) \\ B_{2n}\left(2^k\right) &= \sum_i C_{2n}^{2i} B_{2i}\left(2^{k-1}\right) B_{2(n-i)}\left(2^{k-1}\right) \end{aligned}\right\} \tag{5.39}$$

with $A_{2n}(2) = C_{2n-1}^{n}$ and $B_{2n}(2) = C_{2n}^{n}$. When N is odd, the number of signal patterns is 0. Moreover, we can show the following proposition holds for the proposed code, which suggests that to avoid significant coding rate loss, a longer encoding interval can be used.

Proposition 5.1:

The code given by (5.35) and (5.38) are asymptotically non-redundant, i.e., the code rate $R \to 1$, as $N \to \infty$.

Proof: See Section 5.7.3 for detail. ■

The code rates verus N for different M are shown in Figure 5.8. It shows that the code rate decreases with increasing M. Thus for a larger M, a longer observation interval is needed to avoid a significant coding rate loss.

In Figure 5.9-Figure 5.11, computational results are given to show the performance

BDPSK	BPSK
01110	011010
01011	001011
01001	001101
11010	001110
11111	010011
11101	010101
10101	010110
10111	011001

Table 5.2. Signalling for binary PSK.(N=6)

improvement thanks to our proposed signalling or coding scheme. Table 5.2.[2] lists the signalings used for our computational results[3]. In Figure 5.10 and Figure 5.11, for the sake of comparison and demonstration of the superiority of our new signalling/coding scheme, we also include BER performance for soft decision-decoded (7,4) Hamming code which is the perfect code of a length comparable to our signalling sequence length (N=6). As expected, the good signalling set offers a very strong resistance to narrowband interference, even in the coherent case, when narrowband interference is dominant. Moreover, as seen from Figure 5.11, e.g., for f_JT=0.1, performance of soft decision decoded (7,4) Hamming code which has complexity comparable to our proposed N=6 scheme is about 8dB inferior at BER of, say, 10^{-4}. Consequently, additional complexity required to attain these extra 8dB coding gain can obviously be rather high. In Figure 5.10, it is interesting to note that using (7,4) Hamming code results in a better performance at large E_b/N_J. This is because that when the channel approaches AWGN channels the BER performance is mainly decided by the minimum distance of codes. Clearly, the proposed code has minimum distance of 2, while (7, 4) Hamming code yields a minimum distance of 3.

2. In BDPSK, we assume the differential phase for "0" is 0, and for "1" is π.

3. For the sake of illustration, we just randomly choose 8 out of all possible patterns. However, one may attain a better performance by selecting these patterns optimally.

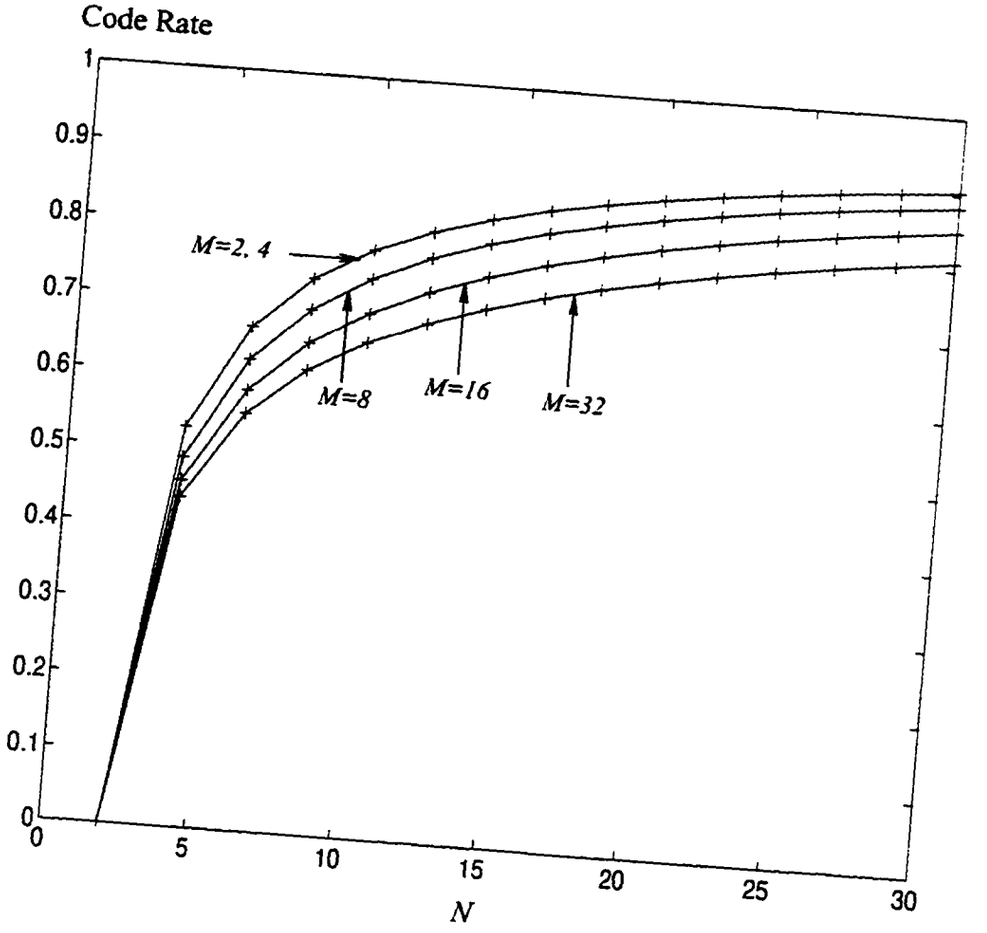

Figure 5.8 Code rate for different N and MDPSK.

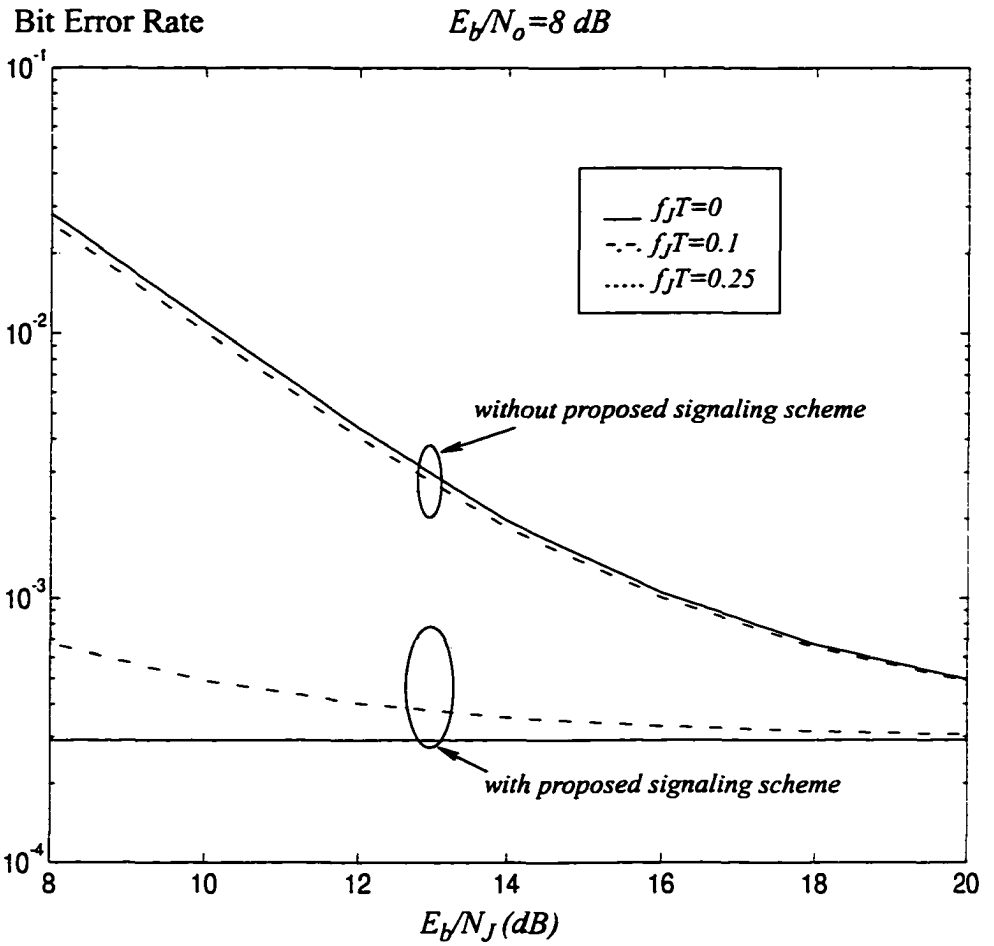

Figure 5.9 BER versus E_b/N_J for multiple symbol differential detection of BDPSK with the use of the proposed signaling scheme for N=6.

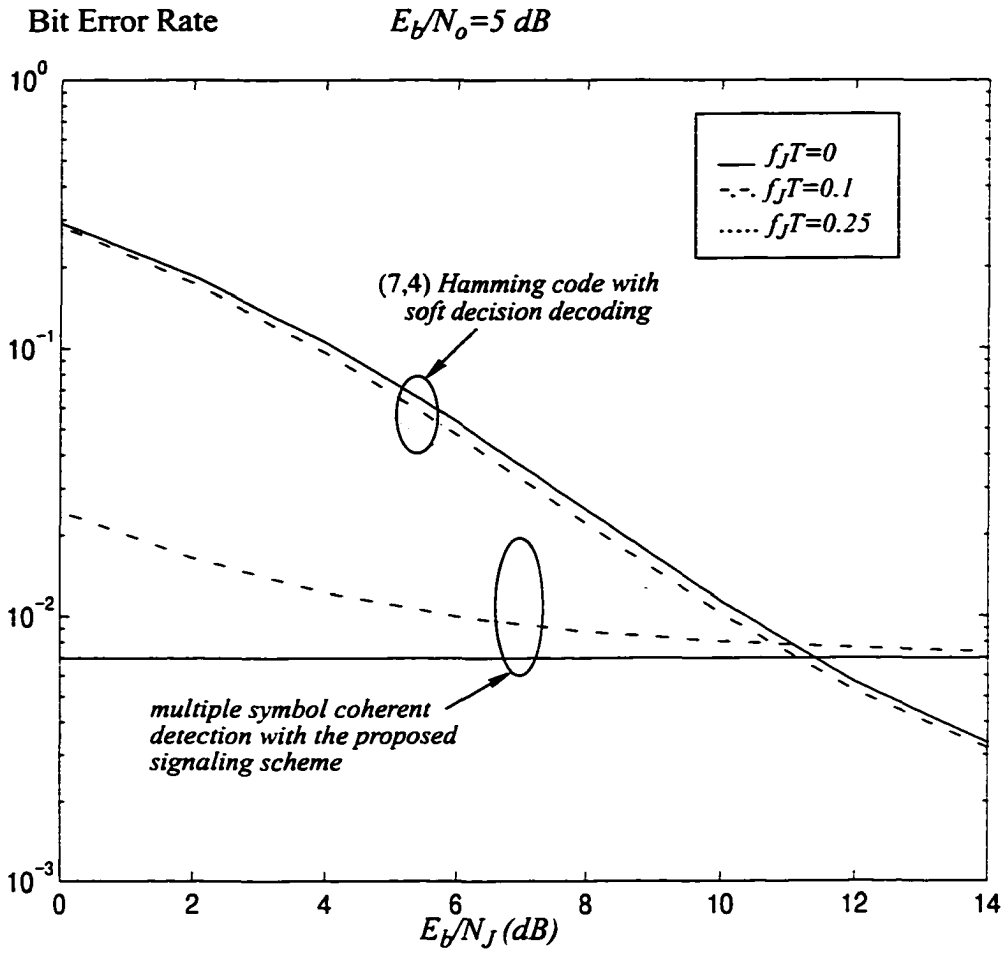

Figure 5.10 BER versus E_b/N_J for multiple symbol coherent detection of BPSK with the use of the proposed signaling scheme for N=6, where E_b/N_0=5 dB.

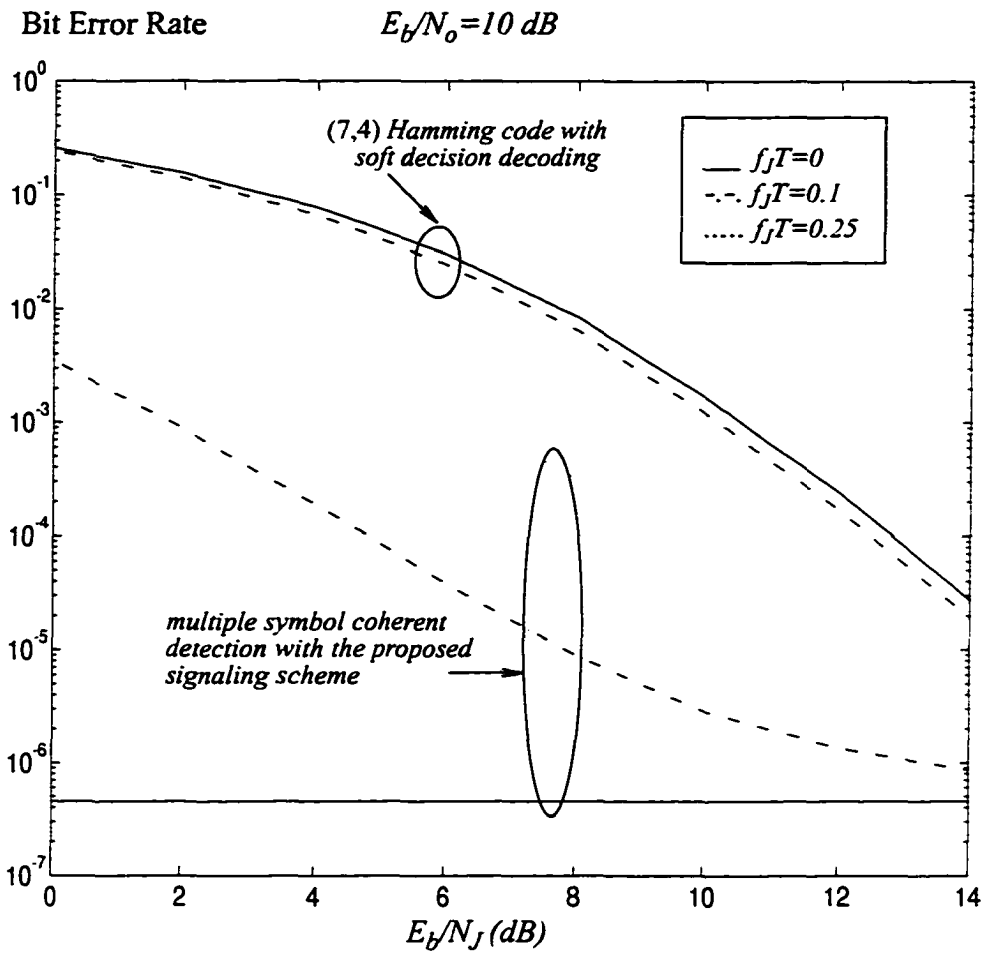

Figure 5.11 BER versus E_b/N_J for multiple symbol coherent detection of BPSK with the use of the proposed signaling scheme for N=6.

5.4.3 Frequency Offset

From a practical point of view, it appears too ideal to assume that the central frequency of the narrowband interference coincides with the signal carrier frequency. Let us now consider the situation where there is an angle frequency offset, denoted by $\Delta\omega$, between them which is known through estimation or otherwise. For the reason explained earlier, we focus on the asymptotic case, i.e. the case with tone interference. Now, we have

$$J_k = Je^{jk\Delta\omega T} \tag{5.40}$$

which suggests that we need modify our signalling scheme given in the previous subsections. For our use here, we define addition between a scaler and a vector as

$$\eta + (\alpha_1,\ldots\ldots,\alpha_{N-1}) = (\alpha_1 + \eta, \ldots\ldots, \alpha_{N-1} + \eta) \tag{5.41}$$

and addition of two vectors as

$$(\eta_0, \ldots\ldots, \eta_{N-1}) + (\theta_0,\ldots\ldots,\theta_{N-1}) = (\eta_0 + \theta_0,\ldots\ldots,\eta_{N-1} + \theta_{N-1}) . \tag{5.42}$$

We now can modify the signaling set as follows
for noncoherent MDPSK:

$$\boldsymbol{C} = \Delta\omega T + \boldsymbol{C}; \tag{5.43}$$

for coherent MPSK:

$$\boldsymbol{C} = (0, \Delta\omega T, \ldots\ldots, \Delta\omega T(N-1)) + \boldsymbol{C}. \tag{5.44}$$

It is noted that while transmitted phases or differential phases are now not necessarily a multiple of $\frac{2\pi}{M}$, the pairwise difference between two phase sequences remains unchanged, which is most important and desirable from the error performance point of view. For MDPSK, (5.43) shows that all differential phases are skewed by the same constant. If we somehow wish to see the transmitted phases or differential phases to be a multiple of $\frac{2\pi}{M}$, we can do the following approximation.

Note that, for any $\Delta\omega T$, there exists a factor $\frac{d}{L_0}$, where $L_0 = 2^n$ with n to be a non-negative integer and d to be odd, that satisfies

$$\left|\Delta\omega T - \frac{2d\pi}{L_0}\right| < \varepsilon, \tag{5.45}$$

where ε represents a small approximation error. Thus, without loss of generality, we only consider such a frequency offset, $\Delta\omega T = \frac{2d\pi}{L_0}$. We then can modify the signalling set as in (5.43) and (5.44) with $\frac{2d\pi}{L_0}$ replacing $\Delta\omega T$ there, for $M \geq L_0$. If $M < L_0$, the transmitted phases or differential phases will simply be a multiple of $\frac{2\pi}{L_0}$.

In all these cases, (5.36) holds. Obviously, the code rate of C' is the same as that of C. It is therefore seen that our signalling scheme can be easily modified to accommodate the frequency offset. For the simplicity of presentation, we omit the frequency offset in the rest of the chapter.

5.5 Application to SFH/DPSK

5.5.1 Performance in Worst Case Jamming

In addition to its wide use in anti-jamming communications[15][8], slow frequency hopped differential phase shift keying (SFH/DPSK) is also very attractive for commercial applications where cost effectiveness is an important consideration in selection of a spread spectrum technique. Improving the performance of SFH/DPSK in various kinds of interference has been the subject of much recent research. It has been found that, under worst case jamming, even when low rate error-control coding and ideal interleaving are employed, the error performance is still disappointing[47]. In this section, we consider the performance of SFH/DPSK under narrowband jamming[4] when the multiple symbol dif-

ferential detection and the proposed signalling scheme are employed. We consider the

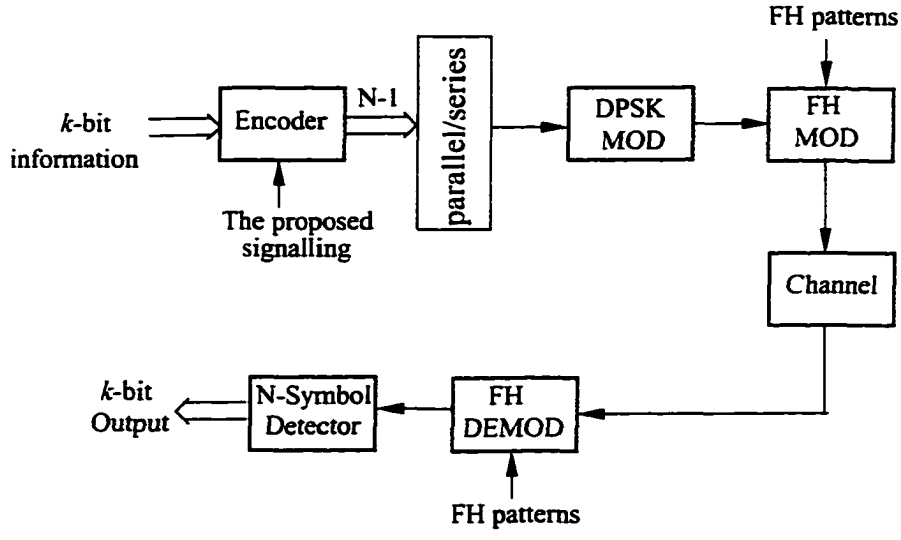

Figure 5.12 Functional block diagram of the proposed SFH/DPSK system

more general case of narrowband jamming than merely tone jamming which has been usually considered in the literature for simplicity. We focus on binary DPSK as an example. The system model considered is shown in Figure 5.12. A block of k-bit information is used to select a sequence of N-1 differential phases based on our proposed signalling scheme. Each differential phase sequence then generates DPSK signal which is transmitted over one hop at the frequency controlled by the FH pattern. The received signal is subject to the background noise modeled as AWGN and narrowband jamming optimized by the jammer. Since our concern is the anti-jam performance of the proposed system, the performance is measured by the worst case BER and compared with the conventional differential detection scheme in which the received differential phase is determined by the difference of only two successively received phases.

Suppose the signal is hopped over L frequencies and jammed with probability ρ.

4. Here we use the word "jamming" instead of interference to emphasize that jamming can be optimized against communications, thus leading to the worst case interference.

At each jammed frequency, there is narrowband jamming of power $\sigma_J^2/2$. With a total jamming power J available, the number of jammed frequency slots is

$$Q = \frac{J}{\sigma_J^2/2} = \frac{J\beta}{A}, \tag{5.46}$$

where A is the signal power and $\beta = \frac{A}{\sigma_J^2/2}$, i.e., power ratio of signal to jamming at a jammed frequency. Suppose T_b is the bit period and $R = T/T_b$ where T is the PSK symbol period.

Then we have the following equation,

$$\rho = \frac{Q}{L} = \frac{J\beta/A \cdot \frac{1}{T}}{L \cdot \frac{1}{T}} = \frac{\beta}{RE_b/N_J}, \tag{5.47}$$

where E_b is the signal energy per bit and N_J is the equivalent broadband jamming power spectral density given by

$$N_J = \frac{J}{L}/\frac{1}{T}, \tag{5.48}$$

which generalizes the definition given in Section 5.3.2 for L=1.

Thus, the average error probability over the entire frequency band is

$$P = (1-\rho) \times P_{AWGN}(E_b/N_0) + \rho \times P_J(E_b/N_0, \rho R(E_b/N_J)), \tag{5.49}$$

where $P_{AWGN}(E_b/N_0)$ is the BER when only AWGN (characterized by E_b/N_0) is present, and $P_J(E_b/N_0, \rho R(E_b/N_J))$ is the BER when both system background noise (AWGN characterized by E_b/N_0) and narrowband jamming (characterized by β or E_b/N_J) are present. For simplicity, we assume, as an approximation, that ρ is continuous. Then the best strategy for jammer (worst case for communicator) is to choose ρ^* to maxi-

mize (5.49).

5.5.2 Computational Results

In this section, selected numerical results are presented for SFH/DPSK. Since the system under study involves a number of parameters such as E_b/N_o, E_b/N_J, f_JT, we can only show results for certain values of these parameters in order to illustrate their influences on system performance. Here, no attempt is made to provide an exhaustive study of all possible combinations of parameter values.

Figure 5.13 and Figure 5.14 show the BER performance of binary DPSK in tone jamming and AWGN. The worst case BER is plotted as a function of signal-to-noise ratio, E_b/N_o, for different signal-to-jamming ratio, E_b/N_J, in Figure 5.13, and as a function of the signal-to-jamming ratio, E_b/N_J, for different signal-to-noise, E_b/N_o, in Figure 5.14, respectively. From these figures, we can see that the proposed system can completely reject the tone jamming. The BER performance does not vary appreciably with the E_b/N_J. Figure 5.15 gives the worst case BER versus E_b/N_J under narrowband jamming of different bandwidths. It shows that when the bandwidth of the narrowband jamming is narrow enough, (e.g. f_JT=0.1), at least 5 dB gain in E_b/N_J can be obtained at a BER 10^{-3} for E_b/N_o=10 dB. In Figure 5.15, we can also see that increasing the bandwidth of jamming will result in a degradation in the performance of the proposed system. This forces the jammer to deviate from the otherwise most powerful narrowband jamming waveform, namely, tone jamming. In other words, in the jamming-antijam game, the proposed narrowband interference rejection scheme offers the communicator a powerful strategy to establish a new equilibrium in his favor.

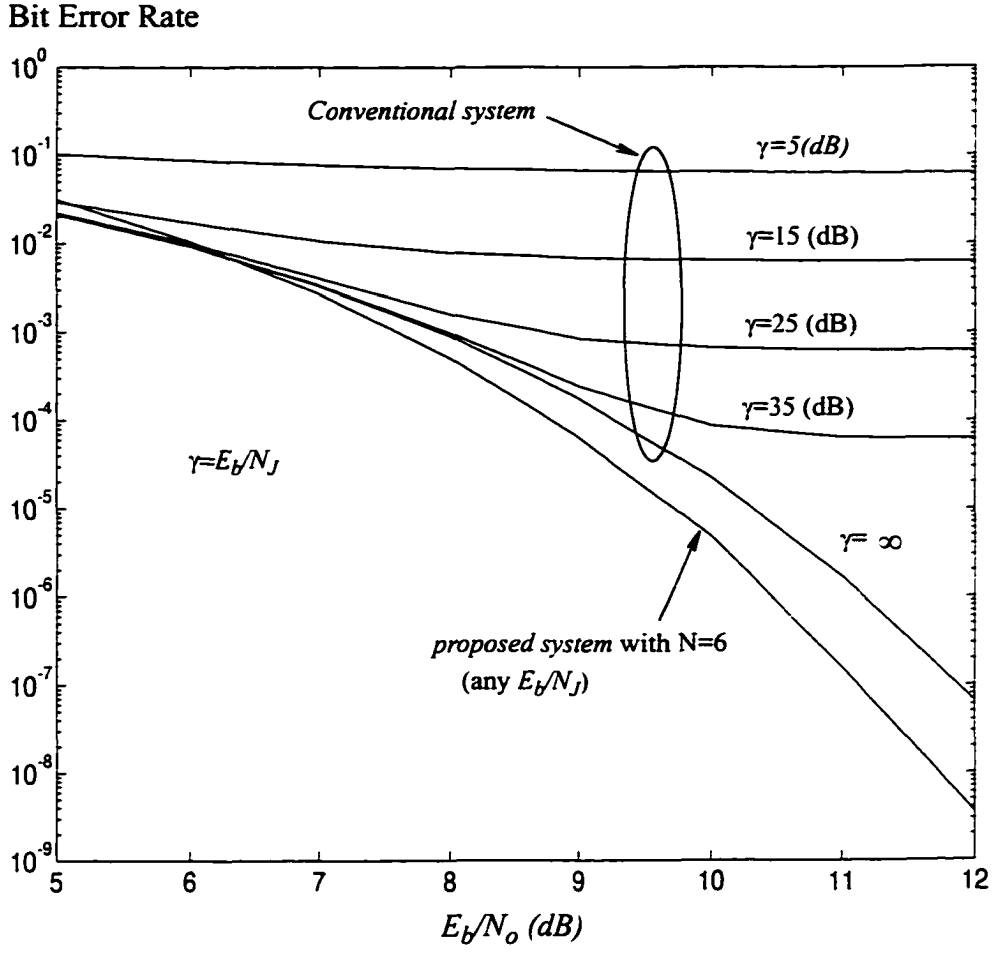

Figure 5.13 Worst case BER versus E_b/N_o for the proposed system with N=6 and the conventional system in tone jamming ($f_JT=0$) for various E_b/N_J and AWGN

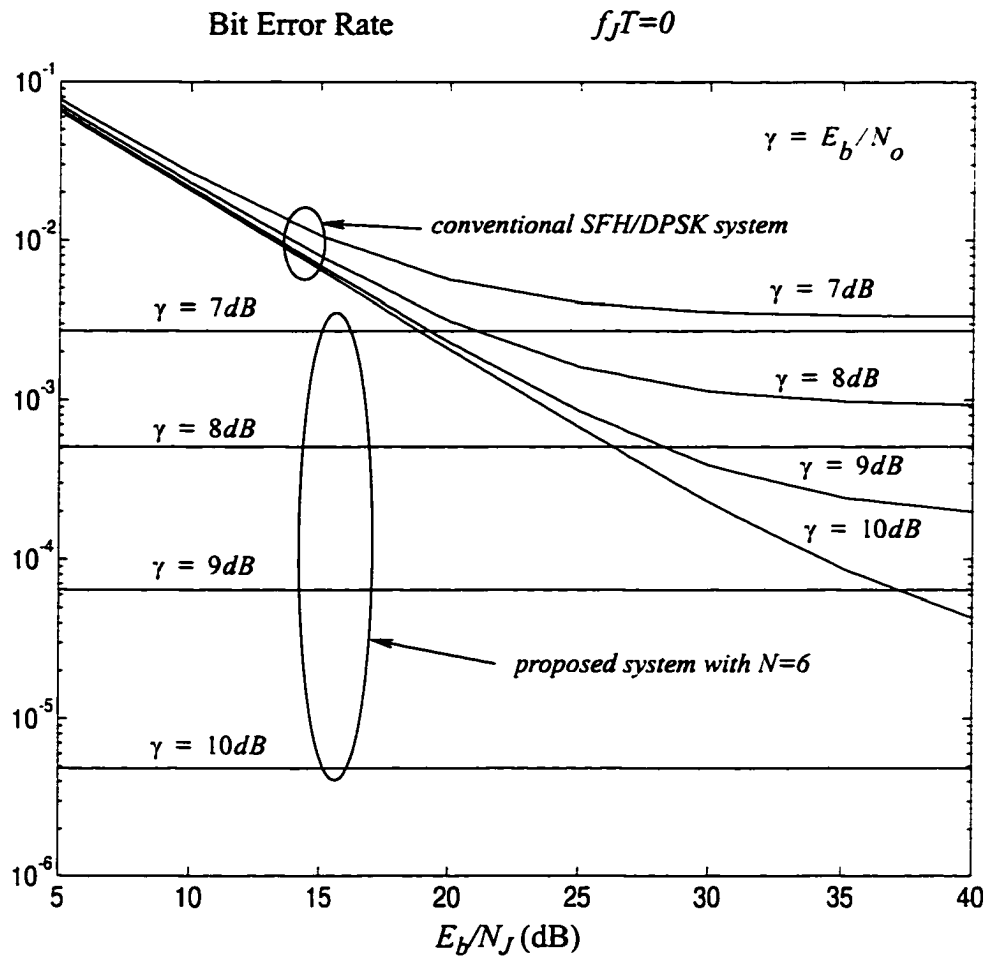

Figure 5.14 Worst case BER versus E_b/N_J for E_b/N_o=7, 8, 9, 10 (dB) in tone jamming and AWGN.

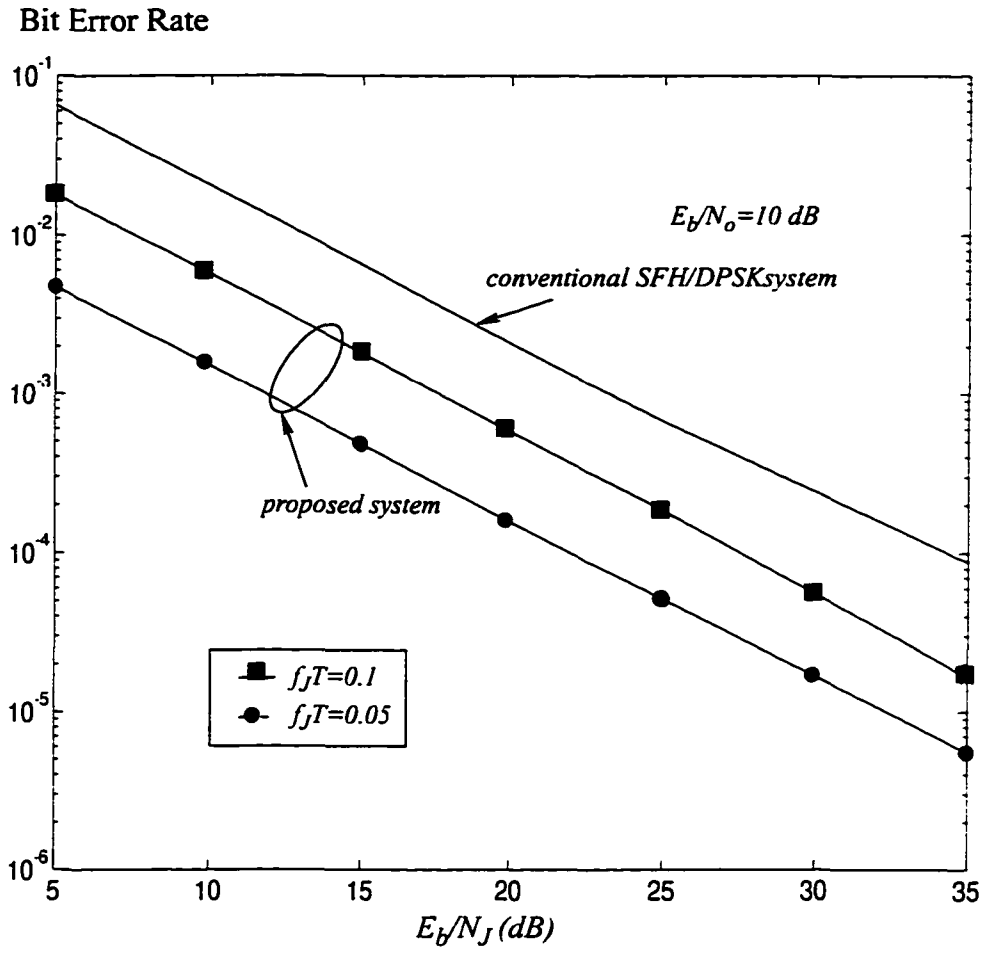

Figure 5.15 Worst case BER versus E_b/N_J for the proposed system with N=6 and the conventional system in narrowband jamming and AWGN.

5.6 Summary

In this chapter, we have considered multiple-symbol detection for MPSK in narrowband interference. A new signalling scheme which offers strong resistance to narrowband interference has been proposed. It has been shown that when multiple symbol detection is employed with the proposed signalling scheme, we can significantly enhance the system robustness against narrowband interference, especially tone jamming which is otherwise the worst case interference. Specifically for SFH/DPSK, the worst case BER performance can be dramatically improved. While the proposed signalling scheme can be viewed as a coding scheme, its implementation is significantly simpler than other error correction coding schemes which might offer the same performance with complexity that might be prohibitively high.

5.7 Detailed Derivations

5.7.1 Derivation of (5.20)-(5.22).

We now evaluate the probability of $Pr\left(|Z_1|^2 < |Z_2|^2\right)$ for complex Gaussian random variables Z_1 and Z_2 with arbitrary variances, means and covariance.

Define

$$f = |Z_1|^2 - |Z_2|^2. \tag{5.50}$$

Then we express it in the form of matrix

$$f = U^{*T} F U \tag{5.51}$$

where superscripts "*" and "T" denote complex conjugate and matrix transpose respectively and

$$U = \begin{bmatrix} Z_1 \\ Z_2 \end{bmatrix} \qquad F = \begin{bmatrix} 1 & 0 \\ 0 & -1 \end{bmatrix}. \tag{5.52}$$

Since f is a quadratic form of Gaussian random variables, its pdf (probability density function) is not an elementary function. Its characteristic function is given by [26]

$$G_f(t) = \frac{\exp\left(jt\langle U\rangle^{*T} F(I-2jtR^{*}F)^{-1}\langle U\rangle\right)}{det(I-2jtR^{*}F)}, \tag{5.53}$$

where "$\langle\rangle$", "I" and "*det*()" denote expected value, identity matrix and determinant, respectively, and

$$R = \frac{1}{2}\langle (U-\langle U\rangle)^{*}(U-\langle U\rangle)^{T}\rangle . \tag{5.54}$$

Thus, we can express the probability in terms of its characteristic function G_f(t) [24] as

$$Pr(f<0) = \frac{-1}{2\pi j}\int_{-\infty+j\varepsilon}^{\infty+j\varepsilon}\frac{G_f(t)}{t}dt, \tag{5.55}$$

where ε is a small positive number.

Denote

$$\sigma_i^2 = var(Z_i),\ i = 1,2,$$

$$U_i = \langle Z_i\rangle,\ i = 1,2, \text{ and}$$

$$\gamma = \langle (Z_1-\langle Z_1\rangle)^{*}(Z_2-\langle Z_2\rangle)\rangle . \tag{5.56}$$

We have

$$R = \frac{1}{2}\begin{bmatrix}\sigma_1^2 & \gamma\\ \gamma^{*} & \sigma_2^2\end{bmatrix}. \tag{5.57}$$

Thus

$$G_f(t) = \frac{1}{t^2\left(\sigma_1^2\sigma_2^2-|\gamma|^2\right)-jt\left(\sigma_1^2-\sigma_2^2\right)+1}\times$$

$$\exp\left(\frac{-t^2\left(\sigma_2^2|U_1|^2+\sigma_1^2|U_2|^2-2Re(\gamma U_1 U_2^*)\right)+jt\left(|U_1|^2-|U_2|^2\right)}{t^2\left(\sigma_1^2\sigma_2^2-|\gamma|^2\right)-jt\left(\sigma_1^2-\sigma_2^2\right)+1}\right). \tag{5.58}$$

Express the exponential function in the form

$$\exp\left(-K_1+\frac{jK_2}{t+jt_1}+\frac{jK_3}{t-jt_2}\right) \tag{5.59}$$

where t_1 *and* t_2 are the roots of $t^2\left(\sigma_1^2\sigma_2^2-|\gamma|^2\right)-jt\left(\sigma_1^2-\sigma_2^2\right)+1=0$, and therefore,

$$\begin{bmatrix}t_1\\ t_2\end{bmatrix}=\frac{\sqrt{\left(\sigma_1^2+\sigma_2^2\right)^2-4|\gamma|^2}\mp\left(\sigma_1^2-\sigma_2^2\right)}{2\left(\sigma_1^2\sigma_2^2-|\gamma|^2\right)}. \tag{5.60}$$

Then a conformal transformation is made from the t-plane onto the z-plane via the change in variable

$$z=\frac{t_1}{t_2}\times\frac{t-jt_2}{t+jt_1}. \tag{5.61}$$

Define

$$a^2=\frac{2}{\left(\sigma_1^2+\sigma_2^2\right)^2-4|\gamma|^2}\left(\sigma_2^2|U_1|^2+\sigma_1^2|U_2|^2-2Re(\gamma U_1 U_2^*)\right)-$$

$$\frac{\sqrt{\left(\sigma_1^2+\sigma_2^2\right)^2-4|\gamma|^2}-\left(\sigma_1^2-\sigma_2^2\right)}{\left(\sigma_1^2+\sigma_2^2\right)^2-4|\gamma|^2}\left(|U_1|^2-|U_2|^2\right),$$

$$b^2=\frac{2}{\left(\sigma_1^2+\sigma_2^2\right)^2-4|\gamma|^2}\left(\sigma_2^2|U_1|^2+\sigma_1^2|U_2|^2-2Re(\gamma U_1 U_2^*)\right)+$$

$$\frac{\sqrt{\left(\sigma_1^2+\sigma_2^2\right)^2-4|\gamma|^2}+\left(\sigma_1^2-\sigma_2^2\right)}{\left(\sigma_1^2+\sigma_2^2\right)^2-4|\gamma|^2}\left(|U_1|^2-|U_2|^2\right). \tag{5.62}$$

As a result, (5.55) can be rewritten as

$$Pr(f<0) = \frac{t_1}{t_1+t_2}\exp\left(-\frac{a^2+b^2}{2}\right)\times\frac{1}{2\pi j}\int_{\Gamma}\frac{(1+t_2/t_1 z)}{z(1-z)}\exp\left(\frac{a^2}{2}\frac{1}{z}+\frac{b^2}{2}z\right)dz, \quad (5.63)$$

where Γ is a circular contour enclosing the origin with radius less than unity.

It can be further simplified by use of the following relations which can be proved easily:

$$\frac{1}{2\pi j}\int_{\Gamma}\frac{1}{p(1-p)}\exp\left(\frac{a^2}{2}\frac{1}{p}+\frac{b^2}{2}p\right) = Q(a,b)\exp\left(\frac{a^2+b^2}{2}\right),$$

$$\frac{1}{2\pi j}\int_{\Gamma}\frac{p}{1-p}\exp\left(\frac{a^2}{2}\frac{1}{p}+\frac{b^2}{2}p\right) = Q(a,b)\exp\left(\frac{a^2+b^2}{2}\right)-I_0(ab)$$

and $Q(a,b)+Q(b,a) = 1+\exp\left(\frac{a^2+b^2}{2}\right)I_0(ab)$,

where $I_o(x)$ is the zeroth order modified Bessel function of the first kind and $Q(x,y)$ is the Marcum's Q-function.

Therefore, it follows that

$$Pr\left(|Z_1|^2<|Z_2|^2\right) = \frac{t_1}{t_1+t_2}Q(a,b)+\frac{t_2}{t_1+t_2}(1-Q(b,a)). \quad (5.64)$$

As a special case when $\sigma_1^2 = \sigma_2^2 = \sigma^2$,

$$Pr\left(|Z_1|^2<|Z_2|^2\right) = \frac{1}{2}[1-Q(b,a)+Q(a,b)], \quad (5.65)$$

where

$$\begin{bmatrix}a^2\\b^2\end{bmatrix} = \frac{1}{2\sigma^2}\left[\frac{|U_1|^2+|U_2|^2-2Re(\rho U_1 U_2^*)}{1-|\rho|^2}\mp\frac{|U_1|^2-|U_2|^2}{\sqrt{1-|\rho|^2}}\right] \quad (5.66)$$

and

$$\rho = \frac{\gamma}{\sigma^2}, \quad (5.67)$$

which is a result in [43].

5.7.2 Derivation of (5.39)

We start our derivation from the following Lemma.

Lemma 5.1:

Let $f(x) \in Z[x]$ and

$$f(x) = g_1\left(x^2\right) + xg_2\left(x^2\right),$$

where $Z[x]$ denotes the ring of polynomials in the variable x with integer coefficients, $g_1\left(x^2\right)$ and $xg_2\left(x^2\right)$ are the polynomials which contain the items with even and odd power of x, respectively. Then,

$$x^{2m} + 1 \,|\, f(x) \text{ if only if } x^m + 1 \,|\, g_1(x) \text{ and } x^m + 1 \,|\, g_2(x).$$

where a|b denotes that a is a divisor of b.

Proof:

If $f(x)$ is divided by $x^{2m}+1$, then

$$\exists h(x) \in Z[x], \text{ and } f(x) = \left(x^{2m} + 1\right)h(x). \tag{5.68}$$

Write $h(x)$ in the form of

$$h(x) = h_1\left(x^2\right) + xh_2\left(x^2\right), \tag{5.69}$$

where $h_1(x), h_2(x) \in Z[x]$.

Substituting (5.69) into (5.68), it follows

$$f(x) = g_1\left(x^2\right) + xg_2\left(x^2\right) = \left(x^{2m} + 1\right)h_1\left(x^2\right) + x\left(x^{2m} + 1\right)h_2\left(x^2\right), \tag{5.70}$$

which implies that

$$g_1\left(x^2\right) = \left(x^{2m} + 1\right)h_1\left(x^2\right) \text{ and } g_2\left(x^2\right) = \left(x^{2m} + 1\right)h_2\left(x^2\right).$$

Thus, we have

$$x^m + 1 \,|\, g_1(x) \text{ and } x^m + 1 \,|\, g_2(x).$$

Conversely, it is obvious. ■

Now, we derived the iteration (5.39).

In MPSK, the transmitted phase have M discrete values, typically given by

$$\theta = \frac{2\pi}{M} i;\ i = 1, 2, \ldots, M. \tag{5.71}$$

Denote

$$\alpha = \exp\left(j\frac{2\pi}{M}\right).$$

Clearly, (5.38) is equivalent to choosing k_i; i=0, 1,...., N-1 so that

$$\sum_{i=0}^{L-1} \alpha^{k_i} = 0. \tag{5.72}$$

In other word, (5.72) can be expressed in terms of a polynomial of α with integer coefficients as

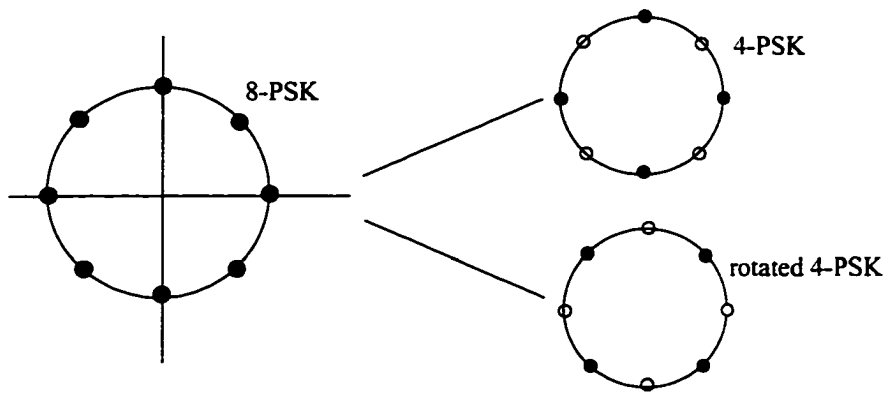

Figure 5.16 Set Partitioning for 8-PSK.

$$f(\alpha) = 0, \tag{5.73}$$

where $f(x) \in Z[x]$.

Therefore, we have

$$f(\alpha) = f_1\left(\alpha^2\right) + \alpha f_2\left(\alpha^2\right) = 0. \tag{5.74}$$

Since α is a root of the irreducible polynomial x^M+1, thus,

$$x^M + 1 | f(x) .$$

From Lemma 5.1, we have

$$f_1(\alpha^2) = 0;\ f_2(\alpha^2) = 0; \tag{5.75}$$

$$2 | f_1(1), f_2(1) . \tag{5.76}$$

If we partition the MPSK constellation into two sets as follows, (see Figure 5.16 for an example)

$$C_0 = \{\alpha^{2i}; i = 0, 1, \ldots M/2-1\} \text{ and } C_1 = \{\alpha^{2i+1}; i = 0, 1, \ldots M/2-1\} .$$

Clearly, C_0 is the constellation of M/2PSK. Therefore, (5.74) and (5.76) imply that the construction of signalling (5.38) can be completed by choosing $2i$ symbols from C_0 and $2(n-i)$ from C_1. Furthermore, (5.75) suggests that the symbols chosen from C_0 is also a "good" signalling for M/2PSK with length of $2i$, i.e., satisfies (5.38) with N=$2i$, and the symbols chosen from C_1 is a "good" signalling for rotated M/2PSK with length of $2(n-i)$. Consequently, the number of "good" signalling patterns, $B_{2n}(M)$, can be calculated as

$$B_{2n}(M) = \sum_i C_{2n}^{2i} B_{2i}(M/2)\, B_{2(n-i)}(M/2) .$$

The results for MDPSK can be derived similarly.

5.7.3 Proof of Proposition 5.1

First, we show the following inequalities which will be used in our proof.

$$\frac{2^{n-1}}{\left\lfloor \frac{n+1}{2} \right\rfloor} < C_n^{\left\lfloor \frac{n+1}{2} \right\rfloor} < 2^n, \tag{5.77}$$

where $\lfloor x \rfloor$ denotes the largest integer less than or equal to x.

Since $C_{2n-1}^n = \dfrac{(2n-1)(2n-2)\ldots 2 \cdot 1}{n!(n-1)!}$

$$= \frac{((2n-1)(2n-3)\ldots 3\cdot 1)((2n-2)(2n-4)\ldots 4\cdot 2)}{n!(n-1)!}$$

$$= \frac{2^{n-1}((2n-1)(2n-3)\ldots 3\cdot 1)}{n!},$$

and using the fact

$$(2n-1)(2n-3)\ldots 3\cdot 1 > (2n-2)(2n-4)\ldots 2 = 2^{n-1}(n-1)! \tag{5.78}$$

and

$$(2n-1)(2n-3)\ldots 3\cdot 1 < (2n)(2n-2)\ldots 4\cdot 2 = 2^{n}n!, \tag{5.79}$$

we have

$$\frac{2^{2n-2}}{n} < C_{2n-1}^{n} < 2^{2n-1}. \tag{5.80}$$

Similarly, we have

$$\frac{2^{2n-1}}{n} < C_{2n}^{n} < 2^{2n}. \tag{5.81}$$

Now we are ready to prove that as $n \to \infty$, $R \to 1$ for any $M = 2^k$.

A). M=2

Since $A_{2n}(2) = C_{2n-1}^{n}$,

using (5.80), we have $\frac{(2n-2)-\log n}{2n-1} < \frac{\log C_{2n-1}^{n}}{2n-1} < 1$.

Therefore, by noting $\frac{(2n-2)-\log n}{2n-1} \to 1$ as $n \to \infty$,

we have $R_{DPSK} \to 1$ as $n \to \infty$.

Similarly we can prove $R_{PSK} \to 1$.

B). M>2

To show the rate $R \to 1$ as $n \to \infty$, we first show the following inequalities by induction on k (i.e. M).

$$\left.\begin{aligned} \frac{2^{k(2n-1)-a(k)}}{n^{2^{k-1}}} < A_{2n}\left(2^k\right) < 2^{k(2n-1)} \\ \frac{2^{k(2n)-b(k)}}{n^{2^{k-1}}} < B_{2n}\left(2^k\right) < 2^{k(2n)} \end{aligned}\right\}; k > 1 \qquad (5.82)$$

where $A_{2n}\left(2^k\right)$ and $B_{2n}\left(2^k\right)$ are given in (5.39); $a(k)$ and $b(k)$ are given by the iteration

$$\left.\begin{aligned} a(k+1) &= a(k) + b(k) + 1 \\ b(k+1) &= 2b(k) + 1 \end{aligned}\right\}; \quad k > 1 \qquad (5.83)$$

with $a(2) = b(2) = 2$.

i). k=2, i.e. M=4

$$A_{2n}(4) = \sum_i C_{2n-1}^{2i} C_{2i}^{i} C_{2(n-i)-1}^{n-i} = \sum_i \frac{(2n-1)!}{i! \cdot i! \cdot (n-i)! \cdot (n-i-1)!}$$

$$= C_{2n-1}^{n} \sum_i C_n^{n-i} C_{n-1}^{i} = \left(C_{2n-1}^{n}\right)^2.$$

Similarly, we have

$$B_{2n}(4) = \left(C_{2n}^{n}\right)^2.$$

Thus, using (5.77), we have

$$\frac{2^{2(2n-1)-2}}{n^2} < A_{2n}(4) < 2^{2(2n-1)}$$

and $$\frac{2^{2(2n)-2}}{n^2} < B_{2n}(4) < 2^{2(2n)}.$$

ii). As the induction hypothesis, suppose that (5.82) is true for k. Then for k+1, by the iteration (5.39), we have

$$A_{2n}\left(2^{k+1}\right) = \sum_i C_{2n-1}^{2i} B_{2i}\left(2^k\right) A_{2(n-i)}\left(2^k\right)$$

$$> \sum_i C_{2n-1}^{2i} \frac{2^{k(2i)-b(k)}}{i^{2^{k-1}}} \frac{2^{k(2n-2i-1)-a(k)}}{(n-i)^{2^{k-1}}} \quad \text{(by induction assumption)}$$

$$> \frac{2^{k(2n-1)-(a(k)+b(k))}}{n^{2^k}} \sum_i C_{2n-1}^{2i} = \frac{2^{k(2n-1)-(a(k)+b(k))}}{n^{2^k}} 2^{2n-2}$$

$$= \frac{2^{(k+1)(2n-1)-a(k+1)}}{n^{2^k}}.$$

Similarly, we have $A_{2n}\left(2^{k+1}\right) < 2^{(k+1)(2n-1)}$

and

$$\frac{2^{(k+1)(2n)-b(k+1)}}{n^{2^k}} < B_{2n}\left(2^{k+1}\right) < 2^{(k+1)(2n)}.$$

Therefore, by induction on k, we have proven (5.82). From (5.82), it is easy to show that

$$R_{DPSK} = \frac{\log A_{2n}(M)}{(2n-1)\log M} \to 1$$

and $$R_{PSK} = \frac{\log B_{2n}(M)}{2n \log M} \to 1 \qquad \text{as } n \to \infty.$$

Thus, from A) and B), we have proven that,

for any $M = 2^k$, $\qquad R \to 1$; as $n \to \infty$.■

Chapter 6

Conclusions

In this chapter, a brief summary of results described in previous chapters is given, and suggestions for further research are made.

6.1 Summary of the Dissertation

This dissertation focused on analysis and cancellation of narrowband interference in wireless systems.

In Chapter 2, a novel method has been presented for determination of the general probability distribution of the differential phase between two random variables. The phase characteristics function has been defined and its properties have been studied.

In Chapter 3, an general expression has been derived for the probability distribution of a DPSK signal corrupted by tone interference and AWGN. It takes the previous results of Simon[11] and Pawula, Rice and Roberts[33] as special cases. Subsequently, we have investigated the performance of a general uncoded SFH/DPSK under partial-band multitone jamming. It has been observed that, without fading, the signaling schemes may affect the performance of SFH/DPSK under tone jamming and the choice of the best signaling scheme is dependent upon M. For example, different binary DPSK signalling can results a degradation in performance of approximately 2.4 dB at a BER of 10^{-3} and E_b/N_o=28dB. Based on the analysis on jamming strategies, we concluded that, to obtain a scheme which is robust against jamming tones with a deliberate frequency offset, DPSK signalling design should be carried out carefully. Furthermore, we have demonstrated that for BDPSK, the band single tone jamming is more effective than band multi-

tone, however, for QDPSK, the effectiveness of single tone jamming will depend on E_b/N_J. These results can provide the basis for signalling design in practical system implementation.

In Chapter 4, a further study of SFH/DPSK under tone interference and fading has been presented. First, we have described fading channel models which are of interests in this research. Based on these channel models, the performance of SFH/DPSK under tone interference has been evaluated in detail for different fading environments. It has been shown that, in fading, we can not expect performance improvement due to different signalling schemes. However, when the signal is subject to light fading, properly chosen signalling schemes are shown to be robust against jamming tone with a deliberate frequency offset. When the signal channel approaches deep fading (i.e., without LOS), the effect of frequency jitter is negligible.

In Chapter 5, we have proposed a new technique for rejection of narrowband interference based on multiple symbol detection of coherent or differential phase shift keying (PSK). We first show that the direct use of multiple symbol detection offers a poor performance when narrowband interference is dominant. Our proposed technique employs a special signalling or vector coding scheme which is shown to be optimum against narrowband interference under certain conditions. We then have evaluated its BER (bit error rate) performance in both narrowband interference and AWGN (additive white Gaussian noise) which may model the background noise. A significant improvement in BER performance has been found. Finally, we have applied our proposed technique to a slow frequency hopped differential PSK system which is suitable for high speed spread spectrum communications such as wireless LAN (local area network). It has been shown that even in the worst case narrowband interference, our proposed technique can offer a significant gain in the power ratio of signal to narrowband interference.

6.2 Suggestions for Further Work

Relevant research suggested as follows may be further pursued in the future.

In addition to the narrowband interference analyzed in this dissertation, co-channels interference is also a common concern in wireless communications, especially in a mobile cellular environment. Clearly, Chapter 2 also provides a promising tool for analysis of such kind of interference. Furthermore, this study can be extended to performance analysis of other phase-shift keying modulation schemes, such as differential detection of GMSK which has been used as a modulation standard in pan-European GSM system.

As shown in Chapter 4, frequency selective fading can drastically degrade the system performance by introducing inter-symbol interference (ISI). Therefore, for the system where high data rate is required, equalization should be employed to eliminate ISI. Moreover, on account of the time-varying characteristics of wireless channels, some sophisticated adaptive equalization techniques, e.g. blind equalization, should be investigated in the future research.

In Chapter 5, a new signalling scheme has been proposed for rejection of narrowband interference. If we rewrite the decision metric of (5.10) and (5.13) as follows

$$\left| \sum_{k=0}^{N-1} \left(s_k e^{j\phi} + n_k \right) s^*_k + \sum_{k=0}^{N-1} J_k s^*_k \right| ; \tag{6.1}$$

$$Re\left\{ \sum_{k=0}^{N-1} \left(s_k + n_k e^{-j\phi} \right) s^*_k + \left(\sum_{k=0}^{N-1} J_k s^*_k \right) e^{-j\phi} \right\} . \tag{6.2}$$

Clearly, the items caused by the narrowband interference J_k can be considered as the responds of signals passing a narrowband filter with coefficients J_k. This suggests that purpose of signalling design is no more than to form certain special spectrum shape. Therefore, a class of coding techniques for spectral shaping of data[45] can be investigated for suppression of narrowband interference.

Furthermore, it has been shown that our new signalling scheme is powerful in its ability to reject narrowband interference. Nevertheless, it is not designed for error correction in general. This suggests that some error-control codes can be concatenated with such a signalling scheme to further improve the system performance.

Moreover, it was stated in Chapter 5 that, to avoid a significant coding rate loss, a longer observation interval is needed to make a multi-symbol decision, especially for a larger M. Since the complexity of demodulation increases drastically as the observation interval increases, research on the implementation of multiple symbol detection is necessary.

Bibliography

[1] V. K. Garg and J. E. Wilkes, *Wireless and Personal Communications Systems*, Prentice Hall PTR, 1996.

[2] K. Feher, *Wireless Digital Communications: Modulation & Spread Spectrum Applications*, Prentice Hall PTR, 1995.

[3] D. L. Schilling, "Spread Spectrum for Commercial Communications," *IEEE Communications Magazine, Vol.* 39, pp. 66-79, April 1991.

[4] D. T. Magill, F. D. Natali and G. P. Edwards, "Spread Spetrum Technology for Commercial Applications," *Proceedings of IEEE, Vol.* 82, pp. 572-583, April 1994.

[5] D. C. Cox, "Wireless Personal Communication: What is it ?" *IEEE Personal Communications, Vol. 2, No. 2*, pp. 20-35, April 1995.

[6] K. Pahlavan, T. H. Probert and M. E. Chase, "Trends in Local Wireless Networks," *IEEE Communications Magazine*, Vol. 33, pp. 88-95, March 1995

[7] R. Kohno, R. Meidan, and L. B. Milstein, "Spread Spectrum Access Methods for Wireless Communications," *IEEE Communications Magazine*, Vol. 33, pp. 58-67, January 1995.

[8] M. K. Simon, J. K. Omura, R. A. Scholtz and B. K. Levitt, *Spread Spectrum Communications*, Rockville, MD: Computer Science Press, 1990.

[9] V. K. Bhargava, D. Haccoun, R. Matyas and P. Nuspl, *Digital Communications by Satellite*, A Wiley-Interscience Publication, 1981.

[10] R. Meidan, "Frequency hopped CDMA and the GSM system," *Proceedings of the Fifth Nordic Seminar on Digital Mobile Radio Communications,* DMR-V, Helsinki, Finland, December 1992.

[11] M. K. Simon, "The Performance of M-ary FH/DPSK in the Presence of Partial-band Multitone Jamming," *IEEE Transactions on Communications*, pp. 953-958, May 1982.

[12] J. S. Lee and L. E. Miller, "Error Performance Analysis of Differential Phase-Shift-Keyed/Frequency-Hopping Spread-Spectrum Communications System in the Partial-Band Jamming Environments," *IEEE Transactions on Communications, Vol.* 30, pp. 943-952, May 1982.

[13] S. W. Houston, "Modulation Techniques for Communication, Part 1: Tone and Noise Jamming Performance of Spread Spectrum M-ary FSK and 2, 4-ary DPSK Waveforms," *NAECON'75 Conference Record*, pp. 51-58.

[14] K. S. Gong, "Performance Analysis of FH/DPSK in Additive White Gaussian Noise and Multitone Jamming," *Proceedings of IEEE MILCOM*, pp. 53.4.1-53.4.7, 1988.

[15] Q. Wang, T. A. Gulliver and V. K. Bhargava, "Probability Distribution of DPSK in Tone Interference and Application to SFH/DPSK," *IEEE Journal on Selected Areas in Communications, Vol. 8*, pp. 895-906, June 1990.

[16] Q. Wang, T. A. Gulliver and V. K. Bhargave, "Performance of SFH/MDPSK in Tone Interference and Gaussian Noise," *IEEE Transactions on Communications, Vol. 42*, pp. 1450-1454, February/March/April 1994.

[17] L. J. Mason, "Error Probability for FH/MDPSK in Multitone Jamming, Fast Rician Fading, and Gaussian Noise," *IEEE Transactions on Communications, Vol. 43*, pp. 545-553, February/March/April 1995.

[18] M. A. Hasan, J. C. Lee and V. K. Bhargava, "A Narrowband Interference Canceller with an Adjustable Center Weight," *IEEE Transactions on Communications, Vol.* 42, pp. 877-880, February/March/April 1994.

[19] L. A. Rush and H. V. Poor, "Multiuser Detection techniques for Narrowband Interference Suppression in Spread Spectrum," *IEEE Transactions on Communications, Vol.* 43, pp. 1725-1737, February/March/April 1995.

[20] L. A. Rusch and H. V. Poor, "Narrowband Interference Suppression in CDMA Spread Spectrum Communications," *IEEE Transactions on Communications, Vol.* 42, pp. 1969-1979, February/March/April 1994.

[21] E. Masry and L. B. Milstein, "Enhanced Signal Interception in the Presence of Interference," *IEEE Transactions on Communications, Vol.* 43, pp. 1089-1096, February/March/April 1995.

[22] A. Y. Wong and V. C. M. Leung, "Single Tone Interference Rejection of Code-phase Multiplexed Direct-Sequence Spread-Spectrum Signalling," *IEEE Transactions on Communications, Vol.* 44, pp. 557-561, May 1996.

[23] H. Fathallah and L. A. Rush, "Enhanced Blind Adaptive Narrowband Interference Suppression in DSSS," *Proceedings of IEEE Global Telecommunications Conference*, pp. 545-561549, Westminster, London, November 1996.

[24] J. Gil-Pelaez, "Note on the inversion theorem," Biometrika, Vol. 38, 1951, pp. 481-482.

[25] G. N. Watson, *A Treatise on the Theory of Bessel Functions*, Cambridge University Press, 1958.

[26] M. Schwartz, W. R. Bennett, and S. Stein, *Communication Systems and Techniques*, New York; McGraw-Hill, 1966.

[27] C. J. Tranter, *Bessel Functions with Some Physical Applications,* Englis University Press Ltd., *1968.*

[28] R. S. Kennedy, *Fading Dispersive Communication Channels*, New York: John Wiley and Sons, 1969

[29] W. C. Jakes, *Microwave Mobile Communications*, New York: John Wiley and Sons, 1974.

[30] J. H. Roberts, *Angle Modulation*, England: Peregrinus, 1977.

[31] G. R. Cooper and R. W. Nettleton, "A Spread Spectrum technique for high capacity mobile communications," *IEEE Transactions on Vehicular Technology*, Vol. 27, pp. 264-275, November 1978.

[32] G. Turin, "Introduction to Spread Spectrum Antimultipath Techniques and Their Application to Urban Digital Radio," *Proceedings of IEEE*, Vol. 68, pp. 328-353, March 1980.

[33] R. F. Pawula, S. O. Rice and J. H. Roberts, "Distribution of the Phase Angle Between Two Vectors Perturbed by Gaussian Noise," *IEEE Transactions on Communications*, *Vol.* 30, pp. 1828-1841, August 1982.

[34] M. Matsumoto and G. R. Cooper, "Performance of a Nonlinear FH/DPSK Spread Spread-Spectrum Receiver with Multiple Narrowband-Band Interfering Signals," *IEEE Transactions on Communications, Vol.* 30, pp. 937-942, May 1982.

[35] H. H. Ma and M. A. Poole, "Error Correcting Codes Against the Worst Case Partial-band Jammer," *IEEE Transactions on Communications*, *Vol.* 32, *No.* 2pp. 124-133, February 1984.

[36] D. Verhulst, M. Mouly and J. Szpirglas, "Slow frequency hopping multiple access for digital cellular radiotelephone," *IEEE Journal on Selected Areas in Communications*, *Vol.* 2, July 1984.

[37] C. Loo, "A Statistical Model for a Land Mobile Satellite Link," *IEEE Transactions on Vehicular Technology, Vol.* 34, pp. 122-127, August 1985.

[38] R. J. C. Bultitude, "Measurement, characterization and modeling of indoor 800/900 MHz radio Channels for Digital Communications," *IEEE Communications Magazine, Vol.* 25, pp. 5-12, June, 1987.

[39] T. S. Rappaport and C. D. Mcgillem, "UHF Fading in Factories," *IEEE Journal on Selected Areas in Communications*, *Vol.* 7, pp. 40-48, January 1989.

[40] R. J. C. Bultitude and G. K. Bedal, "Propagation Characteristics on Microcellular Urban Mobile Radio Channels at 910 MHz," *IEEE Journal on Selected Areas in Communications*, *Vol.* 7, pp. 31-39, January 1989.

[41] J. G. Proakis, *Digital Communications,* (Second Edition), McGraw-Hill, NY, 1989.

[42] D. N. Romalo and Q. Wang, "Implementation of a Frequency Hop Modem," *Proceedings of Canadian Conference on Electrical and Computer Engineering*, pp. 4.2.1-4.2.5, September. 1990.

[43] D. Divsalar and M. K Simon, "Multiple-symbol Differential Detection of MPSK," *IEEE Transactions on Communications, Vol.* 38, No. 3, pp. 300-308, March, 1990.

[44] W. R. Braun and U. Dersch, "A Physical Mobile Radio Channel Model," *IEEE Transactions on Vehicular Technology, Vol.* 40, pp. 472-482, May, 1991.

[45] J. K. Cavers and R. F. Marchetto, "A New Coding Technique for spectral shaping of Data," *IEEE Transactions on Communications*, Vol. 40, pp. 1418-1422, September 1992.

[46] L. B. Milstein, D. L. Schilling, R. Pickholz, V. Erceg, M. Kullback, E. G. Kanterakis, D. S. Fishman, W. H. Biederman and D. C. Salerno, "On the Reasibility of CDMA Overlay for Personal Communications Networks, " *IEEE Journal on Selected Areas in Communications, Vol.* 10, pp. 655-668, May 1992.

[47] Q. Chen, Q. Wang, V. K. Bhargava and L. Mason, "Error Performance of Coded SFH/DPSK in Tone Interference and AWGN," *IEE Proceedings, Part I, Vol.* 140, *No.* 4, pp. 262-268, August 1993.

[48] A. A. Hassan, W. E. Stark and J. E. Hershey, "Frequency-Hopped Spread Spectrum in the Presence of a Follower Partial-Band Jammer," *IEEE Transactions on Communications, Vol.* 41, pp. 1125-1131, July 1993.

[49] H. Hashemi, "Impulse Response Modeling of Indoor Radio Propagation Channels, " *IEEE Journal on Selected Areas in Communications, Vol.* 11, pp. 967-978, September 1993.

[50] Q. Wang, Q. Chen, V. K. Bhargava and L. J. Mason, "Block and Decoded Error Probablity of DPSK in AWGN," *IEEE Transactions on Communications, Vol. 42,* pp. 3065-3068, December 1994.

[51] X. D. Wang and M. Lecours, "The Effect of Delay Spread on a FH/FSK Spread Spectrum Mobile Radio System over Frequency-selective Fading Channels, " *IEEE Transactions on Communications, Vol.* 42, pp. 1312-1324, February/March/April 1994.

[52] J. B. Andersen, T. S. Rappaport and S. Yoshida, "Propagation Measurements and Models for Wireless Communications Channels," *IEEE Communications Magazine*, Vol. 33, pp. 42-49, January 1995.

[53] K. Cheun and W. E. Stark, "Performance of FHSS Systems Employing Carrier Jitter Against One-Dimensional Tone Jamming," *IEEE Transactions on Communications, Vol.* 43, pp. 2622-2629, October 1995.

[54] F. Adachi and M. Sawahashi, "Decision Feedback Differential Phase Detection of M-ary DPSK Signals," *IEEE Transactions on Vehicular Technology*, Vol. 44, pp. 203-210, May 1995.

[55] J. Liu, S. C. Kwatra and J. Kim, "An Analysis of Decision Feedback Detection of Differentially Encoded MPSK Signals," *IEEE Transactions on Vehicular Technology*, Vol. 44, pp. 261-267, May 1995

[56] A. A. Ali, "Worst-case Partial-Band Noise Jamming of Rician Fading Channels," *IEEE Transactions on Communications, Vol.* 44, pp. 660-662, June 1996.

[57] B. A. Bjerke and M. Stojanovic, "A Hypothesis-Test Technique for Narrowband Interference Suppression in Spread Spectrum Systems," *Proceedings of IEEE Global Telecommunications Conference*, pp. 545-561549, Westminster, London, November 1996.

[58] R. C. Robertson and J. F. Sheltry, "Multiple Tone Interference of Frequency-Hopped Noncoherent MFSK Signals Transmitted Over Ricean Fading Channels," *IEEE Transactions on Communications, Vol.* 44, pp. 867-875, July 1996.

Appendix A

Useful Integrals and formula

1. Weber's second exponential integral

$$\int_0^\infty e^{-p^2t^2/2} J_0(at) J_0(bt)\, tdt = \frac{1}{p^2}\exp\left(\frac{a^2+b^2}{2p^2}\right) I_0\left(\frac{ab}{p^2}\right), \tag{A.1}$$

where $J_0(x)$ is the *Bessel function* and modified *Bessel function* of the *first kind* of order zero, and $I_0(x)$ is the modified *Bessel function* of the *first kind* of order zero.

2. Hankel Exponential intergral (which is a special case of (A.1))

$$\int_0^\infty te^{-p^2t^2/2} J_0(at)\, dt = \frac{1}{p^2}\exp\left(\frac{a^2}{2p^2}\right). \tag{A.2}$$

3. Generalisation of the *Weber-Schafheitlin* integral

$$\int_0^\infty J_1(at) J_0(bt) J_0(ct)\, dt = \begin{cases} 0; & a^2 < (b \pm c)^2 \\ \frac{1}{a}; & a^2 > (b \pm c)^2 \\ \frac{1}{\pi a} arc\cos\frac{b^2+c^2-a^2}{2bc}; & otherwise \end{cases}. \tag{A.3}$$

4. *Weber*'s infinite integral,

$$\int_0^\infty J_\nu(t)\, t^{-(\nu-\mu+1)}\, dt = \frac{\Gamma\left(\frac{1}{2}\mu\right)}{2^{\nu-\mu+1}\Gamma\left(\nu-\frac{1}{2}\mu+1\right)}. \tag{A.4}$$

5. Definition of Marcum's Q-function

$$Q(a,b) = \int_b^\infty x\exp\left(-\frac{x^2+a^2}{2}\right)I_o(ax)\,dx. \tag{A.5}$$

6. Some special values of Marcum's Q-function

$$Q(a,0) = 1;\ Q(0,b) = \exp\left(-\frac{b^2}{2}\right). \tag{A.6}$$

7. Neumann's formula

$$J_0\left(\sqrt{x^2+y^2-2xy\cos\theta}\right) = \sum_{r=-\infty}^{\infty} J_r(x)J_r(y)\cos(r\theta), \tag{A.7}$$

where $J_r(x)$ is the *Bessel function* of the *first kind* of order *r*.

8. Basic relation between the *Bessel function* and modified *Bessel funtion* of the *first kind.*

$$I_n(z) = \begin{cases} e^{-\frac{\pi}{2}ni}J_n(iz) & -\pi < \arg z < \frac{\pi}{2} \\ e^{\frac{\pi}{2}ni}J_n(-iz) & \frac{\pi}{2} < \arg z < \pi \end{cases}. \tag{A.8}$$

9. Basic relation between Marcum's Q-functions *Q(a,b)* and *Q(b,a)*

$$Q(a,b) + Q(b,a) = 1 + \exp\left(-\frac{a^2+b^2}{2}\right)I_0(ab). \tag{A.9}$$

10.

$$\frac{d}{dz}\{z^{-v}J_v(z)\} = -z^{-v}J_{v+1}(z). \tag{A.10}$$

11.

$$\int\frac{1}{a+b\cos\theta}d\theta = \frac{2}{\sqrt{a^2-b^2}}arctg\frac{(a-b)\,tg\frac{\theta}{2}}{\sqrt{a^2-b^2}};\ a^2>b^2. \tag{A.11}$$

Appendix B

List of Acronyms

AWGN	additive white Gaussian noise
BER	bit error rate
BDPSK	binary differential phase shift-keying
BPSK	binary phase shift-keying
CW	continuous wave
DS	direct sequence
FFH	fast frequency hopping
GSM	Global system for Mobile
ISI	intersymbol interference
ISM	industrial, scientific and medical
LAN	local area network
LOS	line-of-sight
MDPSK	M-ary differential phase shift-keying
MFSK	M-ary frequency shift-keying
ML	maximum-likelihood
MPSK	M-ary phase shift-keying
NBI	narrowband interference
PCS	personal communication services
QDPSK	quaternary differential phase shift-keying
SFH	slow frequency hopping
SS	spread spectrum